FLOW OF NON-NEWTONIAN FLUIDS WITHIN A DOUBLE POROSITY RESERVOIR UNDER PSEUDOSTEADY-STATE INTERPOROSITY TRANSFER CONDITIONS

A Thesis

by

JORGE ROBERTO GARCIA

Submitted to the Office of Graduate and Professional Studies of
Texas A&M University
in partial fulfillment of the requirements for the degree of

MASTER OF SCIENCE

Chair of Committee,	Thomas A. Blasingame
Co-Chair of Committee,	Maria A. Barrufet
Committee Members,	Eduardo Gildin
Head of Department,	A. Daniel Hill

August 2015

Major Subject: Petroleum Engineering

ABSTRACT

Heavy and extra heavy oil are fluids with high ranges of viscosity at both reservoir and surface conditions. These fluids have complex production processes due to factors such as high sulfide content, carbon dioxide (or other fluid injection reactions), flow assurance, and water breakthrough. The rheological properties of heavy and extra heavy oil modify the fluid in such a manner that these fluids cannot be treated as traditional Newtonian fluids. The behavior of such fluids is well documented in the petroleum industry and serves as the motivation for this work.

This work develops and presents a new reservoir model which accounts for the behavior of a non-Newtonian fluid within a double porosity reservoir. We propose a new interporosity function for "pseudosteady-state" flow with non-Newtonian phenomena. The non-Newtonian fluid type that we have chosen to use in this work is the "pseudoplastic" plastic fluid type.

We review and adopt certain aspects from the prior studies that have been performed to describe the behavior of a non-Newtonian fluid through porous media in a homogeneous reservoir system. We also provide an extensive literature review on this topic and the behavior of "double porosity" (or "naturally fractured") reservoir systems. In this work we only consider the classic case of "pseudosteady-state" interporosity flow introduced by Warren and Root as this represents the "base" case (or starting point).

Specifically, in this work, we derive the partial differential equation for non-Newtonian flow within a double porosity reservoir under pseudosteady-state interporosity transfer conditions. All solutions assume the "constant rate" inner boundary condition, the outer boundary conditions used in this work include the infinite-acting reservoir, circular reservoir with a "no flow" outer boundary, circular reservoir with a "constant pressure" outer boundary. "Type curve" plots are provided to illustrate the behavior of the dimensionless pressure and dimensionless pressure derivative behavior as a function of dimensionless time.

Illustrative examples are provided using synthetic cases. In these examples the entire workflow is illustrated, including diagnostic identification and radial flow analyses.

DEDICATION

To the love of my life — Adriana Morales. I would not be here without her support, encouragement, patience and most of all, her love.

ACKNOWLEDGEMENTS

I would like to thank:

Dr. Blasingame for all his support, strictness, courage, and patience during my Masters studies, and I give him my special thanks for being my "Abuelito." You are my school dad.

My advisory committee members Dr. Barrufet and Dr. Gildin for their support and valuable comments during my Masters studies.

Mr. Alex Valdes for his dedication, guidance, support, patience and his sincere friendship during my Masters studies, his mentoring and collaboration made very significant contributions to this work.

My parents, Julieta and Francisco for all their support and love.

My big brother Francisco, A.K.A. Paquirri.

My mother- and sister-in-law, Linda and Gaby.

Dr. Victor Arana for his support and teaching at a distance — no matter what the subject, especially for his friendship and his guidance on life experiences.

My PEMEX advisor, Dr. Fernando Rodriguez de la Garza, from the very first time I talked to him about my interest to study abroad he gave me his unconditional support and guidance

The "Wettability Group" at Texas A&M (Uriel, Erick and Pedro) for their friendship.

PEMEX and CONACYT for my sponsorship and the opportunity to study abroad.

All of my teachers during my Masters studies, and to Texas A&M University for letting me achieve one of the most valuable experiences of my life.

TABLE OF CONTENTS

ABSTRACT ii

DEDICATION iii

ACKNOWLEDGEMENTS iv

TABLE OF CONTENTS v

LIST OF FIGURES vii

LIST OF TABLES x

CHAPTER I INTRODUCTION 1

I.1 Motivation 1
I.2 Objectives 1
I.3 Basic concepts 1
I.4 Rheological models 4
I.5 Power law model 8

CHAPTER II LITERATURE REVIEW 10

II.1 Double porosity model with pseudosteady-state interporosity transfer 10
II.2 Flow of non-Newtonian fluids through homogeneous reservoirs 14
II.3 Flow of non-Newtonian fluids within a double porosity reservoir with pseudosteady-state interporosity transfer and Newtonian interaction between media 16
II.4 Flow of non-Newtonian fluids within a double porosity reservoir with transient interporosity transfer and Newtonian interaction between media 17

CHAPTER III PROPOSED MODEL 21

III.1 Assumptions 21
III.2 Partial differential equation 22
III.3 Dimensionless analysis 23

CHAPTER IV SOLUTIONS AND RESULTS 25

IV.1 General solution 25
IV.2 Initial and boundary conditions 25
IV.3 Solution for infinite acting reservoir and constant flowrate 26
IV.4 Solution for closed reservoir and constant flowrate 35
IV.5 Solution for constant pressure at the outer boundary and constant flowrate 37
IV.6 Early and long time approximations from Laplace domain to real domain 39
IV.7 Inclusion of effects around the wellbore. 42

CHAPTER V SYNTHETIC CASE 45

CHAPTER VI SUMMARY, CONCLUSIONS, AND RECOMMENDATIONS FOR FUTURE WORK 56

REFERENCES 58

NOMENCLATURE 60

APPENDIX A DERIVATION OF A RADIAL FLOW-DUAL POROSITY MODEL (PSEUDO-STATE INTERPOROSITY FLOW) 62

APPENDIX B DERIVATION OF A RADIAL MODEL FOR NON-NEWTONIAN FLUID THROUGH POROUS MEDIUM 69

APPENDIX C PROPOSED DUAL POROSITY MODELINCLUDING NON-NEWTONIAN FLUID FLOW (PSEUDOSTEADY-STATE INTERPOROSITY FLOW) 76

APPENDIX D CLOSED RESERVOIR AT THE OUTER BOUNDARY AND CONSTANT RATE AT THE WELLBORE 89

APPENDIX E CONSTANT PRESSURE AT THE OUTER BOUNDARY AND CONSTANT RATE AT THE WELLBORE 92

APPENDIX F WELLBORE STORAGE 95

APPENDIX G SKIN FACTOR 98

APPENDIX H EARLY-TIME APPROXIMATIONS 100

APPENDIX I LATE-TIME APPROXIMATIONS 103

LIST OF FIGURES

Page

Fig. 1 ─ Laminar flow steady state (modified from Bird et al., 2002) 2

Fig. 2 ─ Time-Independent non-Newtonian fluids 3

Fig. 3 ─ Bingham model graphical representation 4

Fig. 4 ─ Power law graphical representation 5

Fig. 5 ─ Viscosity behavior as function of the shear rate 5

Fig. 6 ─ Herschel-Bulkley graphical representation 6

Fig. 7 ─ Casson model graphical representation 7

Fig. 8 ─ Idealization of heterogeneous porous media 10

Fig. 9 ─ Double porosity reservoir semilog plot λ cases 12

Fig. 10 ─ Double porosity reservoir log-log dimensionless pressure derivative 13

Fig. 11 ─ Double porosity reservoir log-log plot with wellbore storage 14

Fig. 12 ─ Dimensionless pressure vs dimensionless time for pseudoplastic non-Newtonian fluids in an infinite acting reservoir 15

Fig. 13 ─ Semi-log plot non-Newtonian cases 16

Fig. 14 ─ Log-log dimensionless derivative pressure (Escobar et al., 2011) 17

Fig. 15 ─ Dimensionless pressure, *n* selected cases (Olarewaju, 1992) 19

Fig. 16 ─ Dimensionless pressure derivative, *n* selected cases (Olarewaju, 1992) 20

Fig. 17 ─ Schematic representation of the proposed model 22

Fig. 18 ─ Log-log plot for selected values of dimensionless matrix contribution *D*, *n*=0.1 27

Fig. 19 ─ Log-log plot for selected values of dimensionless matrix contribution *D*, *n*=0.25 28

Fig. 20 ─ Log-log plot for selected values of dimensionless matrix contribution *D*, *n*=0.50 28

Fig. 21 ─ Log-log plot for selected values of dimensionless matrix contribution *D*, *n*=0.75 29

Fig. 22 ─ Log-log plot for selected values of dimensionless matrix contribution *D*, *n*=1.0 29

Fig. 23 ─ Log-log plot for selected values of interporosity flow coefficient λ, *n*=0.10 30

Fig. 24 ─ Log-log plot for selected values of interporosity flow coefficient λ, *n*=0.25 31

Fig. 25 ─ Log-log plot for selected values of interporosity flow coefficient λ, n=0.50 31

Fig. 26 ─ Log-log plot for selected values of interporosity flow coefficient λ, n=0.75 32

Fig. 27 ─ Log-log plot for selected values of interporosity flow coefficient λ, n=1.0 32

Fig. 28 ─ Log-log plot for selected values of storativity ratio ω, n=0.1 33

Fig. 29 ─ Log-log plot for selected values of storativity ratio ω, n=0.25 33

Fig. 30 ─ Log-log plot for selected values of storativity ratio ω, n=0.50 34

Fig. 31 ─ Log-log plot for selected values of storativity ratio ω, n=0.75 34

Fig. 32 ─ Log-log plot for selected values of storativity ratio ω, n=1.0 35

Fig. 33 ─ Closed reservoir and constant flowrate at the wellbore for selected values of n, r_{eD}=5000 36

Fig. 34 ─Closed reservoir and constant flowrate at the wellbore for selected values of n, r_{eD}=10000 37

Fig. 35 ─ Constant pressure at the outer boundary and constant flowrate at the wellbore, r_{eD}=5000 38

Fig. 36 ─ Constant pressure at the outer boundary and constant flowrate at the wellbore, r_{eD}=10000 39

Fig. 37 ─ Early time approximations for dimensionless pressure, selected values of n 40

Fig. 38 ─ Early time approximations for dimensionless pressure derivative, selected values of n 41

Fig. 39 ─ Long time approximations for dimensionless pressure, selected values of n 42

Fig. 40─ Long time approximations for dimensionless pressure derivative, selected values of n 42

Fig. 41 ─ Dimensionless wellbore storage when n=0.25 43

Fig. 42 ─ Dimensionless wellbore storage when n=0.50 43

Fig. 43 ─ Dimensionless wellbore storage when n=0.75 44

Fig. 44 ─ Dimensionless wellbore storage when n=1.0 44

Fig. 45 ─ Pressure drop and pressure drop derivative vs time 47

Fig. 46 ─ Specialized graph 48

Fig. 47 ─ Semi-analytical approximation 49

Fig. 48 ─ Pressure drop data vs time 51

Fig. 49 ─ Early data- Cartesian plot 52

Fig. 50 ─ Specialized graph 54

Fig. 51 ─ Semi-analytical approximation 55

LIST OF TABLES

Page

Table 1 — Well test data for case 1 (no skin or wellbore storage effects) 45

Table 2 — Well test data for case 2 (effects around the wellbore) 50

CHAPTER I

INTRODUCTION

I.1 Motivation

The motivation of this work originally started generating a model which was able to characterize only fluids with high ranges of viscosity. As part of the development of the research, in the classification of non-Newtonian fluids are integrated fluids whether are produced (heavy and extraheavy oils) or injected (EOR methods: polymers and foams) therefore the statement of the problem can assist characterizing fluids which rely on the classification of non-Newtonian, specifically in this study for *pseudoplastic* fluids. More detailed of this classification is found in the basic concepts chapter.

I.2 Objectives

The main objectives of the work are to:

- *Develop* a double porosity model to describe the physics of pseudosteady state interporosity transfer for non-Newtonian fluid.
- *Provide* an interporosity transfer model for depicting the non-Newtonian effects experienced during interaction between the fracture and the matrix.
- *Generate* solutions suitable for pressure transient analysis.

I.3 Basic concepts

In order to generate a model which takes into account the behavior of non-Newtonian fluids and their nature this chapter define basic concepts to understand such phenomena.

Rheology may be defined as the study of the flow and deformation of materials. There are two basic kinds of flow with relative movement of adjacent particles of liquid; they are called *shear* and *extensional*. Shear flows liquid elements flow over or past each other, while in extensional flow, adjacent elements flow towards or away from each other. All flows are resisted by *viscosity*, stating that for a given *velocity*, the resulting force increases when the viscosity is increased, whereas for a given force, the velocity is reduced when the viscosity is increased. Consider a pair of large parallel plates, each one with area *A*, separated by a distance *Y* as shown in **Fig. 1**. This system is initially at rest, at *t=0* the lower plate is set in motion in the positive x-direction at a constant velocity *V* under laminar flow conditions. As time proceeds, the fluid gains *momentum* and ultimately the linear steady-state velocity profile is established. When the final state of steady motion has been attained, a constant force *F* is required to maintain the motion of the lower plate. The force should

be proportional to the area and to the velocity, and inversely proportional to the distance between the plates. The constant of proportionality μ is a property of the fluid defined as *viscosity*:

$$\frac{F}{A} = \mu \frac{V}{Y}, \quad \text{(I.1)}$$

where: *F/A* is the shear rate, and *V/Y* is the shear stress.

The model given by Eq. 1 is used to determine the viscosity of Newtonian fluids, i.e., for fluids with constant viscosity regardless the *shear rate* and *shear stress*.

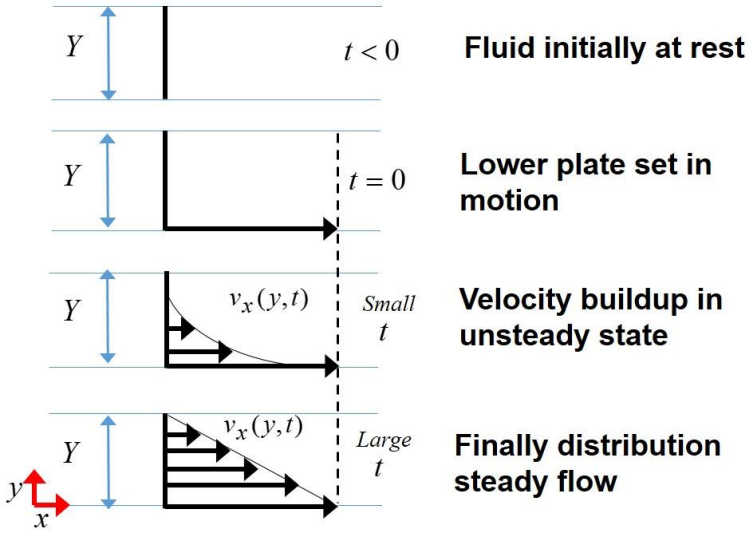

Fig. 1 — Laminar flow steady state (modified from Bird et al., 2002)

Therefore, the viscosity can be defined as a measure of the energy dissipated by a fluid in motion as it resists an applied shearing force. Shear stress is the force per unit area applied to the deformed body, where the force is applied tangentially to the surface of the body. Shear rate is the rate of relative deformation. Hence, eq.1 can be expressed as:

$$\tau = \mu \dot{\gamma}, \quad \text{(I.2)}$$

where, comparing between Eq.1 and Eq.2:

$$\tau = \frac{F}{A}, \quad \text{(I.3)}$$

and:

$$\dot{\gamma} = \frac{V}{Y} \quad \text{..... (I.4)}$$

Eq.2 is often called *Newton's Law of Viscosity* and the fluids that have this behavior are called Newtonian fluids. This expression is known as a rheological model and describes the flow behavior of a liquid in a linear relationship between shear rate and shear stress. Typically μ is known as *viscosity* and it is commonly used to characterize the fluid's resistance to flow.

On the other hand, non-Newtonian fluids are those which do not obey the Newton's Law of Viscosity, it means that, even under isothermal conditions, when shear rate or shear stress varies, viscosity changes by many orders of magnitude.

A classification of the non-Newtonian fluids is given as follows:

1. Time-Independent non-Newtonian Fluids (see **Fig. 2**).
   a. Pseudoplastic fluids: apparent viscosity decreases with increase of shear rate.
   b. Dilatant fluids: apparent viscosity increases with increase of shear rate.
   c. Bingham plastics: no relation between shear rate and shear stress
2. Time-Dependent non-Newtonian Fluids
3. Viscoelastic non-Newtonian Fluids: have the effect of partial elastic recovery and may be non-Newtonian and time-dependent.

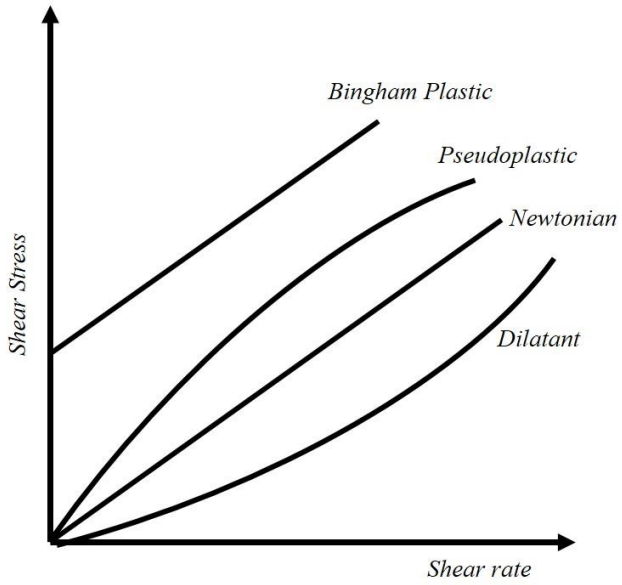

Fig. 2 ─ Time-Independent non-Newtonian fluids

The shear rate ant the shear stress are parameters that have been investigated for a variety of fluids, and there are some important rheological models that describe the fluid flow behavior. Due to the assumptions that we will make for our mathematical model, *we will focus only on power law models*. Next are described several rheological models which not obey to the Newtonian's Law of viscosity.

I.4 Rheological models

Bingham Model. This model plastic materials which behave as solids, unless a stress greater than the yield stress is applied: The viscosity for these fluids is known as *plastic viscosity*, μ_p, (Pa•s).

$$\tau = \tau_y + \mu_p \dot{\gamma} \quad \text{..... (I.5)}$$

A Bingham plastic fluid will not flow until the applied shear stress τ exceeds a certain minimum value τ_y known as the yield stress. After the fluid has been exceed, changes in shear stress are proportional to changes in shear rate; a graphical representation is shown on **Fig. 3.**

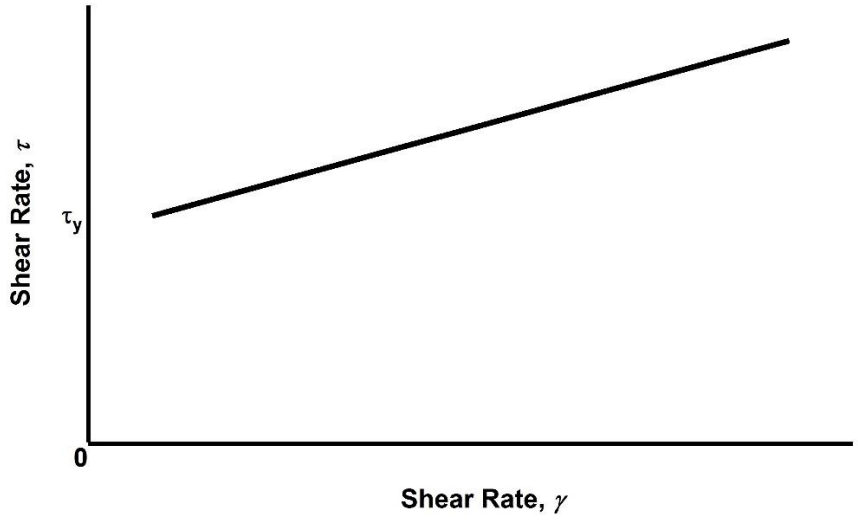

Fig. 3 ─ Bingham model graphical representation

*Power Law (de Waele)***.** For most of the fluids, the relations hip between shear stress and shear rate is not the linear form shown in Eq.I.2, many fluids show rapid changes in viscosity as a function of the shear rate. The next expression is used to represent the behavior of such fluids:

$$\tau = H\dot{\gamma}^n, \quad \text{..... (I.6)}$$

where:

H the consistency coefficient (Pa•s^n) and

n flow behavior index (dimensionless).

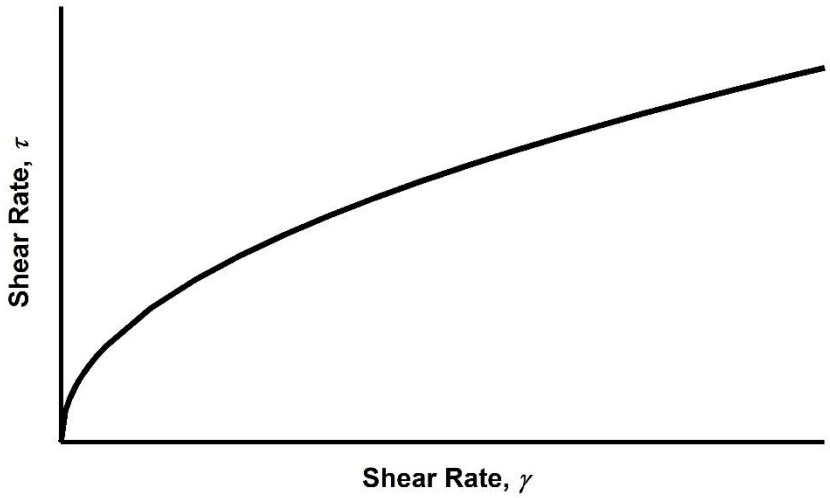

Fig. 4 ─ Power law graphical representation

The deviation of the flow behavior index characterizes the degree to which the fluid behavior is non-Newtonian. For power law fluids, $n<1$indicates that the viscosity decreases as shear rate increases. This is called a pseudoplastic fluid. When $n>1$ the fluids are called dilatants, showing an increase in viscosity as the shear rate increases. The Newtonian fluid relies when $n=1$. **Fig. 2 and Fig. 5** shows graphically this explanation.

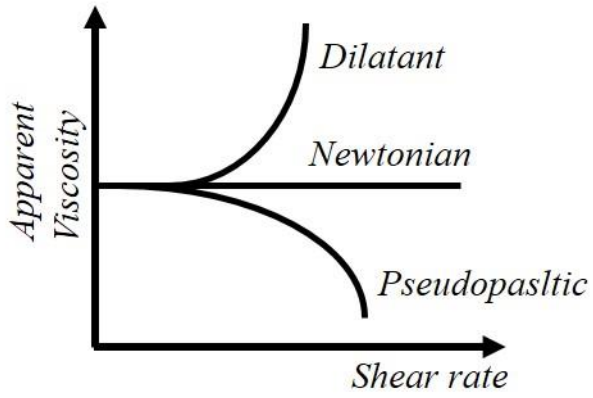

Fig. 5 ─ Viscosity behavior as function of the shear rate

Hershel-Buckley Model. In this model when $\tau < \tau_0$ the material does not flow.

$$\tau = \tau_y + H\dot{\gamma}^n \quad \text{..... (I.7)}$$

The model combines the characteristics of the Bingham and power law models and requires three parameters for fluid characterization. The Herschel-Bulkley model can be used to represent a yield-pseudoplastic fluid (n<1), a dilatant fluid (n>1), a pseudoplastic fluid (τ_y = 0, n<1) a plastic fluid (n=1), or a Newtonian fluid (τ_y = 0, n=1). Eq. (I.7) is valid only for laminar flow.

Like the Bingham plastic model, a fluid represented by this model will not flow until the applied shear stress τ exceeds a minimum value τ_y, which is called the yield stress. The fluid behaves like a solid until the applied force is high enough to exceed the yield stress. The Herschel-Bulkley model is represented graphically in **Fig. 6.**

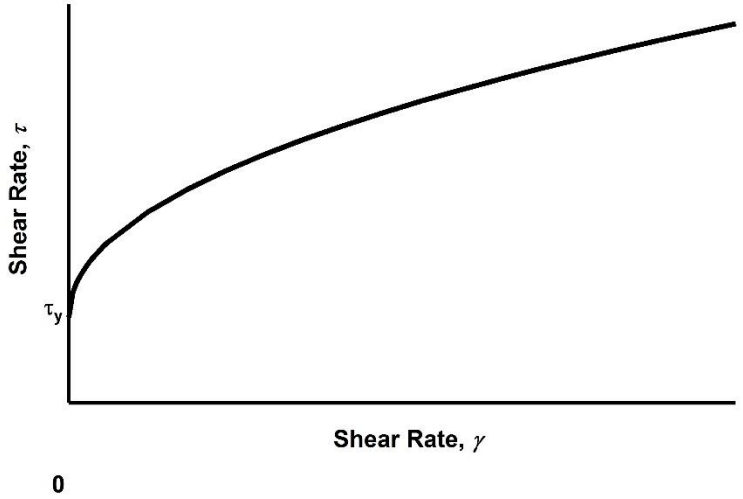

Fig. 6 ─ Herschel-Bulkley graphical representation

Generally, the rheological parameter that characterizes a model are determined by using analytical equations based on a data set of measurements from rotational viscometer, as reported by the API 13 standards. However, to improve the accuracy of calculation on the rheological parameters, statistical regression methods are used. They are applied to complete set (τ, γ) of measurements performed on a sample of the fluid in the rotational viscometer. Outcomes are higher accuracy in determining the rheological parameters that characterizes the behavior of the tested fluid, and as consequence a better evaluation of flow parameters such as velocity profile, flow regime, and pressure drop.

Casson Model. Is often used to simulate drilling fluids and cement slurries with plastic behavior, with higher accuracy than the Bingham plastic model. The model is defined by:

$$\sqrt{\tau} = \sqrt{\tau_y} + \sqrt{\mu_p}\sqrt{\dot{\gamma}} \quad \text{.....(I.8)}$$

Eq. I.8 is valid only for laminar flow. Generally, the model is plotted with coordinates ($\tau^{1/2}$, $\gamma^{1/2}$) instead of (τ, $\dot{\gamma}$) to still maintain the liner trend. Like the Bingham model, Casson model requires two parameters for fluid characterization. A fluid represented by this model requires a finite shear stress, τ_y below it will not flow. Above the finite shear stress, referred to as the *yield stress*, changes in shear stress are proportional to changes in shear rate, and the constant of proportionality is called the plastic viscosity, μ_p. A graphical representation is shown in **Fig. 7.**

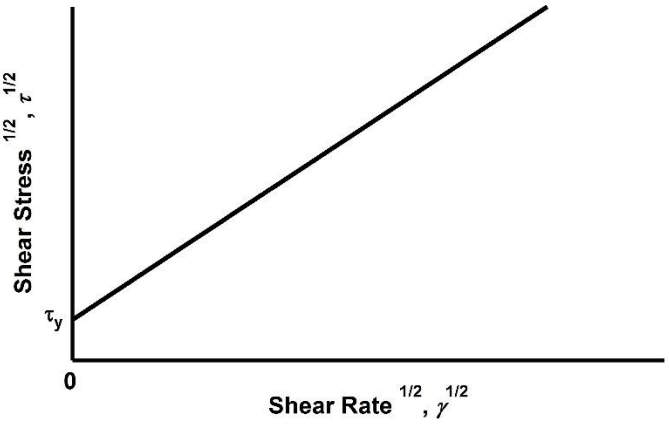

Fig. 7 ─ Casson model graphical representation

In addition to the model previously reported, there are many other empirical mathematical descriptions that can describe with high accuracy the behavior of the viscous forces of some petroleum fluids.

Three-Parameter models. These models require three constant parameters for fluid characterization The Graves Collins model is defined by:

$$\tau = (1 - e^{-\beta\gamma})(\tau_0 + \mu\gamma), \quad \text{.....(I.9)}$$

The constants parameters are τ_0, μ and β. The model can approximate with good accuracy pseudoplastic fluids at low shear rates and plastic fluids at high shear rates.

The Gucuyener model is defined by

$$\tau^{\frac{1}{m}} = \tau_y^{\frac{1}{m}} + \eta\gamma^{\frac{1}{2}} \quad \text{.....(I.10)}$$

The constant parameters of the model are τ_y, η and m. The model predicts the behavior of yield-pseudoplastic fluids. In addition, it can be used to represent pseudoplastic fluids (τ_y=0) plastic fluids (m=2) and Newtonian fluids (τ_y =0, m=2).

The Sisko model is defined by

$$\tau = a\gamma + b\gamma \quad \text{(I.11)}$$

The constants parameters of the model are a, b and c. The model can describe the behavior of pseudoplastic fluids (a=0) and Newtonian fluids (b=0).

Four-Parameter Models. These models require four constant parameters for fluid characterization. The Shulman model is defined by:

$$\tau^{\frac{1}{n}} = \tau_0^{\frac{1}{n}} + (\eta\gamma)^{\frac{1}{m}} \quad \text{(I.12)}$$

The constant parameters of the model are τ_0, η, m, and n. The model approximates with high accuracy the properties of yield-pseudoplastic fluids (n=1), pseudoplastic fluids (τ_0=0, n=1), plastic fluids (n=m=1 for Bingham plastic fluids, and n=m=2 for Casson fluids), and Newtonian fluids (τ_0=0, n=m=1).
The Zhu model is defined by

$$\tau = \tau_0(1 - e^{-m\gamma}) + \eta_1 e^{-t_1\gamma}\gamma \quad \text{(I.13)}$$

The constant parameters of the model are τ_0, η_1, m and t_1. The model can approximate with high accuracy the behavior of yield-pseudoplastic fluids.
Five-Parameter models. These models require five constant parameters for fluid characterization. The Maglione model is defined by

$$\tau^{\frac{1}{n}} = a^{\frac{1}{n}} + (b\gamma)^{\frac{1}{m}} + (c\gamma)^{\frac{1}{m}+1} \quad \text{(I.13)}$$

The five constant parameters of the model are a, b, c, n and m. The parameter a is the yield stress, parameters b and c are related to the fluid viscosity, and n and m are related to the flow behavior index of the fluid. The model approximates with high accuracy the properties of yield-pseudoplastic fluids (c=0, n=1), pseudoplastic fluids (a=c=0, n=1), plastic fluids (c=0, and n=m=1 for Bingham plastic fluids, c=0 and n=m=2 for Casson fluids), and Newtonian fluids (a=c=0, n=m=1).

I.5 Power law model

The Blake and Kozeny (1956) model is a semi-empirical flow model for Newtonian fluid through a packed bed was extended by Christopher et al. (1965), to be applied when there is a power-law fluid flowing in a porous media. Such modification is given by:

$$v_o = \frac{n\phi}{3n+1}\left[\frac{D_p\,\phi}{3(1-\phi)}\right]^{\frac{n+1}{n}}\left[\frac{6\Delta p}{25\,HL}\right]^{\frac{1}{n}}, \quad \text{(I.14)}$$

where:

D_p = Particle diameter [cm]

L = Length [cm]

Δp = Pressure change [g/cm • s^2]

And the permeability is given by:

$$k = \frac{D_p^2\,\phi^3}{150\,(1-\phi)^2}, \quad \text{(I.15)}$$

Combining Eq.I.7 and Eq.I.8, we obtain:

$$v_o = \left[\frac{k}{\mu_{eff}}\frac{\Delta p}{L}\right]^{\frac{1}{n}}, \quad \text{(I.16)}$$

Where μ_{eff} is the *effective viscosity*, and is defined by:

$$\mu_{eff} = \frac{H}{12}\left[9+\frac{3}{n}\right]^{n}\left(150\,k\phi\right)^{\frac{1-n}{2}}. \quad \text{(I.17)}$$

We state that Eq.I.9 can be written in radial coordinates as follows:

$$v_r^n = \frac{k}{\mu_{eff}}\frac{\partial p}{\partial r} \quad \text{(I.18)}$$

Eq. I.18 is the analog for Darcy's Law using a Non-Newtonian fluid. It is important to note that this equation was used for the development of the proposed model.

CHAPTER II

LITERATURE REVIEW

This chapter summarize the models found in the literature to characterize a double porosity model and a non-Newtonian fluid through porous media.

II.1 Double porosity model with pseudosteady-state interporosity transfer

Double porosity flow models can be categorized in three main types: pseudosteady-state (Warren et al., 1963 and Najurieta, 1980), transient (Cinco-Ley et al., 1982, Serra, et al., 1983 and Streltsova, 1982) and interporous skin (Moench, 1984, Cinco-Ley et al., 1985), nevertheless this work will focused in pseudosteady-state.

Two classes of porosity are described:

1. Matrix: Intergranular and controlled by deposition and lithification.
2. Fracture: '*foramenular*' (which means, orifice, perforation or small opening) and controlled by fracturing, jointing and/or solution

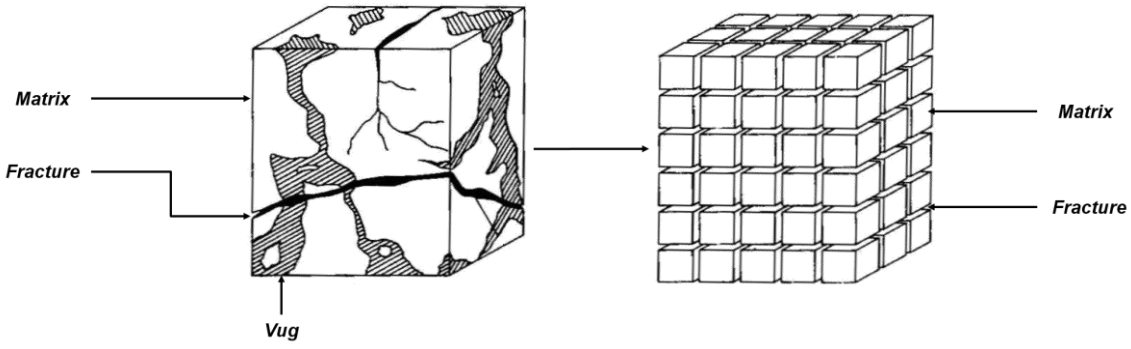

Fig. 8 ─ Idealization of heterogeneous porous media

Fig. 8 represents the idealization of a heterogeneous porous media. Such idealization provides a starting point to model the complexity of multiporosity reservoirs.

II.1.1 Pseudosteady-state interporosity transfer in double porosity media flow model (Warren et al. 1963)

This model is based on the following assumptions:

- Matrix blocks are in a systematic array of identical rectangular parallelepipeds.
- Matrix blocks are homogeneous and isotropic.
- Matrix blocks contain matrix porosity ϕ_m.
- Fracture network is arrayed as an orthogonal system of continuous and uniform fractures.

- Fracture porosity is expressed as ϕ_f.
- The double porosity character is assumed to be homogeneously distributed throughout the media.
- Flow occurs towards the wellbore only through fractures.
- Flow occurs between the matrix blocks and fractures, but there is no flow between matrix blocks.

The parameters and solution of Warren et al. (1963) model are presented below, and the detailed derivation of the model is given in Appendix A. The dimensionless diffusivity equation for the flow of fluid in the fracture is defined by

$$\frac{1}{r_D}\frac{\partial}{\partial r_D}\left[r_D\frac{\partial p_{fD}}{\partial r_D}\right]=\omega\frac{\partial p_{fD}}{\partial t_D}+(1-\omega)\frac{\partial p_{mD}}{\partial t_D}, \quad \text{(II.1)}$$

where ω is the *storativity ratio* expressed as:

$$\omega=\frac{(\phi c_t)_f}{(\phi c_t)_f+(\phi c_t)_m}. \quad \text{(II.2)}$$

Whereas, the *dimensionless interface condition* is given by:

$$\frac{\partial p_{mD}}{\partial t_D}=\alpha\frac{k_m}{k_f}r_w^2\frac{(\phi c_t)_m+(\phi c_t)_f}{(\phi c_t)_m}(p_{fD}-p_{mD}), \quad \text{(II.3)}$$

where the *interporosity flow coefficient* (λ) is:

$$\lambda=\alpha\, r_w^2\frac{k_m}{k_f}. \quad \text{(II.4)}$$

The solution of Eq. II.1 in the Laplace domain is given by:

$$\bar{p}_{fD}(r_D,u)=\frac{1}{u}\frac{K_o(r_D\sqrt{u\,f(u)})}{\sqrt{u\,f(u)}\,K_1(\sqrt{u\,f(u)})}, \quad \text{(II.5)}$$

where the *interporosity flow function* is:

$$f(u)=\frac{u(1-\omega)\omega+\lambda}{u(1-\omega)+\lambda}. \quad \text{(II.6)}$$

An approximate solution of Eq. II.5 in the real domain is:

$$p_{fD}(r_D,t_D)\approx\frac{1}{2}\ln\left[\frac{4}{e^{\gamma}}\frac{t_D}{r_D}\right]-\frac{1}{2}E_1\left[\frac{\lambda}{\omega(1-\omega)}t_D\right]+\frac{1}{2}E_1\left[\frac{\lambda}{(1-\omega)}t_D\right]. \quad \text{(II.7)}$$

Well testing derivative of time:

$$p'_{fD}(r_D, t_D) \approx \frac{1}{2} + \frac{1}{2}\exp\left[\frac{-\lambda}{\omega(1-\omega)}t_D\right] - \frac{1}{2}\exp\left[\frac{-\lambda}{(1-\omega)}t_D\right] \quad \text{..... (II.8)}$$

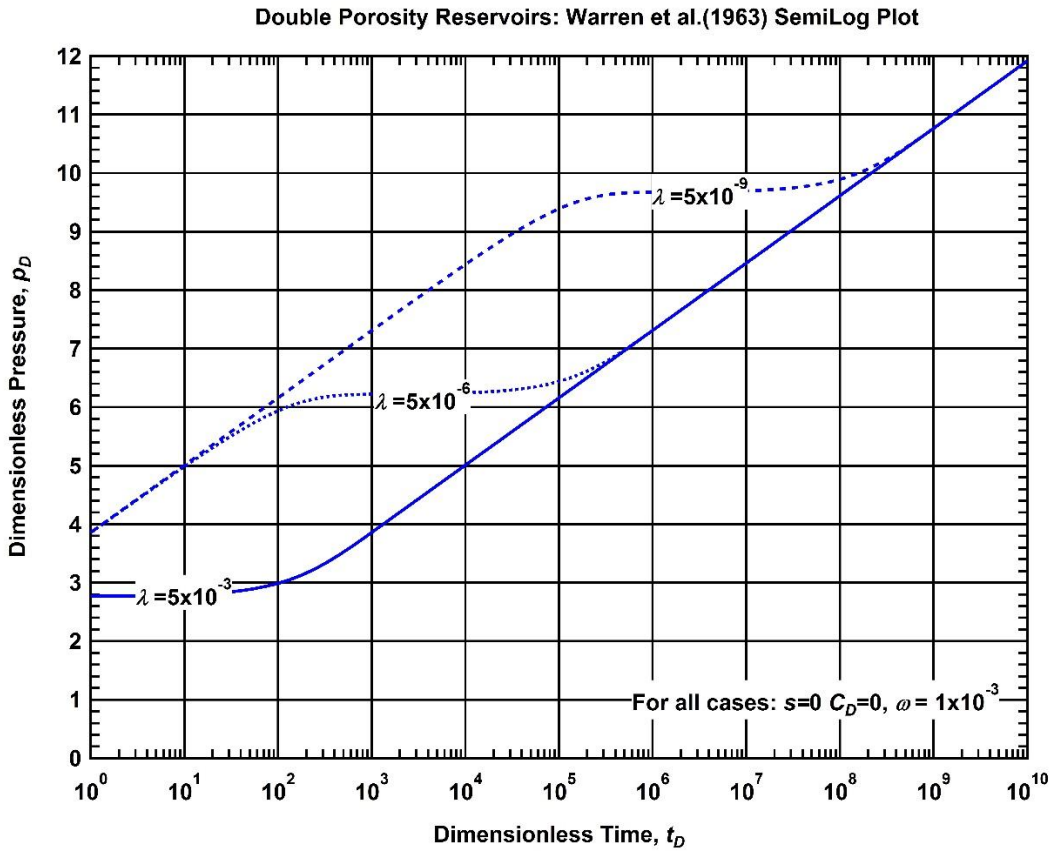

Fig. 9 ─ Double porosity reservoir semilog plot λ cases

Fig. 9 shows the effect of the interporosity flow coefficient in the dimensionless pressure response along time in semi-log scale with no wellbore storage and no skin factor. For all the cases ω=1x10^{-3}. The interporosity flow coefficient controls the speed of the fluid transfer interaction from the matrix through the fracture network. For example, when λ is equal to zero the dual porosity model converges to a homogenous model. The reason why an interporosity flow coefficient approaches to zero could be because there is a fracture-vugular dominated system, and the matrix system will take much more time to appear.

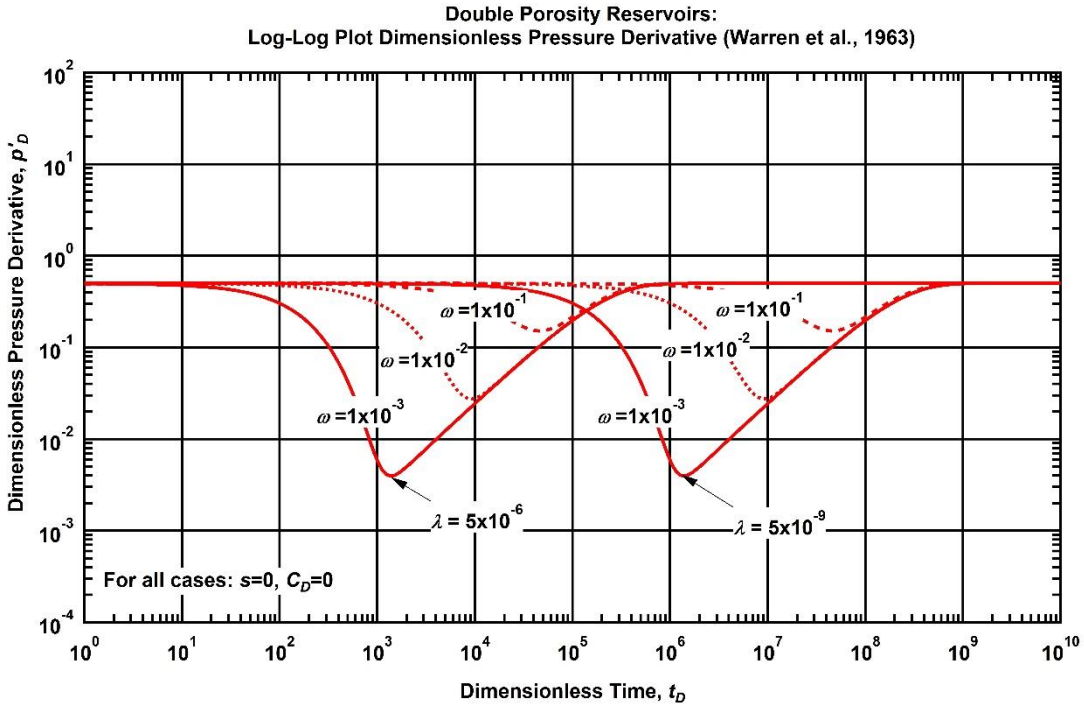

Fig. 10 ─ Double porosity reservoir log-log dimensionless pressure derivative

Fig. 10 shows the log-log plot of the pressure derivative function of the model proposed by Warren et al. (1963). Selected cases for the storativity ratio and the interporosity flow coefficient are plotted. It should be noticed that the higher ω values the less abrupt are the chan ges in the pressure derivative response. The storativity ratio values, may go from 0 to 1. A ω=0 would imply that there is no expansion within fracture network; a ω=1 means that all the expansion in the reservoir is attributed to the fracture expansion

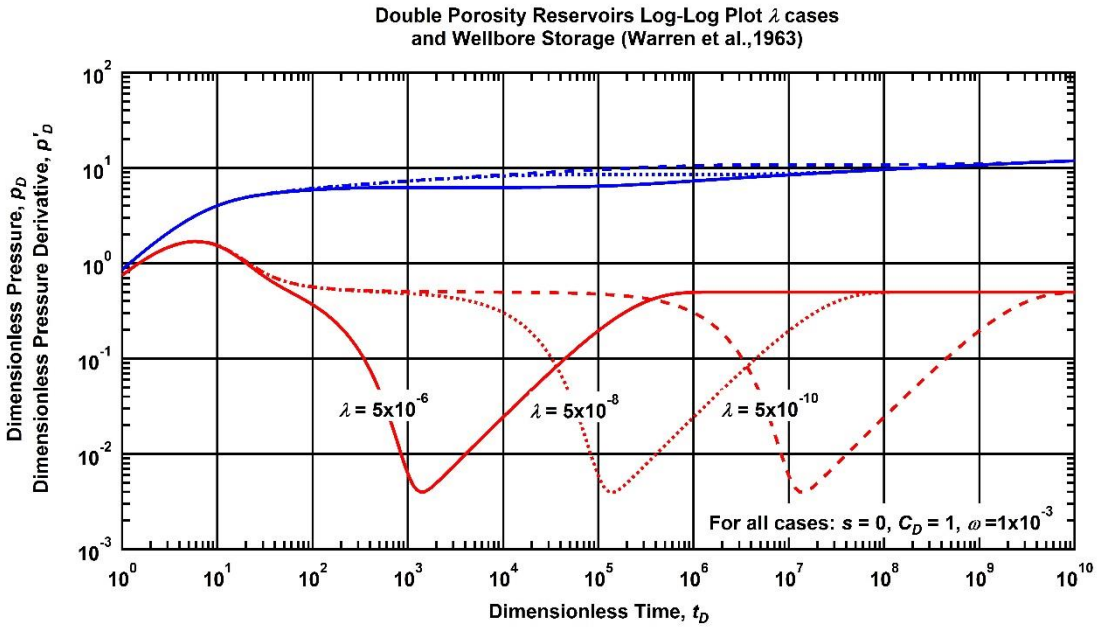

Fig. 11 ─ Double porosity reservoir log-log plot with wellbore storage

Fig.11 shows the log-log plot of the dimensionless pressure and pressure derivative function versus dimensionless time of the model proposed by Warren et al. (1963) including wellbore storage for selected values of interporosity flow coefficient λ. It is observed that the shape of the pressure derivative is the same but the response is delayed.

II.2 Flow of non-Newtonian fluids through homogeneous reservoirs

Ikoku et al. (1979) proposed a model to characterize homogeneous reservoirs where a non-Newtonian fluid is flowing. They combined the motion expression proposed by Christopher et al. (1965) for non-Newtonian fluids and the continuity equation. The resulting model is defined by:

$$\frac{\partial^2 p}{\partial r^2} + \frac{n}{r}\frac{\partial p}{\partial r} = G\, r^{1-n}\, \frac{\partial p}{\partial t}, \quad \text{..... (II.9)}$$

where *apparent hydraulic diffusivity coefficient* is:

$$G = \frac{n\,\phi\, c_t\, \mu_{eff}}{k}\left[\frac{2\pi h}{q}\right]^{1-n}, \quad \text{..... (II.10)}$$

The dimensionless form of Eq. II.9 is given as:

$$\frac{\partial^2 p_{DNN}}{\partial r_D^2} + \frac{n}{r_w^2}\frac{\partial p_{DNN}}{\partial r_D} = r_D^{1-n}\,\frac{\partial p_{DNN}}{\partial t_{DNN}}\,, \quad \text{..... (II.11)}$$

The general solution of Eq. II.11 assuming uniform pressure distribution, constant flowrate and infinite acting reservoir in the Laplace domain is defined by:

$$\overline{p}_{DNN}\ (r_D, u) = \frac{r_D^{\frac{1-n}{2}}\ K_{\frac{1-n}{3-n}}\left[r_D^{\frac{3-n}{2}}\ \frac{2}{3-n}\sqrt{u}\right]}{u^{\frac{3}{2}} K_{\frac{2}{3-n}}\left[\frac{2}{3-n}\sqrt{u}\right]}\,, \quad \text{..... (II.12)}$$

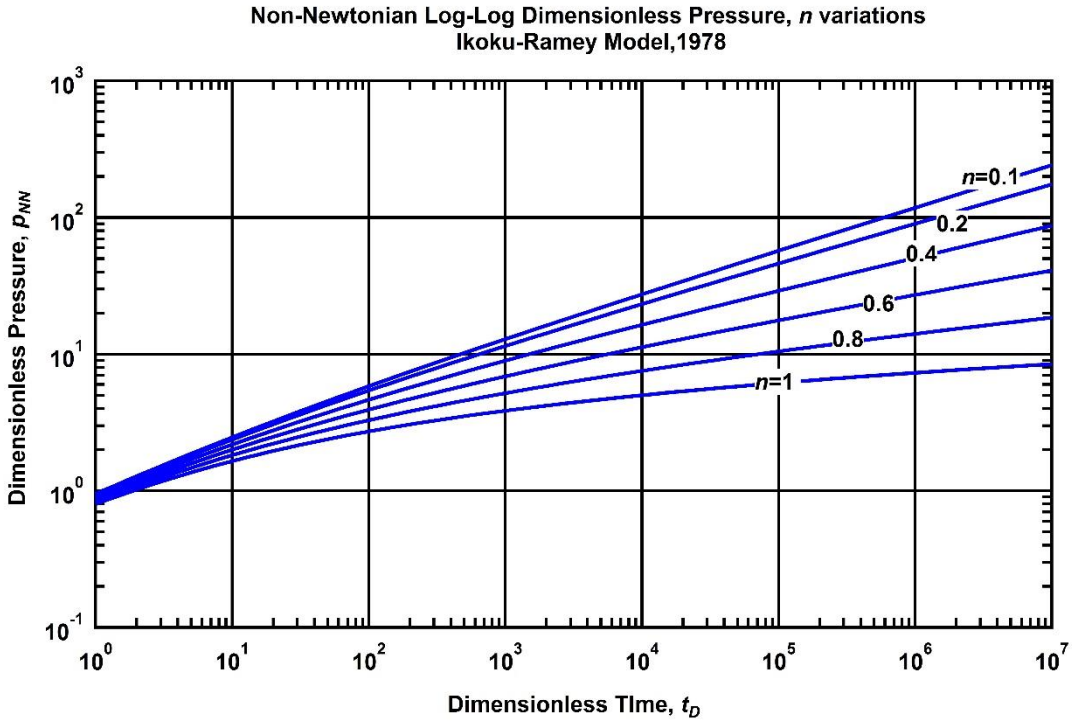

Fig. 12 ─ Dimensionless pressure vs dimensionless time for pseudoplastic non-Newtonian fluids in an infinite acting reservoir

Fig. 12 shows the impact of the flow behavior index for the dimensionless pressure response. The impact in semi log scale is shown in **Fig. 13**.

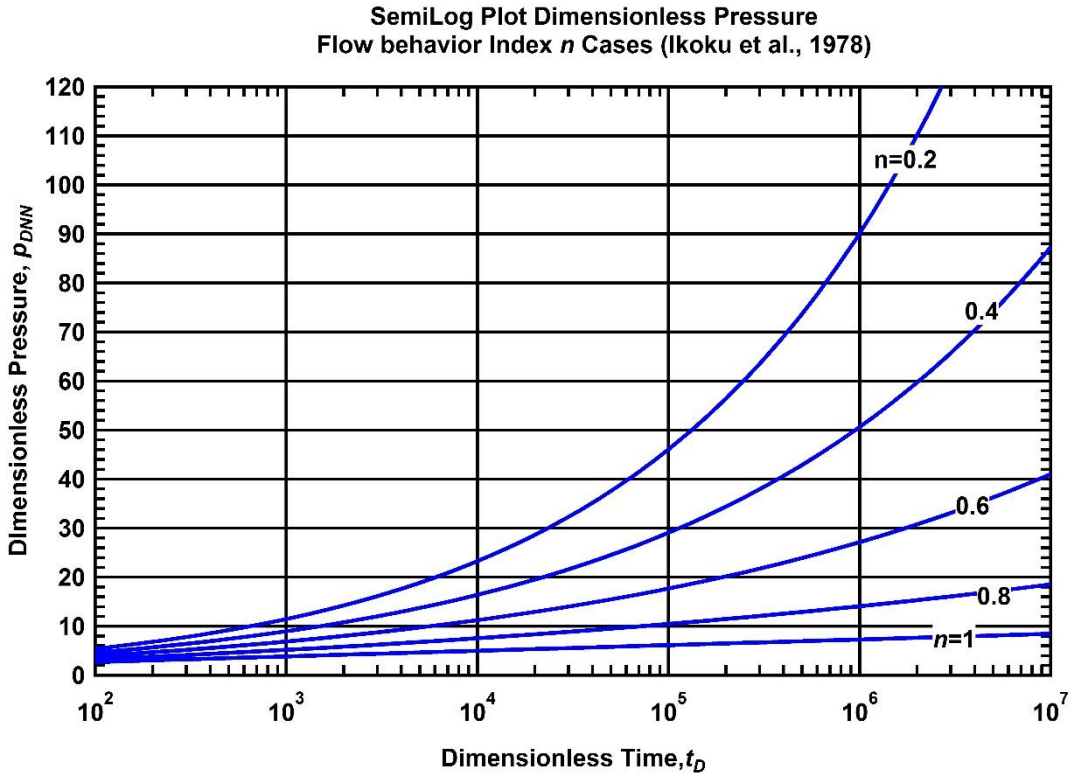

Fig. 13 ─ Semi-log plot non-Newtonian cases

II.3 Flow of non-Newtonian fluids within a double porosity reservoir with pseudosteady-state interporosity transfer and Newtonian interaction between media

After Ikoku et al. (1979) some efforts have been made in order to model the flow of non-Newtonian fluids within a double porosity reservoir. Escobar et al. (2011), introduced the pseudosteady-state interporosity transfer function for double porosity systems, into the non-Newtonian radial diffusivity model for homogeneous reservoir. The proposed equation is defined by:

$$\bar{p}_{DNN}(u) = \frac{K_{\frac{1-n}{3-n}}\left[\frac{2}{3-n}\sqrt{uf(u)}\right]}{u\left[\sqrt{uf(u)}K_{\frac{2}{3-n}}\left[\frac{2}{3-n}\sqrt{uf(u)}\right]\right]}, \quad \text{(II.13)}$$

where the interporosity flow function is exactly the same defined previously by Warren et al. (1963):

$$f(u) = \frac{u(1-\omega)\omega + \lambda}{u(1-\omega) + \lambda}. \quad \text{(II.14)}$$

Fig. 14 shows the response of the pressure derivative function for different values of w, according to the model developed by Escobar et al. (2011).

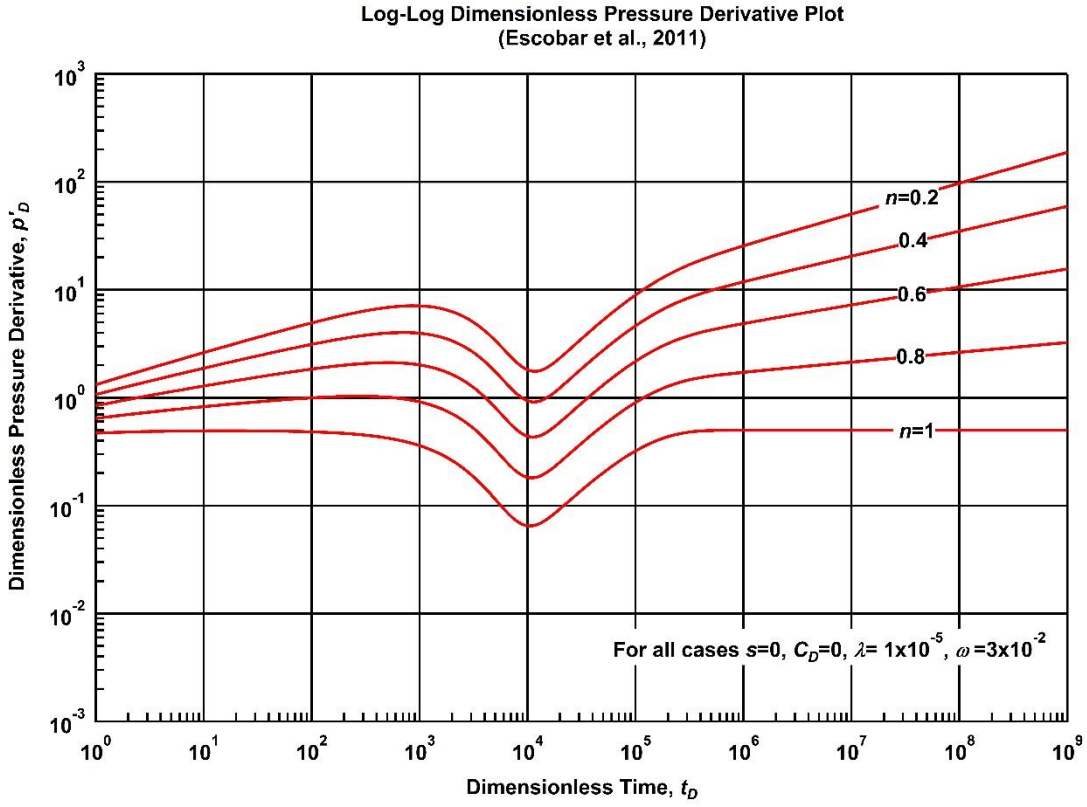

Fig. 14 ─ Log-log dimensionless derivative pressure (Escobar et al., 2011)

II.4 Flow of non-Newtonian fluids within a double porosity reservoir with transient interporosity transfer and Newtonian interaction between media

Olarewaju (1992) included the non-Newtonian effect in the fracture network of the transient interporosity transfer model. The equation proposed is defined by:

$$\frac{\partial^2 p}{\partial r^2} + \frac{n}{r_D}\frac{\partial p}{\partial r} = G\, r^{1-n}\,\frac{\partial p}{\partial t} - n\, A_{fm}\left[\frac{k_m}{k_f}\right]^{\frac{1}{n}} \int_0^t \frac{\partial \Delta p}{\partial \tau}(\tau)\nabla.\Delta p_m(t-\tau)\,d\tau \quad \text{, ... (II.15)}$$

whose dimensionless form is:

$$\frac{\partial^2 p_{fD}}{\partial r_D{}^2} + \frac{n}{r_D}\frac{\partial p_{fD}}{\partial r_D} - n\, r_D^{1-n}\left[\omega\frac{\partial p_{fD}}{\partial t_D} - (1-\omega)\,A_{fD}\int_0^t \frac{\partial p_{fD}}{\partial \tau}(\tau).F_D(\lambda, t_D - 1)d\tau\right] = 0 \text{ , ...} \quad \text{(II.16)}$$

and its general solution in the Laplace domain is given as:

$$\overline{p}_{wD}(u) = \frac{K_{\frac{1-n}{3-n}}\left[\frac{2}{3-n}\sqrt{u\,h(u)}\right]}{u\left[\sqrt{u\,h(u)}\,K_{\frac{2}{3-n}}\left[\frac{2}{3-n}\sqrt{u\,h(u)}\right]\right]}, \quad \text{(II.17)}$$

where the interporosity transfer function is:

$$h(u) = \omega + \left[\frac{\lambda(1-\omega)}{3u}\right]^{\frac{1}{2}}\tanh\left[\frac{3(1-\omega)}{\lambda}\right]^{\frac{1}{2}}. \quad \text{(II.18)}$$

Fig. 15 and **Fig. 16** show the log-log plot of the dimensionless pressure and dimensionless pressure derivative, respectively, for different values of the flow behavior index taking into account wellbore storage effects through a double porosity reservoir.

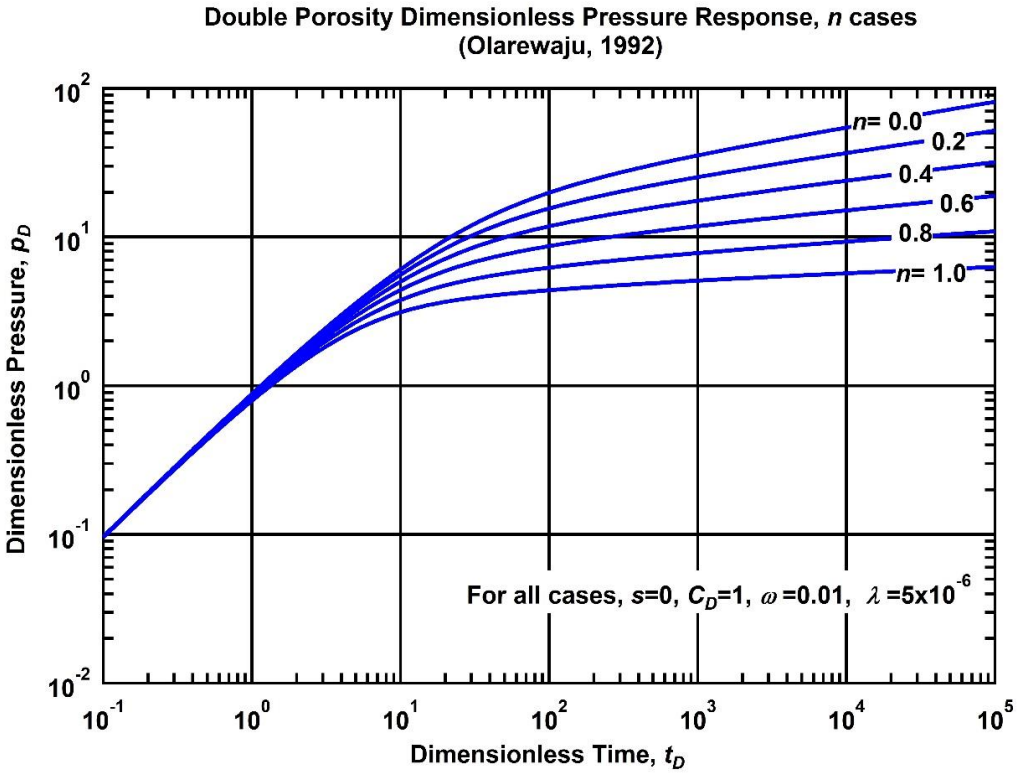

Fig. 15 ─ Dimensionless pressure, *n* selected cases (Olarewaju, 1992)

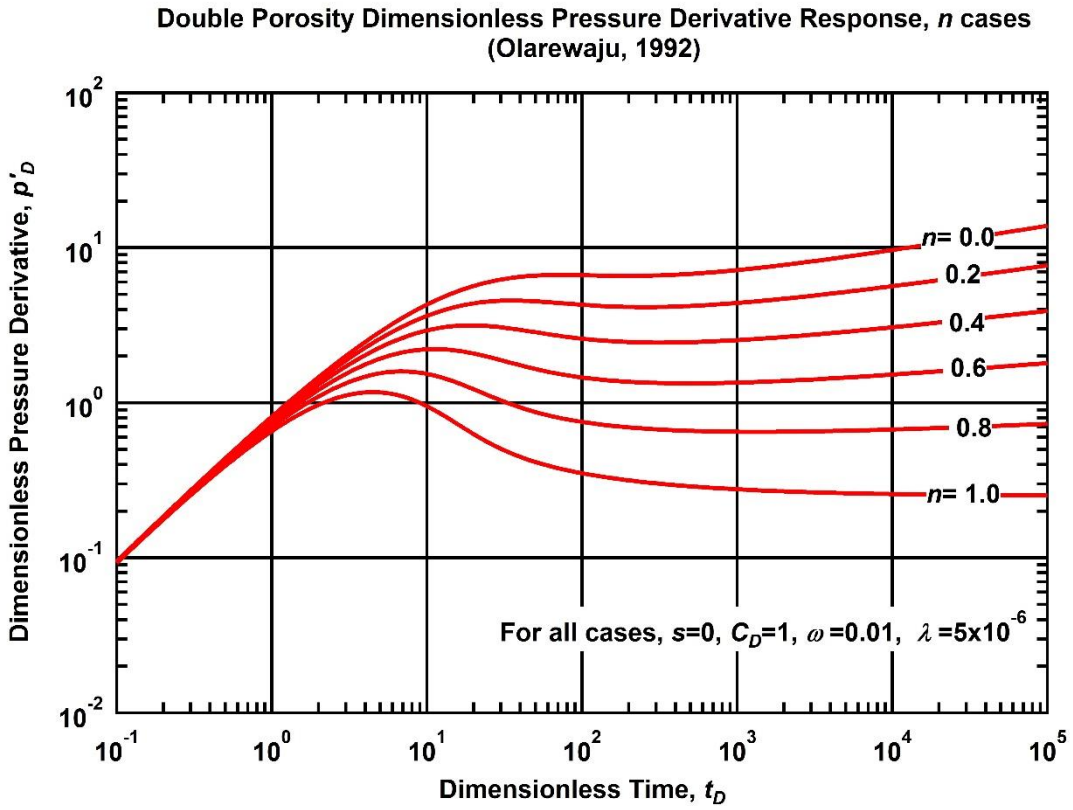

Fig. 16 ─ Dimensionless pressure derivative, *n* selected cases (Olarewaju, 1992)

Other relevant works related to the flow of non-Newtonian fluids in reservoirs are the ones published by Vongvuthipornchai et al. (1987), Liu Ci-qun (1988) and Valdes-Perez et al., (2013).

CHAPTER III

PROPOSED MODEL

For the proposed model, a description of fluid flow through porous media may be obtained from the following physical principles:

- Law of Conservation of Mass.
- Transport Equation.
- Equation of State.

A conservation equation may be derived from the Law of Conservation of Mass which, in combination with the Transport Equation and the Equation of Sate yield a partial differential equation which represents the time-dependent flow through a given porous media. The proposed model describes the flow behavior of non-Newtonian fluids using a specialized interporosity transfer which considers "pseudosteady-state" conditions. The detailed derivation of the proposed model is found in **Appendix C**.

III.1 Assumptions

The following specific assumptions are made in this work:

- A vertical well penetrates the entire thickness of the reservoir.
- The reservoir thickness is uniform (constant).
- The matrix blocks are in a systematic array of identical rectangular parallelepipeds.
- The matrix blocks are homogeneous and isotropic.
- The matrix blocks have a constant porosity (ϕ_m).
- The fracture network is array as an orthogonal system of continuous and uniform fractures.
- The fracture porosity (ϕ_f) is unique to the fracture system (*i.e.*, is constant)
- The double porosity media is considered to be homogeneously distributed.
- Flow to the wellbore occurs only through the fracture network.
- Flow occurs only between the matrix blocks and fracture network (no flow between matrix blocks).
- The reservoir (matrix) and fracture permeabilities are constant.
- The system contains a "slightly compressible" fluid.
- The effects of gravity are negligible.
- The pressure gradients are small.
- Non-Newtonian fluids obey the Oastwald de Waele power law relationship over the flow regime of interest.
- The fluid is considered to be pseudoplastic, which means that it is non-time dependent and the flow behavior index values are from 0 to 1, being 1 the Newtonian fluid. .

An scheme of the proposed model is shown in **Fig. 17**

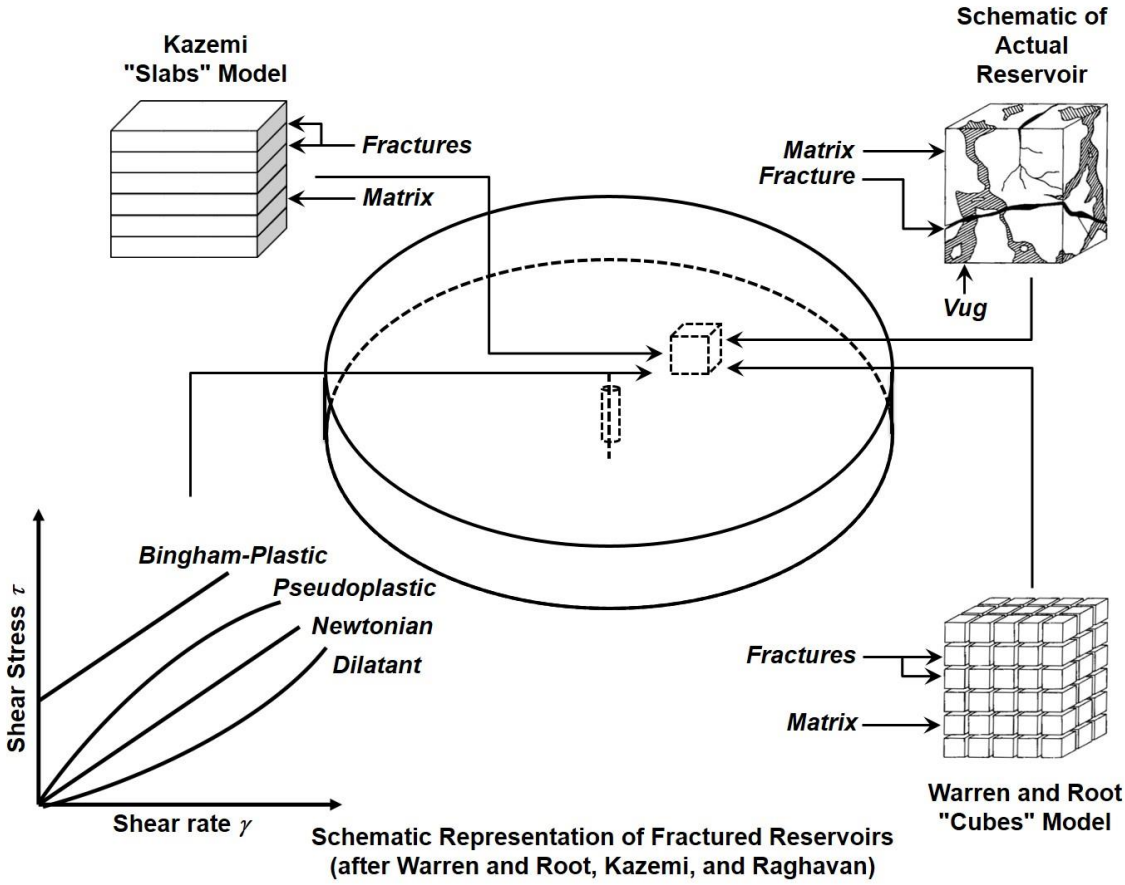

Fig. 17 ─ Schematic representation of the proposed model

III.2 Partial differential equation

The proposed model is a double porosity medium and takes into account two networks: the fracture system, which is the main flow path, and the matrix system, which is the source term. Combining the physical principles and following the assumptions that were established previously, the partial differential equation for the double porosity medium is defined by:

$$\frac{\partial^2 p_f}{\partial r^2} + \frac{n}{r}\left[\frac{\partial p_f}{\partial r}\right] = \frac{n\mu_{eff}}{k_f}\left[\frac{q}{2\pi hr}\right]^{n-1}\left[(\phi c_t)_f \frac{\partial p_f}{\partial t} + (\phi c_t)_m \frac{\partial p_m}{\partial t}\right], \quad \text{(III.1)}$$

and the equation which takes into account the source term adding fluids to the fracture is defined by:

$$\frac{\partial p_m}{\partial t} = \frac{\alpha}{(\phi c_t)_m}\frac{k_m}{\mu_{eff}}\left[\frac{q_m}{\Delta L^2}\right]^{1-n}(p_f - p_m) \quad \text{(III.2)}$$

In the process of deriving Eq. III.2, we proposed a linearization in order to obtain the pressure difference between the fracture and the matrix elevated to 1. The validation of Eq. III.1 and Eq. III.2 is that when the fluid behaves as a Newtonian fluid, both equations collapse and become the well-known Warren et al. model (1963). The detailed derivation can be found in Appendix C.

III.3 Dimensionless analysis

In order to transform Eq. III.1 and III.2 to a dimensionless form, following dimensionless variables have been stated.

Dimensionless pressure in the fracture network,

$$p_{fD} = \frac{(2\pi h)^n k_f}{q^n \mu_{eff} r_w^{1-n}} (p_i - p_f), \quad \text{(III.3)}$$

dimensionless pressure in the matrix,

$$p_{mD} = \frac{(2\pi h)^n k_f}{q^n \mu_{eff} r_w^{1-n}} (p_i - p_m), \quad \text{(III.4)}$$

dimensionless time,

$$t_D = \frac{q^{1-n} k_f}{n (\phi c_t)_t (2\pi h)^{1-n} \mu_{eff} r_w^{3-n}} t, \quad \text{(III.5)}$$

where the *total expansion* of the reservoir is;

$$(\phi c_t)_t = (\phi c_t)_f + (\phi c_t)_m, \quad \text{(III.6)}$$

and the dimensionless radius is

$$r_D = \frac{r}{r_w}. \quad \text{(III.7)}$$

If we substitute the dimensionless variables in Eq. III.1 and Eq. III.2, the dimensionless form of the proposed model is defined, respectively, by;

$$\frac{\partial^2 p_{fD}}{\partial r_D^2} + \frac{n}{r_D} \frac{\partial p_{fD}}{\partial r_D} = r_D^{1-n} \left[\omega \frac{\partial p_{fD}}{\partial t_D} + (1-\omega) \frac{\partial p_{mD}}{\partial t_D} \right], \quad \text{(III.8)}$$

where the *storativity ratio* is defined as;

$$\omega = \frac{(\phi c_t)_f}{(\phi c_t)_t} . \quad \text{(III.9)}$$

For the source term the dimensionless form is defined by;

$$\frac{\partial p_{Dm}}{\partial t_D} = \frac{n\,\lambda}{(1-\omega)} D^{1-n} (p_{fD} - p_{mD}) , \quad \text{(III.10)}$$

where the *interface interporosity coefficient* λ is

$$\lambda = \alpha \frac{k_m}{k_f} r_w^2 , \quad \text{(III.11)}$$

and the *dimensionless matrix contribution, D,* defined as;

$$D = \frac{q_m}{q} \frac{2\pi h r_w}{\Delta L^2} , \quad \text{(III.12)}$$

The dimensionless form of the source term (Eq. III.10) differs from the dimensionless form of the conventional source term because Eq. III.10 takes non-Newtonian behavior into account. The dimensionless matrix contribution *D,* describes the non-Newtonian behavior through the matrix and functions as a linearization to obtain a partial differential equation.

CHAPTER IV

SOLUTIONS AND RESULTS

This chapter summarizes the solutions of the proposed model using the Laplace transform definition. Initial and boundary conditions are defined to obtain the specific solution for each case. Plots presented show the non-Newtonian behavior in a double porosity reservoir.

IV.1 General solution

The general solution obtained in the dimensionless form and the Laplace domain is defined by:

$$\bar{p}_{fD}(r_D, u) = r_D^{\frac{1-n}{2}} \left[C_1 I_\nu (r_D^{\varepsilon} h(u)) + C_2 K_\nu (r_D^{\varepsilon} h(u)) \right], \quad \text{(IV.1)}$$

where u is the Laplace variable and the variables ν ε and h, are defined as:

$$\nu = \frac{1-n}{3-n}, \quad \text{(IV.2)}$$

$$\varepsilon = \frac{3-n}{2}, \quad \text{(IV.3)}$$

$$h(u) = \frac{2\sqrt{u\, g(u)}}{3-n}, \quad \text{(IV.4)}$$

and the *interporosity flow function, g* is defined by:

$$g(u) = \frac{u(1-\omega)\omega + n\lambda D^{1-n}}{u(1-\omega) + n\lambda D^{1-n}} \quad \text{(IV.5)}$$

The constants C_1 and C_2 will depend on the inner and outer boundary conditions, which are defined below.

IV.2 Initial and boundary conditions

Given the general solution in the Laplace domain, initial and boundary conditions are given in the same domain. For all the cases, the Initial Condition is:

$$\bar{p}_{fD}(r_D, u = 0) = 0, \quad \text{(IV.6)}$$

the reservoir has uniform pressure distribution.

Similar to the initial condition, the inner boundary condition will be the same for all the cases defined by:

$$\left[r_D \frac{d\,\bar{p}_{fD}(r_D,u)}{dr_D} \right]_{r_D=1} = -\frac{1}{u}, \quad \text{.....(IV.7)}$$

the flowrate is constant at any time.

Three outer boundary conditions are established: Infinite Acting Reservoir (no outer boundaries felt), Closed Reservoir (no flux at the outer boundary) and Constant Pressure (the bottomhole pressure is constant at any time). Infinite Acting Reservoir is defined by:

$$\lim_{r_D \to \infty} \bar{p}_{Df}(r_D,u) = 0 \quad \text{.....(IV.8)}$$

Closed reservoir is defined by:

$$\left. \frac{d\,\bar{p}_{fD}(r_D,u)}{dr_D} \right|_{r_D=r_{eD}} = 0, \quad \text{.....(IV.9)}$$

where r_{eD} is the dimensionless external radius drainage.

Constant Pressure at the outer boundary is defined by;

$$\bar{p}_{fD}(r_D = r_{eD},u) = 0 \quad \text{.....(IV.10)}$$

IV.3 Solution for infinite acting reservoir and constant flowrate

If we use Eq. IV.7 and Eq. IV.8, the constants C_1 and C_2 are:

$$C_1 = 0, \quad \text{.....(IV.11)}$$

and

$$C_2 = \frac{1}{u} \frac{1}{\sqrt{u\,g(u)}\,K_{\frac{2}{3-n}}\left[\frac{2\sqrt{ug(u)}}{3-n}\right]}, \quad \text{.....(IV.12)}$$

Therefore the solution in the Laplace domain for an infinite acting reservoir with constant flowrate at the well is defined by;

$$\bar{p}_{fD}(r_D,u)=\frac{r_D^{\frac{1-n}{2}}K_{\frac{1-n}{3-n}}\left[r_D^{\frac{3-n}{2}}\frac{2\sqrt{ug(u)}}{3-n}\right]}{u\sqrt{ug(u)}K_{\frac{2}{3-n}}\left[\frac{2\sqrt{ug(u)}}{3-n}\right]}, \quad \text{.....(IV.13)}$$

To invert eq. IV.13 into the real domain, the Gaver-Stehfest numerical inversion is used because the equation cannot be solved directly from tables. Next are presented plots describing the behavior for selected variables in an Infinite Acting Reservoir.

The first variable is the dimensionless matrix contribution, *D*, and is evaluated for several values of the flow behavior index, going from *n*=0.10 to *n*=1. **Fig. 18** through **Fig**.**22** depict this variation in a Log-log plot for dimensionless pressure and dimensionless pressure derivative. The interporosity flow coefficient λ = 5x10^{-6} and the storativity ratio ω=1x10^{-3}.were kept constant Wellbore storage and skin effects are not considered yet.

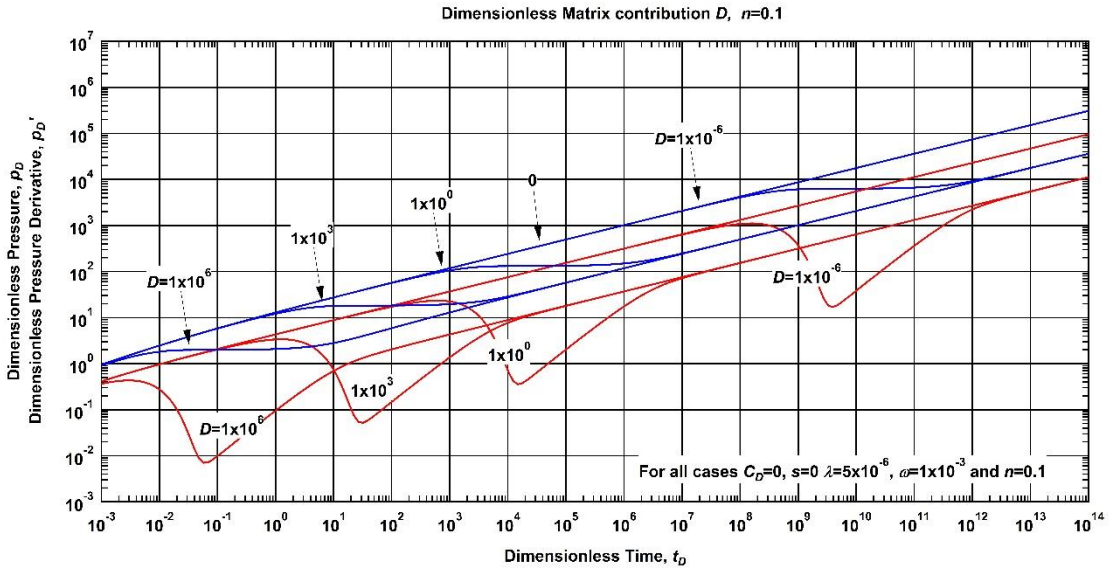

Fig. 18 ─ Log-log plot for selected values of dimensionless matrix contribution *D*, *n*=0.1

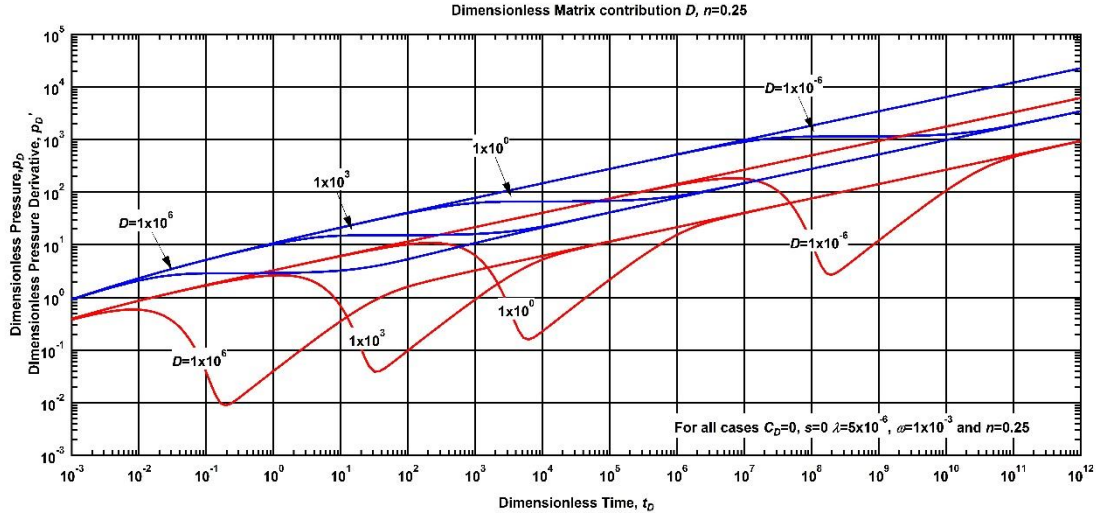

Fig. 19 ─ Log-log plot for selected values of dimensionless matrix contribution *D*, *n*=0.25

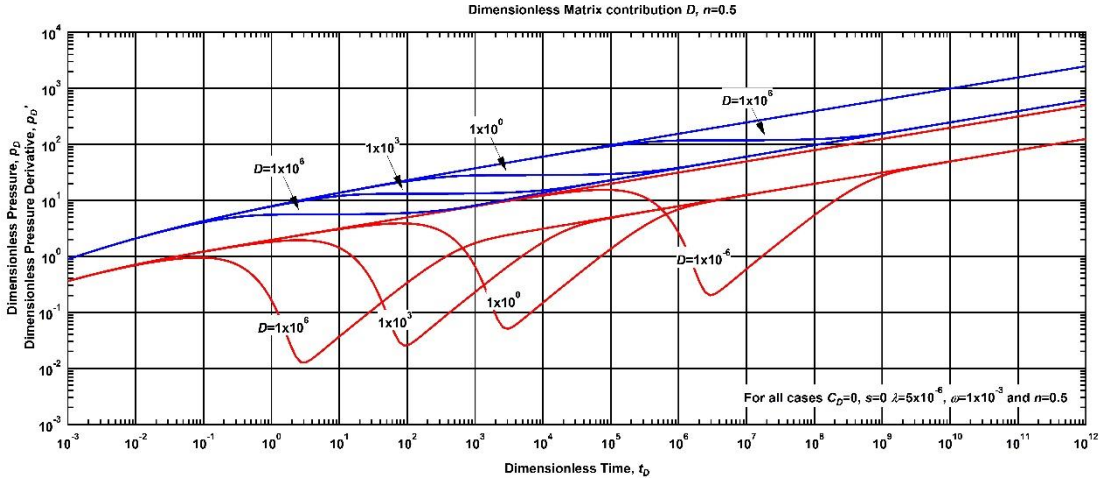

Fig. 20 ─ Log-log plot for selected values of dimensionless matrix contribution *D*, *n*=0.50

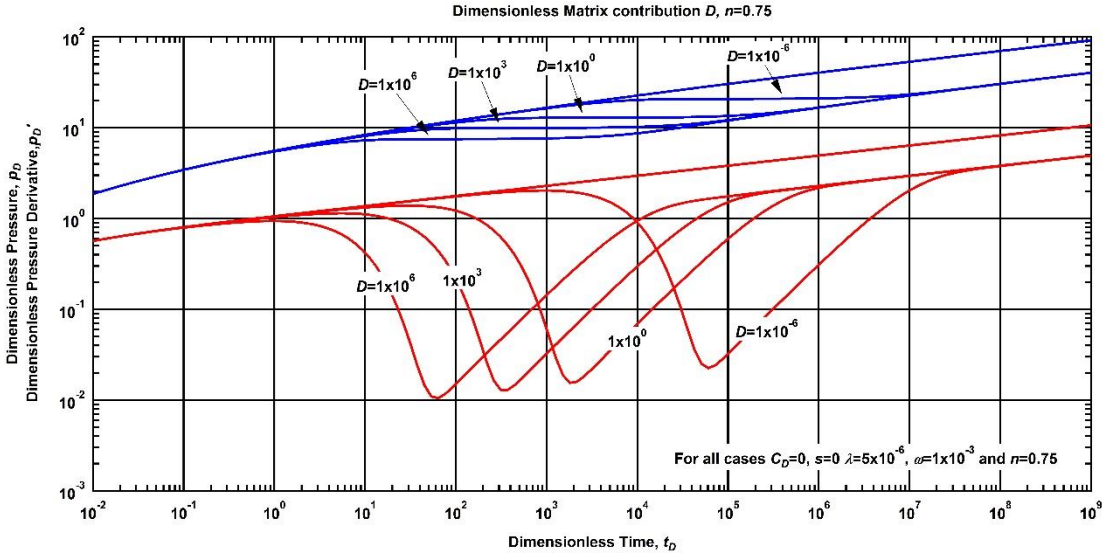

Fig. 21 ─ Log-log plot for selected values of dimensionless matrix contribution *D*, *n*=0.75

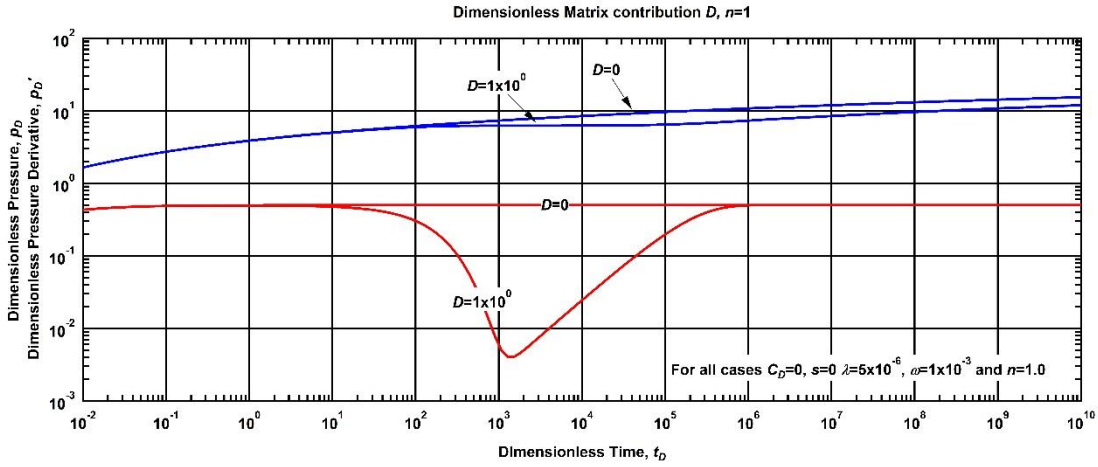

Fig. 22 ─ Log-log plot for selected values of dimensionless matrix contribution *D*, *n*=1.0

From **Fig. 18** to **Fig. 22** the plots in time may be divided as early, middle and late time. Early time is when the fracture system is expanding; middle time is when the interporosity transfer under pseudosteady-state conditions between the matrix and fracture is underway (valley); the late time is when the total system is being expanded, which translates as the sum of expansions between the matrix and the fracture. The variations went from $1x10^{-6}$ to 10^{6}. The dimensionless matrix contribution is defined by a ratios of flowrates (matrix-total) and an area ratio (wellbore-matrix blocks). Here, the numbers are simply variations, and the physical meaning is based on these ratios. A low number means that we have a total flowrate higher than

the matrix, and when we have a greater number physically, it may be explained as we have a wellbore area higher than a matrix block.

The 'valley' is defined by the interporosity flow coefficient λ and the storativity ratio ω. However, the impact on the response or delay of the valley also depends on the dimensionless matrix contribution, which is highly related to the flow behavior index. As we can see in Eq. IV.5, D is also related to the interporosity flow coefficient. For that reason, when the value approaches to 0, the behavior of the plot relies as a homogeneous reservoir with non-Newtonian or Newtonian behavior, whatever the case may be. In **Fig. 21**, two variations are shown; when D=1 the model behaves just as the Warren et al. model (1963), and when D=0 the model behaves as a homogenous reservoir.

The next variation is the interporosity flow coefficient λ, which goes from $1x10^{-9}$ to $1x10^{0}$ for selected cases of the flow behavior index. From **Fig. 23** to **Fig.27** depict these variations in a Log-log plot for the dimensionless pressure and the dimensionless pressure derivative. The dimensionless matrix contribution D=$1x10^{-4}$ and the storativity ratio ω=$1x10^{-3}$ were kept constant. Wellbore storage and skin effects are not considered yet.

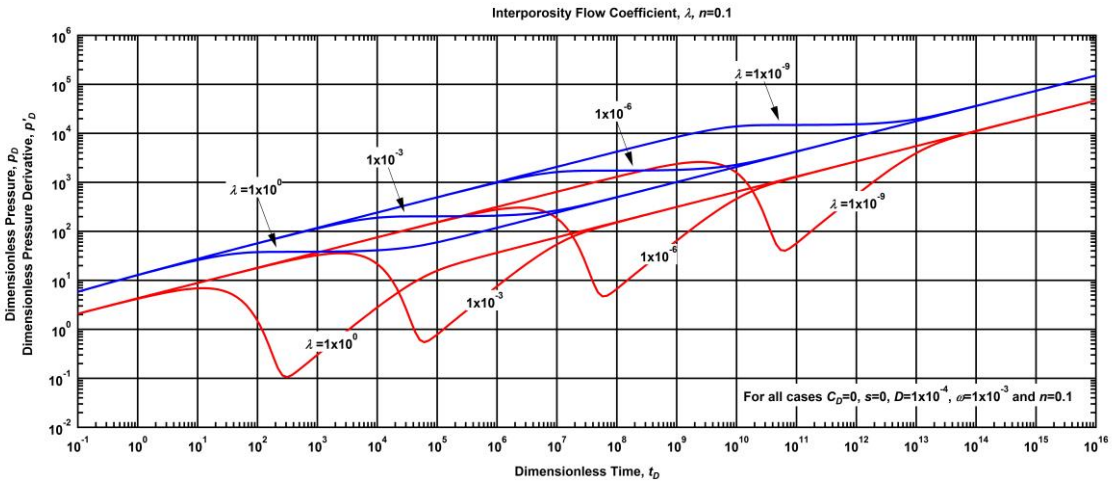

Fig. 23 ─ Log-log plot for selected values of interporosity flow coefficient λ, n=0.10

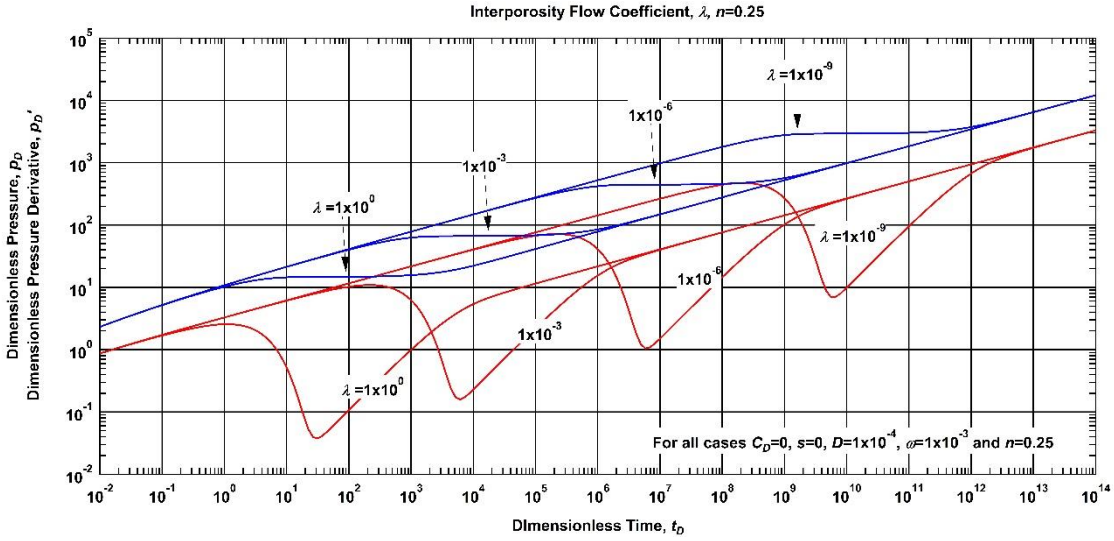

Fig. 24 ─ Log-log plot for selected values of interporosity flow coefficient λ, n=0.25

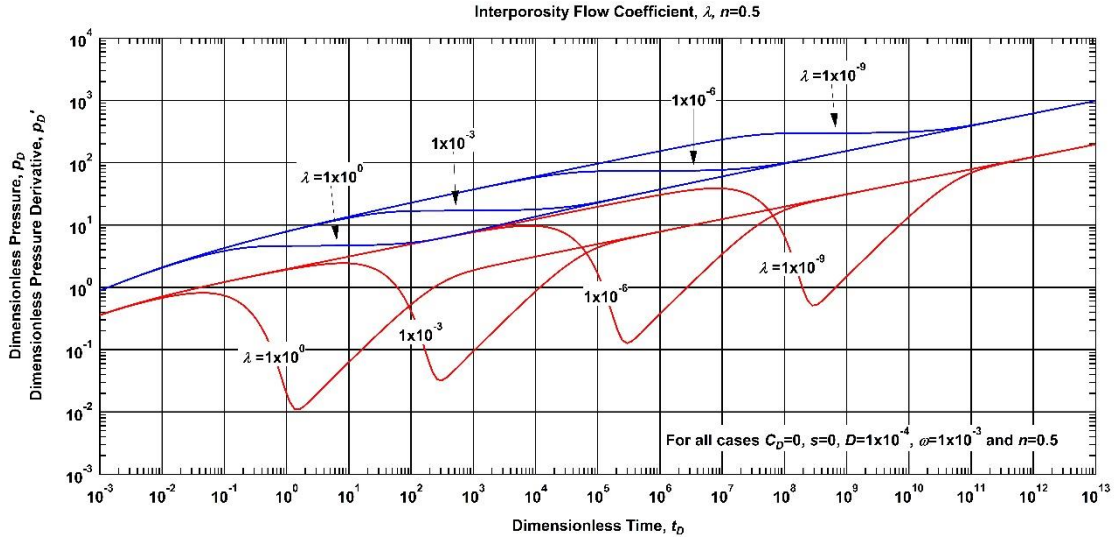

Fig. 25 ─ Log-log plot for selected values of interporosity flow coefficient λ, n=0.50

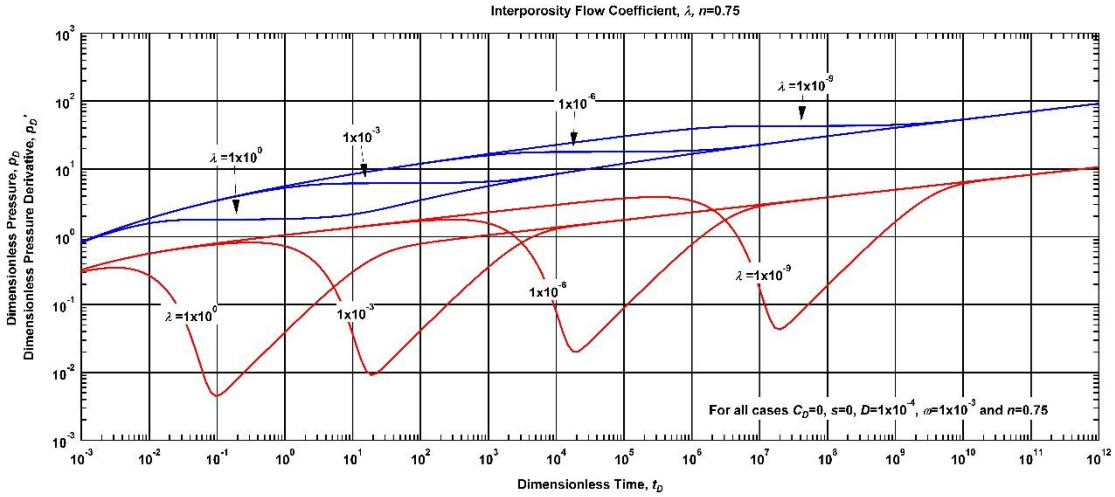

Fig. 26 ─ Log-log plot for selected values of interporosity flow coefficient λ, n=0.75

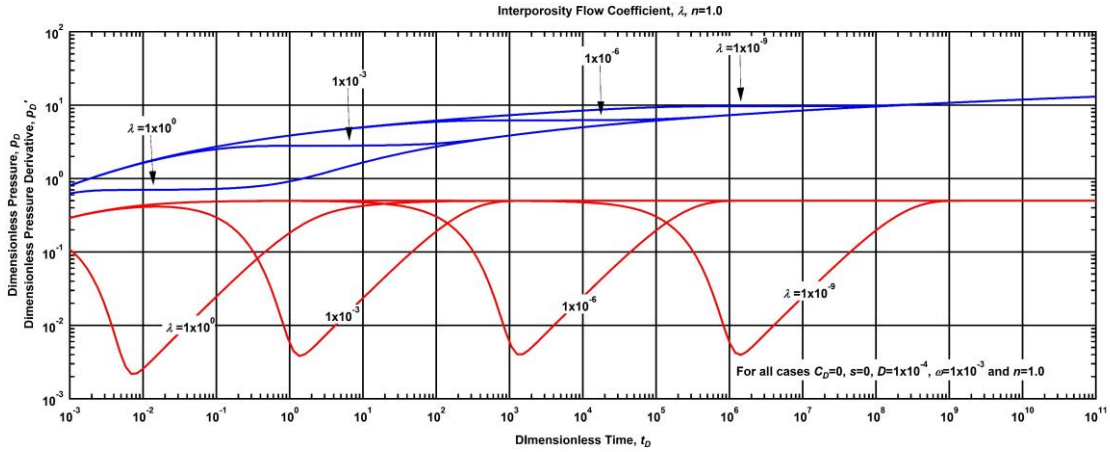

Fig. 27 ─ Log-log plot for selected values of interporosity flow coefficient λ, n=1.0

From **Fig. 23** to **Fig. 27** similar to the dimensionless matrix contribution, the impact of the interporosity flow coefficient λ is dependent in how fast or delayed the response of the interporosity transfer is. This is due to the permeability ratio to the matrix system and the fracture system. It should be noted that the interporosity flow coefficient is exactly the same as that derived by Warren et al (1963).

The next variation is the storativity ratio ω, which goes from $1x10^{-3}$ to $1x10^{0}$ for selected cases of the flow behavior index. From **Fig. 28** to **Fig.32** depict these variations in a Log-log plot for the dimensionless pressure and the dimensionless pressure derivative. The dimensionless matrix contribution D=$1x10^{-4}$ and

the interporosity flow coefficient λ=5x10^{-6} were kept constant. Wellbore storage and skin effects are not considered yet.

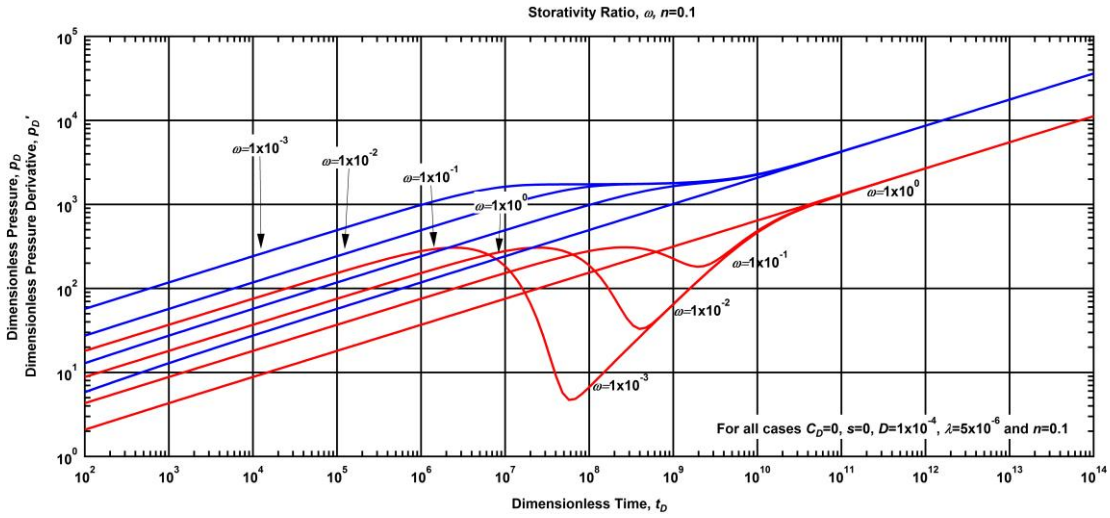

Fig. 28 ─ Log-log plot for selected values of storativity ratio ω, n=0.1

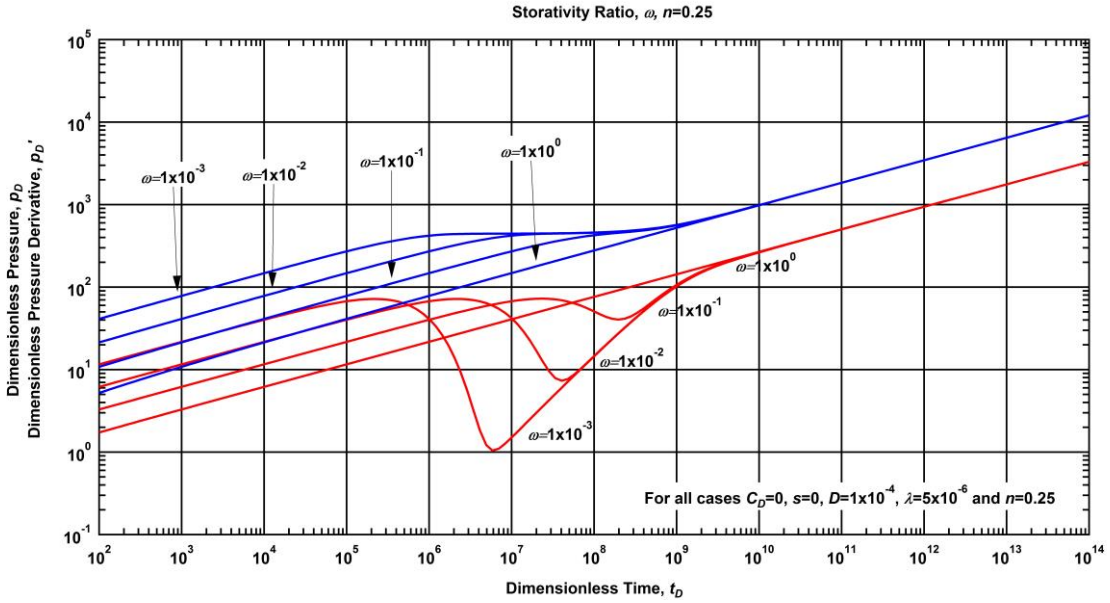

Fig. 29 ─ Log-log plot for selected values of storativity ratio ω, n=0.25

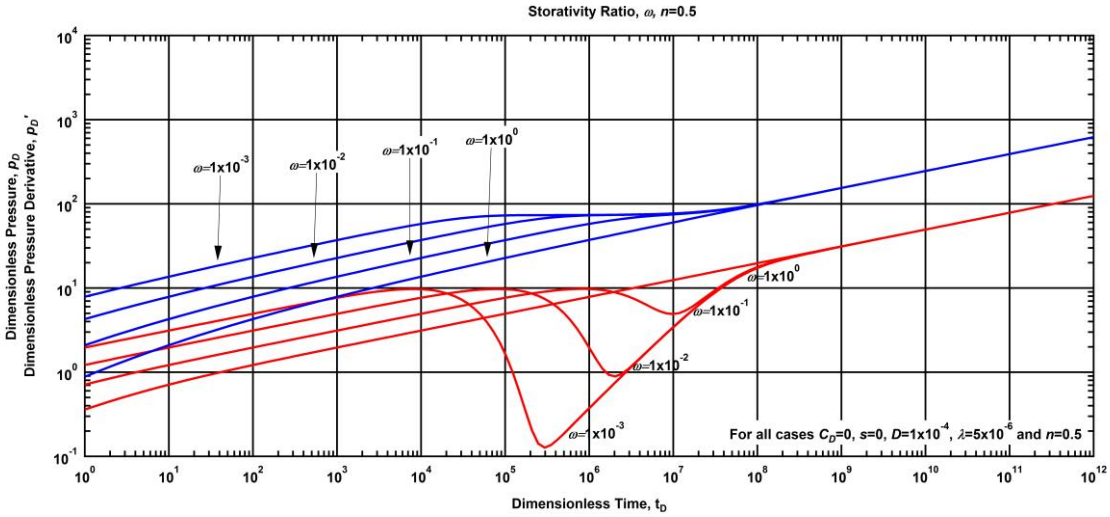

Fig. 30 ─ Log-log plot for selected values of storativity ratio ω, n=0.50

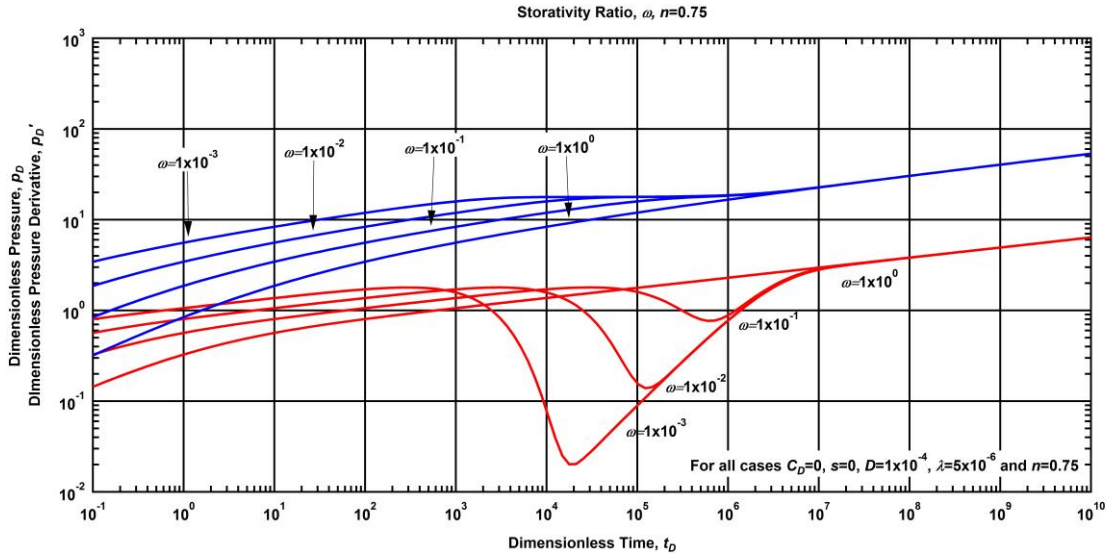

Fig. 31 ─ Log-log plot for selected values of storativity ratio ω, n=0.75

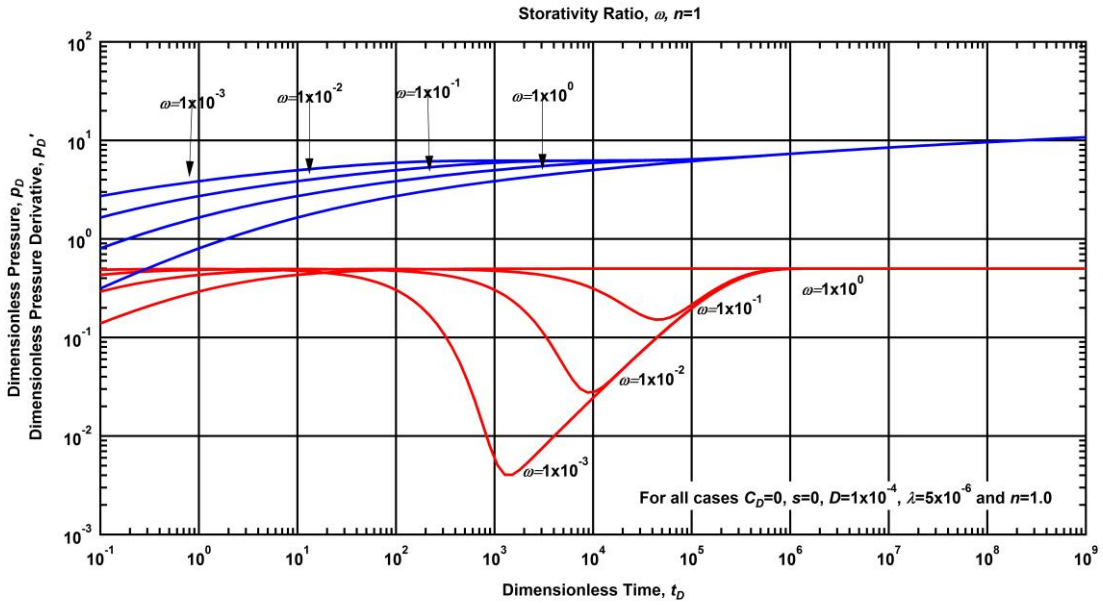

Fig. 32 ─ Log-log plot for selected values of storativity ratio ω, n=1.0

The storativity ratio affects the interporosity transfer. The effect is shown in each log-log plot on the size of the "valley". The size of the "valley" is due to the storativity ratio, which physical meaning is the ratio to the expansion of both systems, fracture and matrix. If the valley is relatively large, that means that the fracture system is small compared to the total system. When the valley is relatively small may be approaching a homogeneous reservoir. Note that this storativity ratio is exactly the same as the one derived by Warren et al

IV.4 Solution for closed reservoir and constant flowrate

If we use Eq. IV.7 and Eq. IV.9, the constants C_1 and C_2 in this particular case are:

$$C_1 = \frac{1}{u\,h(u)\,\varepsilon}\left[\frac{K_{\nu-1}(r_{eD}^{\varepsilon}\,h(u))}{K_{\nu-1}(h(u))\,I_{\nu-1}(h(u)r_D^{\varepsilon}) - K_{\nu-1}(h(u)\,r_D^{\varepsilon})\,I_{\nu-1}(h(u))}\right], \quad \text{.....(IV.14)}$$

and

$$C_2 = \frac{1}{u\,h(u)\,\varepsilon}\left[\frac{I_{\nu-1}(r_{eD}^{\varepsilon}\,h(u))}{K_{\nu-1}(h(u))\,I_{\nu-1}(h(u)r_D^{\varepsilon}) - K_{\nu-1}(h(u)\,r_D^{\varepsilon})\,I_{\nu-1}(h(u))}\right]. \quad \text{.....(IV.15)}$$

Therefore the solution in the Laplace domain for a closed reservoir with constant flowrate at the well is defined by;

$$\bar{p}_{fD}(r_D,u) = r_D^{\frac{1-n}{2}} \frac{1}{u\,h(u)\,\varepsilon}\left[\frac{K_{\nu-1}(r_{eD}^{\varepsilon}h(u))I_{\nu}(h(u)r_D^{\varepsilon}) + I_{\nu-1}(r_{eD}^{\varepsilon}h(u))K_{\nu}(h(u)r_D^{\varepsilon})}{K_{\nu-1}(h(u))\,I_{\nu-1}(h(u)r_D^{\varepsilon}) - K_{\nu-1}(h(u)\,r_D^{\varepsilon})\,I_{\nu-1}(h(u))}\right] \quad \text{.....(IV.16)}$$

In order to invert Eq.IV.16 into the real domain, the Gaver-Stehfest numerical inversion is used because the equation cannot be solved directly from tables. Plots describing the behavior for selected variables in the closed reservoir at the outer boundary case are presented next.

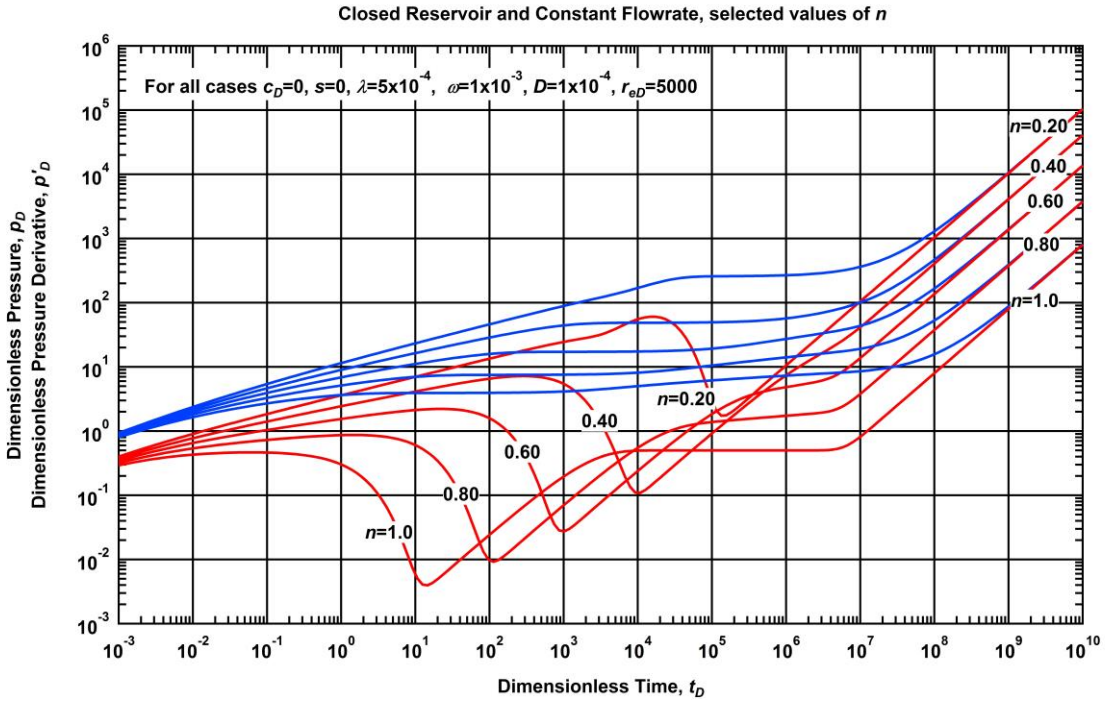

Fig. 33 – Closed reservoir and constant flowrate at the wellbore for selected values of *n*, r_{eD}=5000

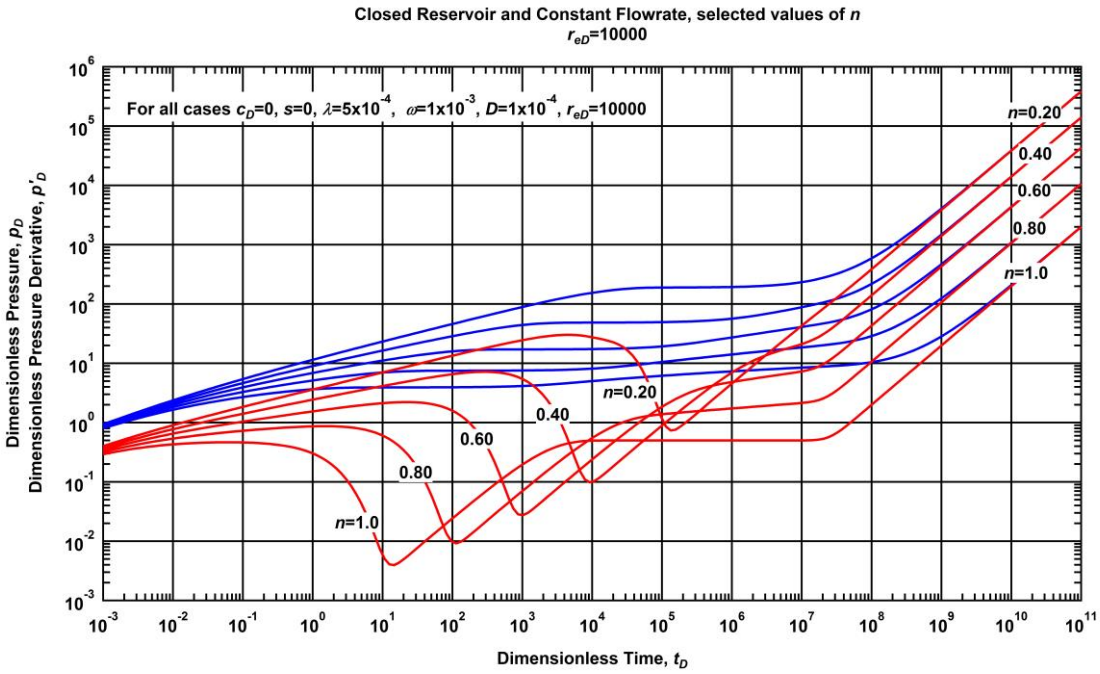

Fig. 34 ─Closed reservoir and constant flowrate at the wellbore for selected values of *n*, r_{eD}=10000

Fig. 33 and **Fig. 34** show the effect of a closed boundary at the outer boundary, and constant flowrate at the wellbore in a log-log plot where the external drainage radius r_{eD} is 5000 and 10000 respectively The interporosity flow coefficient λ = 5x10^{-4}, the storativity ratio ω=1x10^{-3}.and the dimensionless matrix contribution D=1x10^{-4} were kept constant Wellbore storage and skin effects are not considered yet.

IV.5 Solution for constant pressure at the outer boundary and constant flowrate

If we use Eq. IV.7 and Eq. IV.10, the constants C_1 and C_2 in this particular case are:

$$C_1 = -\frac{1}{uh(u)\,\varepsilon}\left[\frac{K_\nu(r_{eD}^{\varepsilon}h(u))}{K_\nu(r_{eD}^{\varepsilon}h(u))I_{\nu-1}(h(u)) + K_{\nu-1}(h(u))I_\nu(r_{eD}^{\varepsilon}h(u))}\right], \quad \text{(IV.17)}$$

and

$$C_2 = \frac{1}{uh(u)\,\varepsilon}\left[\frac{I_\nu(r_{eD}^{\varepsilon}h(u))}{K_\nu(r_{eD}^{\varepsilon}h(u))I_{\nu-1}(h(u)) + K_{\nu-1}(h(u))I_\nu(r_{eD}^{\varepsilon}h(u))}\right]. \quad \text{(IV.18)}$$

Therefore the solution in the Laplace domain for constant pressure at the outer boundary with constant flowrate at the well is defined by;

$$\bar{p}_{fD}(r_D,u) = r_D^{\frac{1-n}{2}} \frac{1}{u\,h(u)\,\varepsilon} \left[\frac{I_\nu(r_{eD}^{\varepsilon} h(u)) K_\nu(h(u) r_D^{\varepsilon}) - K_\nu(r_{eD}^{\varepsilon} h(u)) I_\nu(h(u) r_D^{\varepsilon})}{K_\nu(r_{eD}^{\varepsilon} h(u)) I_{\nu-1}(h(u)) + K_{\nu-1}(h(u)) I_\nu(r_{eD}^{\varepsilon} h(u))} \right] \quad \text{.....(IV.19)}$$

In order to invert Eq.IV.16 into the real domain, the Gaver-Stehfest numerical inversion is used because the equation cannot be solved directly from tables. The plots describing non-Newtonian flow behavior for selected variables of Constant Pressure at the outer boundary are presented next.

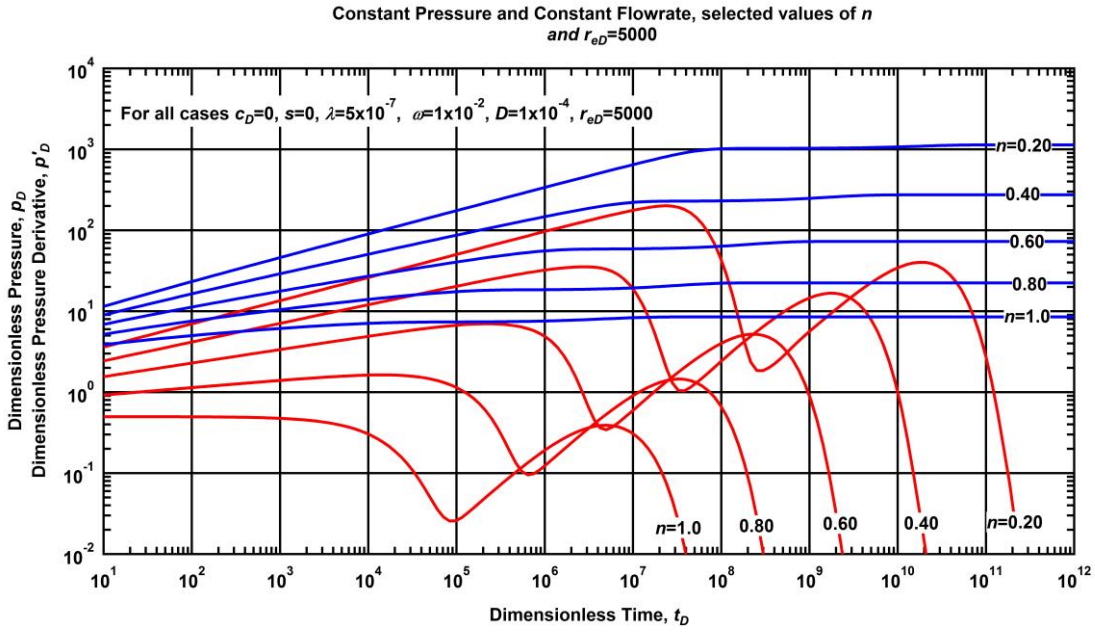

Fig. 35 ─ Constant pressure at the outer boundary and constant flowrate at the wellbore, r_{eD}=5000

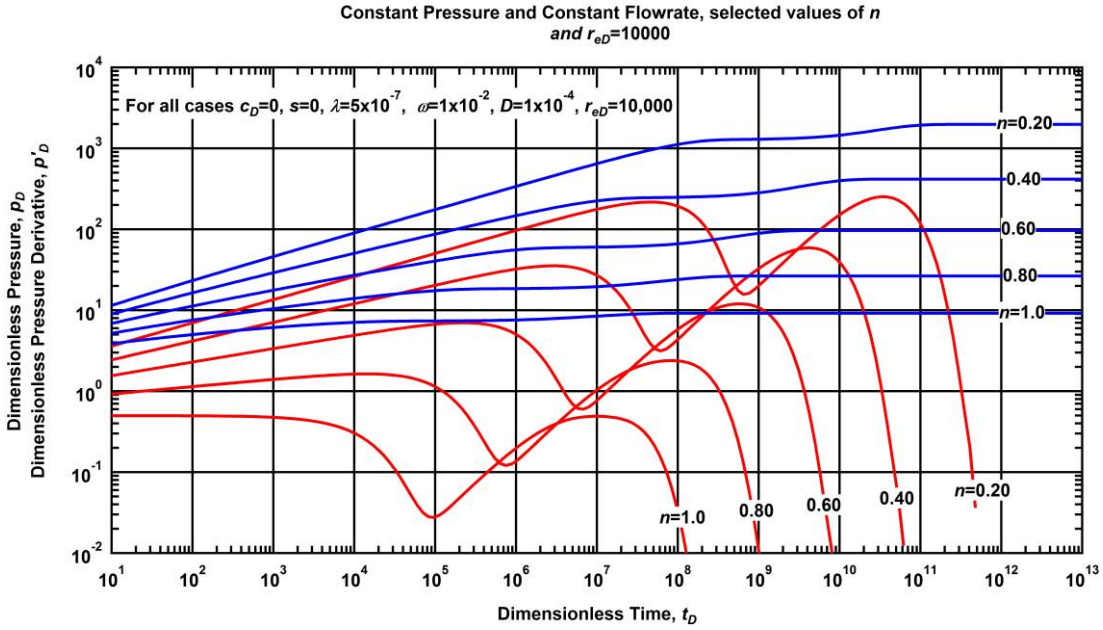

Fig. 36 ─ Constant pressure at the outer boundary and constant flowrate at the wellbore, r_{eD}=10000

Fig. 35 and **Fig. 36** show the effect of constant pressure at the outer boundary, and constant flowrate at the wellbore in a log-log plot where the external drainage radius r_{eD} is 5000 and 10000 respectively The interporosity flow coefficient λ = 5x10^{-7}, the storativity ratio ω=1x10^{-2}.and the dimensionless matrix contribution D=1x10^{-4} were kept constant wellbore storage and skin effects are not considered yet.

IV.6 Early and long time approximations from Laplace domain to real domain

In order to approach a suitable solution from the Laplace domain to the real domain at early times, the Laplace variable was approached to infinity. ($u \approx \infty$). Early approximations in real domain are presented next. The detailed derivation can be found in APPENDIX H

$$p_{fD}(t) \approx \frac{\Gamma\left[\frac{1-n}{3-n}\right]\left[\frac{1}{3-n}\right]^{\frac{n+1}{3-n}}(\omega)^{\frac{n-1}{3-n}}}{\Gamma\left[\frac{2}{3-n}\right]\Gamma\left[-\frac{2(n-2)}{3-n}\right]}(t_D)^{\frac{1-n}{3-n}}, \quad \text{(IV.20)}$$

and the derivative of Eq. IV.20 for well testing purposes is

$$t_D \frac{dp_{fD}(t)}{dt_D} \approx \frac{\Gamma\left[\frac{1-n}{3-n}\right]\left[\frac{1}{3-n}\right]^{\frac{n+1}{3-n}}(\omega)^{\frac{n-1}{3-n}}}{\Gamma\left[\frac{2}{3-n}\right]\Gamma\left[-\frac{2(n-2)}{3-n}\right]}\left[\frac{1-n}{3-n}\right](t_D)^{\frac{1-n}{3-n}} \quad \text{.....(IV.21)}$$

The early time approximation plots are shown in **Fig. 37** for the dimensionless pressure and **Fig. 38** for the dimensionless pressure derivative.

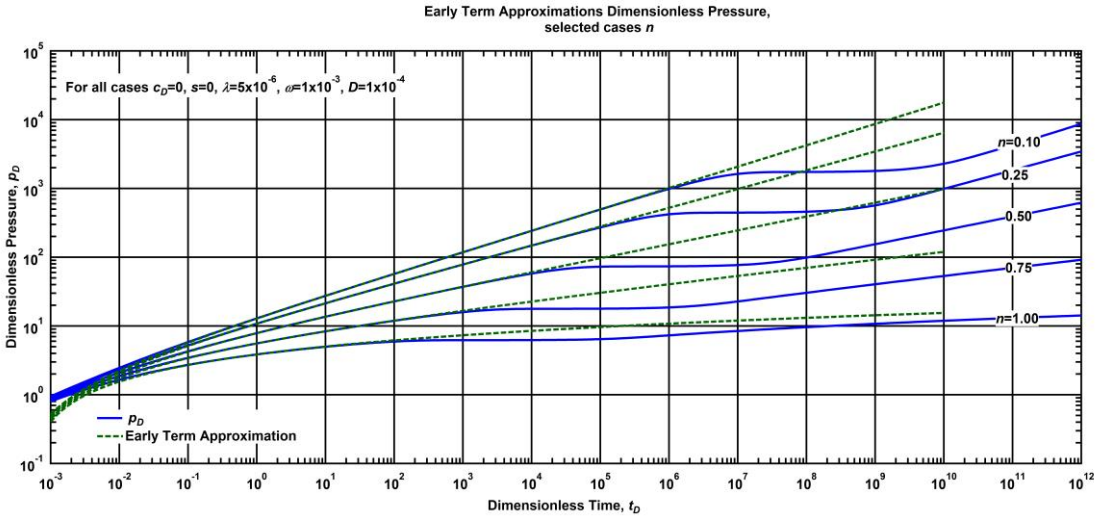

Fig. 37 ─ Early time approximations for dimensionless pressure, selected values of *n*

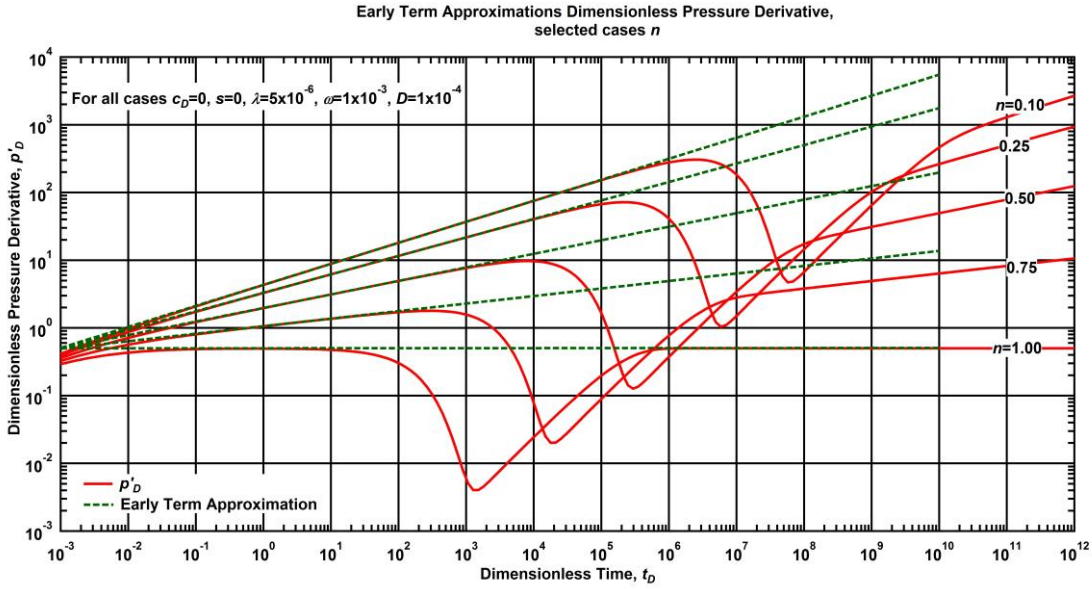

Fig. 38 ─ Early time approximations for dimensionless pressure derivative, selected values of *n*

For the long time approximation, the Laplace variable was approached to zero. ($u \approx 0$). Long approximations in real domain are presented next. The detailed derivation can be found in APPENDIX I

$$p_{Df}(t_D) \approx \frac{(3-n)^{\frac{2(1-n)}{3-n}}}{\Gamma\left[\frac{2}{3-n}\right](1-n)} t_D^{\frac{1-n}{3-n}}, \quad \text{(IV.22)}$$

and the derivative of Eq. IV.20 for well testing purposes is

$$t_D \frac{dp_{Df}(t_D)}{dt_D} = \frac{(3-n)^{\frac{-(1+n)}{3-n}}}{\Gamma\left[\frac{2}{3-n}\right]} t_D^{\frac{1-n}{3-n}}. \quad \text{(IV.23)}$$

The long time approximation plots for selected values of the flow behavior index *n* are shown in **Fig. 39** for the dimensionless pressure and **Fig. 40** for the dimensionless pressure derivative

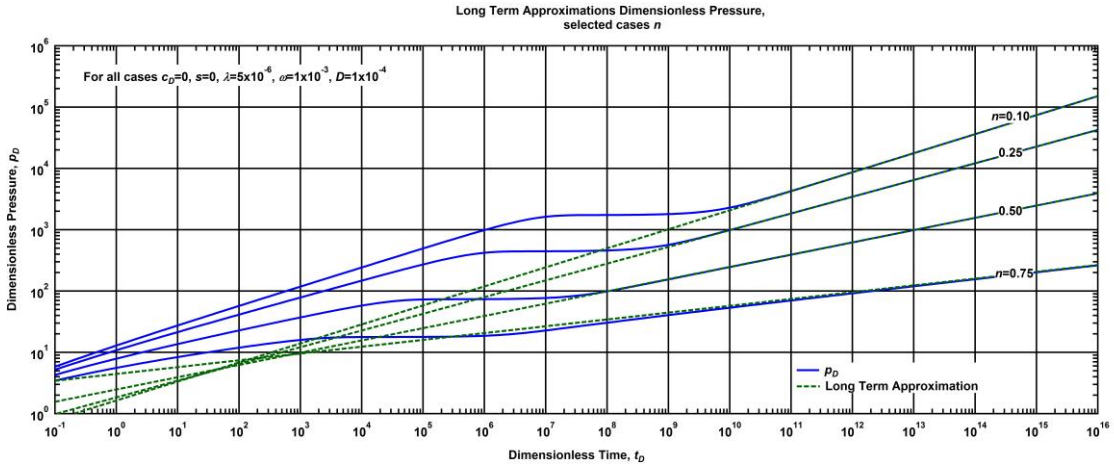

Fig. 39 ─ Long time approximations for dimensionless pressure, selected values of *n*

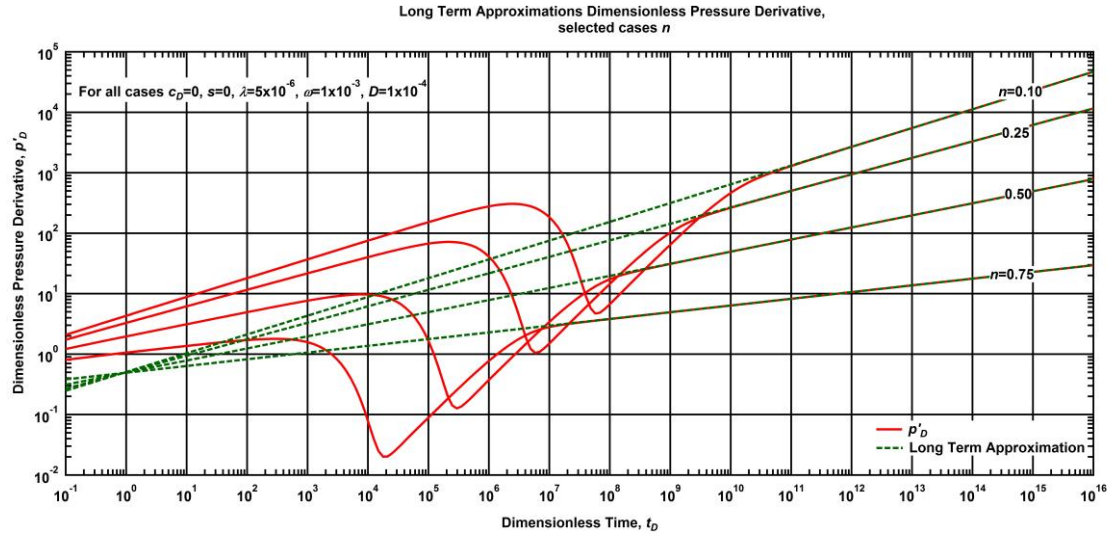

Fig. 40─ Long time approximations for dimensionless pressure derivative, selected values of *n*

IV.7 Inclusion of effects around the wellbore

The dimensionless wellbore storage of the proposed model is defined by:

$$\left[r_D^{\,n} \frac{dp_{fD}(t_D)}{d r_D} \right]^{\frac{1}{n}} = 1 - C_D \frac{dp_{fD}(t_D)}{dt_D}, \quad \text{.....(IV.24)}$$

where

$$C_D = \frac{24\,C}{n\,(\phi c_t)_t\,(2\pi h) r_w^2} \quad \text{.....(IV.25)}$$

Detailed derivation can be found in APPENDIX F. The plots showing the wellbore storage are presented next for selected values of the flow behavior index. The storativity ratio ω, the interporosity flow coefficient λ and the dimensionless matrix contribution D were kept constant.

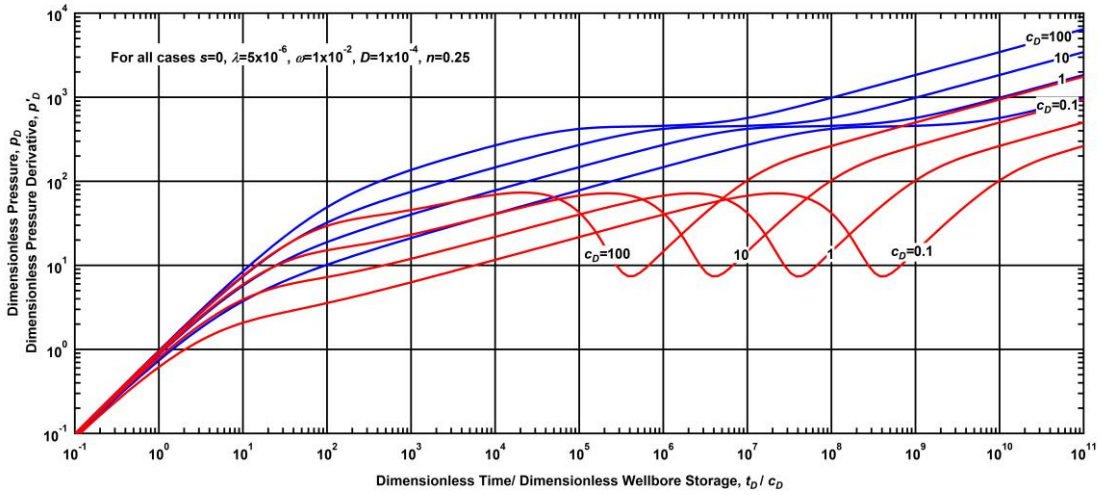

Fig. 41 – Dimensionless wellbore storage when n=0.25

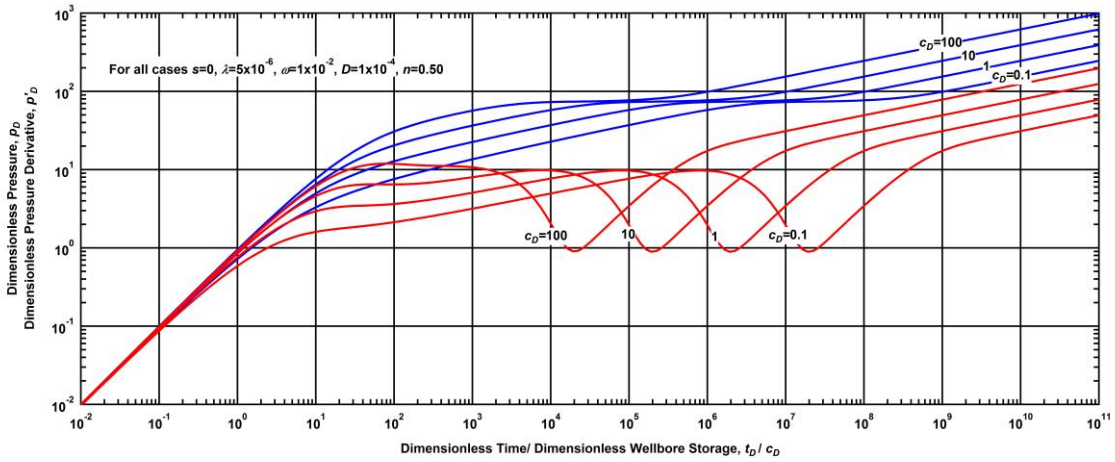

Fig. 42 – Dimensionless wellbore storage when n=0.50

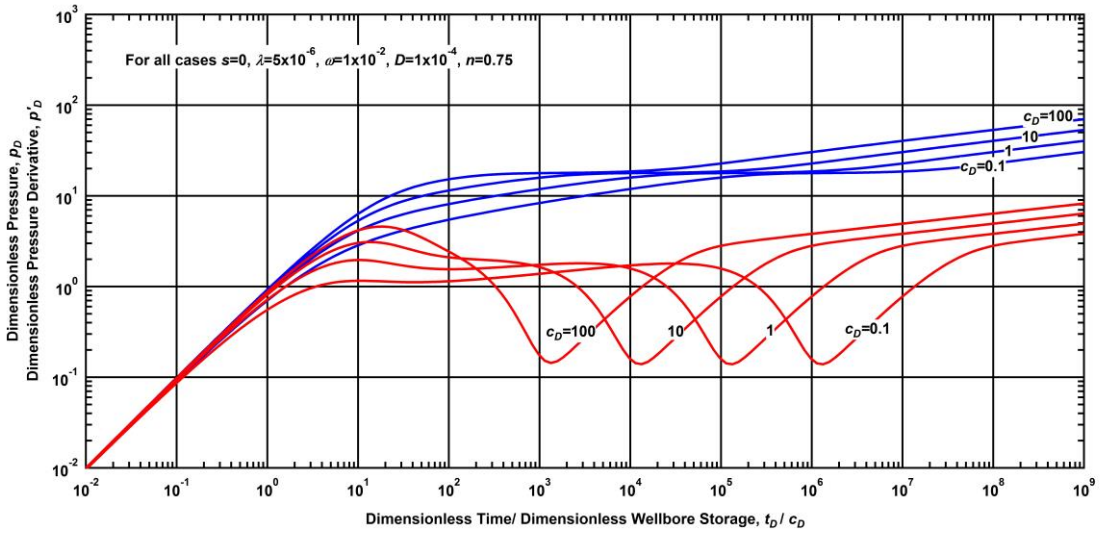

Fig. 43 ─ Dimensionless wellbore storage when n=0.75

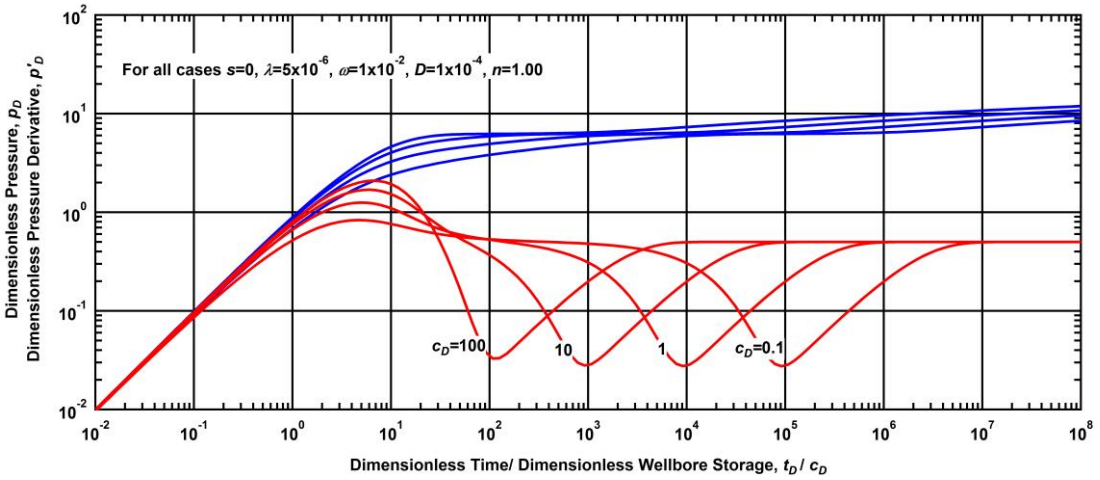

Fig. 44 ─ Dimensionless wellbore storage when n=1.0

The skin factor is defined by:

$$s = \Delta p_s \left[\frac{2\pi h}{q}\right]^n \frac{\mu_{eff}}{k_f} r_w^{1-n} \quad \text{.....(IV.25)}$$

Where Δp_s is the additional pressure drop that results across the skin zone. Detailed derivation can be found in APPENDIX G.

CHAPTER V

SYNTHETIC CASE

This chapter presents a synthetic case of a non-Newtonian fluid within a double porosity reservoir under pseudosteady-state transfer conditions.

This chapter presents two synthetic cases of a non-Newtonian fluid within a double porosity reservoir under pseudosteady-state transfer conditions. The first one as a base case with no skin or wellbore storage effects, and the second with wellbore storage and skin factor. Table 1 shows the reservoir and fluid properties.

Reservoir properties:

ϕ=0.080 (fraction) r_w=0.2917 ft h=150 ft

Oil properties: (initial reservoir pressure unknown)

B_o=1.19 RB/STB μ_o=0.120 cp c_t=24.5x10^{-6} psia^{-1}

Production parameters:

Drawdown Test Sequence

q_o=5000 STB/D (constant)

Case 1: Well Test Data (Base Case No skin or Wellbore storage effects)

Point	t, hr	Δp, psi	$\Delta p'(t)$, psi
0	0.00028	7.471	1.104
1	0.00033	7.600	1.041
2	0.00040	7.895	1.042
3	0.00048	8.067	0.894
4	0.00058	8.245	1.145
5	0.00069	8.404	1.287
6	0.00083	8.695	0.970
7	0.00100	8.919	1.273
8	0.00119	9.094	0.967
9	0.00143	9.305	1.119
10	0.00172	9.384	1.296
11	0.00206	9.705	1.143
12	0.00248	9.901	1.269
13	0.00297	10.143	1.115
14	0.00357	10.220	1.202
15	0.00428	10.640	1.275
16	0.00514	10.695	1.364
17	0.00616	10.959	1.292
18	0.00740	11.306	1.321
19	0.00887	11.402	1.141
20	0.01065	11.735	1.239
21	0.01278	11.874	1.134

Table 1 — Well test data for case 1(no skin or wellbore storage effects)

Point	t, hr	Δp, psi	$\Delta p'(t)$, psi
22	0.01534	12.197	0.969
23	0.01840	12.299	1.337
24	0.02208	12.468	1.192
25	0.02650	12.864	1.361
26	0.03180	12.951	1.259
27	0.03816	13.337	1.181
28	0.04579	13.379	1.056
29	0.05495	13.558	1.021
30	0.06594	13.884	1.101
31	0.07913	13.955	1.004
32	0.09495	14.343	0.955
33	0.11394	14.375	0.915
34	0.13673	14.594	1.120
35	0.16407	14.682	0.786
36	0.19689	14.904	0.709
37	0.23627	15.081	0.799
38	0.28352	15.063	0.492
39	0.34022	15.484	0.878
40	0.40827	15.618	1.007
41	0.48992	15.526	1.039
42	0.58791	15.753	1.386
43	0.70549	16.153	1.085
44	0.84659	16.345	1.509
45	1.01591	16.376	1.372
46	1.21909	16.831	1.443
47	1.46290	17.186	1.642
48	1.75549	17.314	1.522
49	2.10658	17.507	1.666
50	2.52790	17.871	1.492
51	3.03348	18.097	1.551
52	3.64018	18.409	1.536
53	4.36821	18.967	1.771
54	5.24185	19.019	1.875
55	6.29022	19.525	2.063
56	7.54827	19.885	2.214
57	9.05792	20.168	2.011
58	10.86951	20.367	1.788
59	13.04341	20.859	2.034
60	15.65209	21.074	1.507
61	18.78250	21.751	1.619
62	22.53901	21.891	2.171
63	27.04681	22.255	2.191
64	32.45617	22.678	2.484
65	38.94740	23.184	2.318
66	46.73688	23.322	1.846
67	56.08426	24.049	2.043
68	67.30111	24.549	3.209
69	80.76133	24.795	3.452

Table 1 Continued

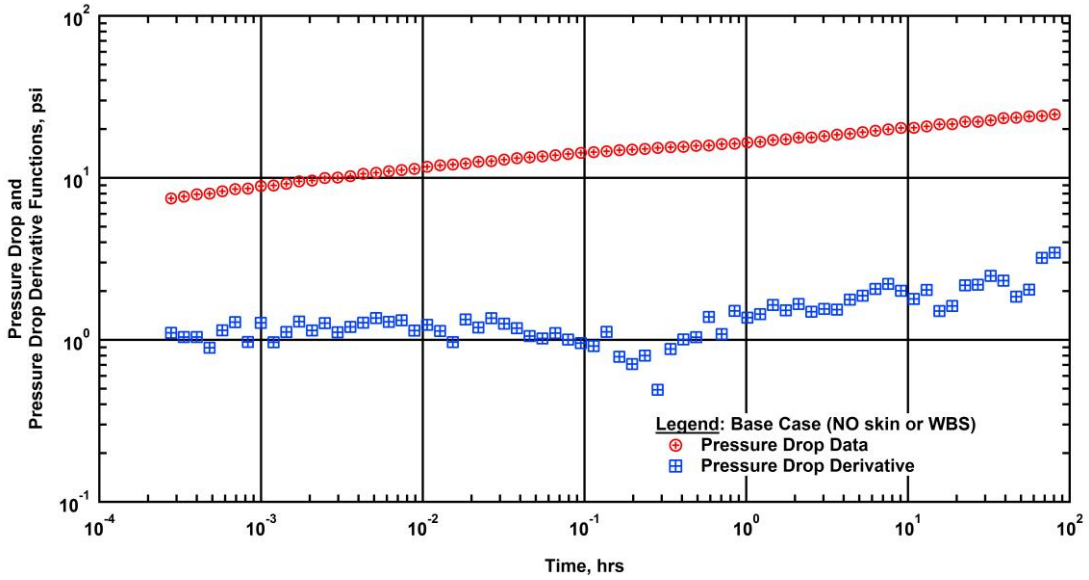

Fig. 45 ─ Pressure drop and pressure drop derivative vs time

Solution:

The log-log plot shown in **Fig. 45** depicts a non-Newtonian behavior. The slope ν from the straight line observed at late times is equal to 0.0691. Also the slope ν in terms of the flow behavior index is defined by:

$$\nu = \frac{1-n}{3-n}, \quad \text{.....(V.1)}$$

The slope from the pressure drop data at late times in the log-log plot is ν=0.0691 and solving for the flow behavior index gives:

$$n = \frac{1-3\nu}{1-\nu} = \frac{1-3(0.0691)}{1-(0.0691)} = 0.852 \quad \text{.....(V.2)}$$

The next step consists to obtain a relation between the time and the pressure drop. Recalling the approximation at late times Eq. IV.22,

$$p_{Df}(t_D) = \frac{(3-n)^{\frac{2(1-n)}{3-n}}}{\Gamma\left[\frac{2}{3-n}\right](1-n)} t_D^{\frac{1-n}{3-n}} \quad \text{.....(V.3)}$$

Substituting Eq.V.3 by Eq.III.3 and Eq.III.5 gives the next expression:

$$\frac{(2\pi h)^n k_f}{q^n \mu_{eff}\, r_w^{1-n}}(p_i - p_f) = \frac{(3-n)^{\frac{2(1-n)}{3-n}}}{\Gamma\left[\frac{2}{3-n}\right](1-n)}\left[\frac{q^{1-n} k_f}{n(\phi c_t)_t (2\pi h)^{1-n}\, \mu_{eff}\, r_w^{3-n}} t\right]^{\frac{1-n}{3-n}} \quad \text{.....(V.4)}$$

An slope m_{SL} is obtained from Eq.V.4 as follows:

$$m_{SL} = \frac{(p_i - p_f)}{t^{\frac{1-n}{3-n}}}, \quad \text{.....(V.5)}$$

and having known the compressibility and the porosity we may calculate the mobility ratio with this equation:

$$\frac{k_f}{\mu_{eff}} = \left[m_{SL}\, \Gamma\left[\frac{2}{3-n}\right](1-n)\right]^{\frac{n-3}{2}}\left[\frac{(3-n)^2}{n\phi c_t}\right]^{\frac{1-n}{2}}\left[\frac{q}{2\pi h}\right]^{\frac{n+1}{2}} \quad \text{.....(V.6)}$$

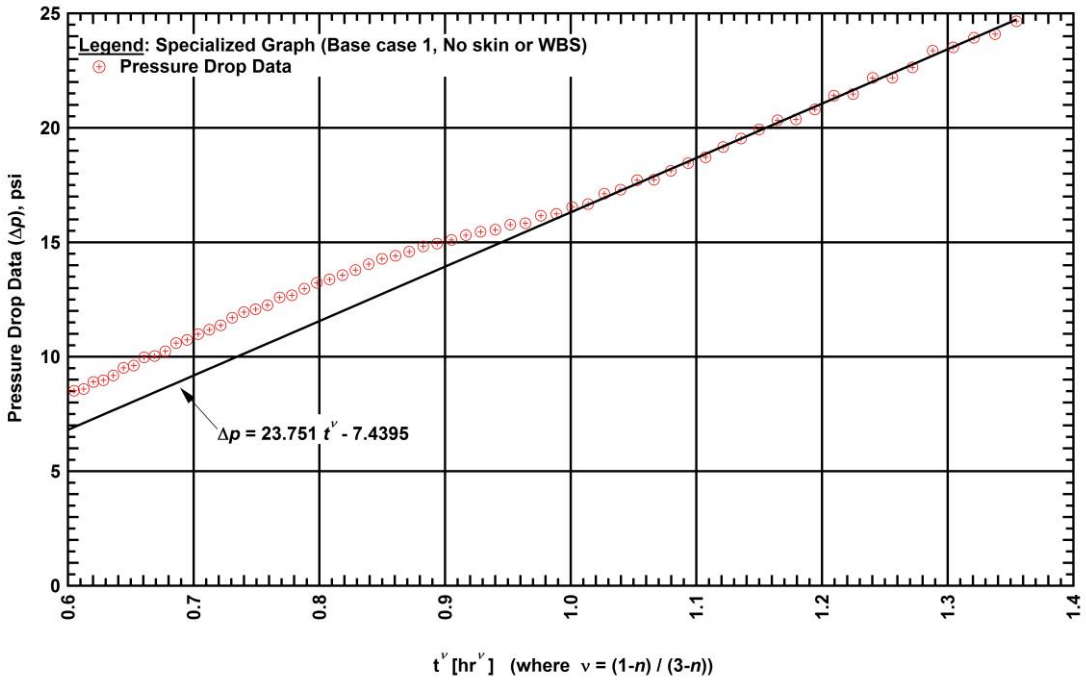

Fig. 46 ─ Specialized graph

From the specialized graph Δp vs t^{ν} the slope m_{SL} is equal to 23.751 [psi/hr$^{\nu}$] and substituting in Eq.V.6 in field units:

$$\frac{k_f}{m_{eff}} = \left[23.751[psi/hr^{0.0691}]\left[\frac{1atm}{14.696psi}\right]\left[\frac{1hr}{3600\sec}\right]^{0.0691}\right]G\left[\frac{2}{3-0.852}\right](1-0.852)^{\frac{0.852-3}{2}} \cdot$$

$$\left[\frac{(3-0.852)^2}{0.852(0.08)(24.5\times 10^{-6}psi^{-1})(14.696psi)}\right]^{\frac{1-n}{2}} \cdot$$

....(V.7)

$$\left[\frac{5000[STB]\left[\frac{5.615Bbl}{1ft^3}\right]\frac{(30.48ft)^3}{(1cm)^3}\frac{1D}{24hr}\frac{1hr}{3600\sec}\left[1.19\frac{RB}{STB}\right]^{\frac{0.852+1}{2}}}{2\pi(150ft)\frac{30.48ft}{1cm}}\right] = 8.188\frac{md}{cp}$$

For this synthetic case the effective viscosity is known but in the real field data in order to get the permeability the consistency factor *H* has to be known. At reservoir conditions this parameter may be very difficult to find. Calculating the permeability in the fracture form the effective mobility in field units is:

$$k_f\left[\frac{1darcy}{1000\ md}\right] = \mu_{eff}\ [cp]\left[8.188\ \frac{md}{cp}\right] = (1000\ md)(0.12\,cp)\left[8.188\ \frac{md}{cp}\right] = 982.52\,md \quad .....(V.8)$$

Fig. 47 shows semi-analytical early and long time approximation in a log-log plot.

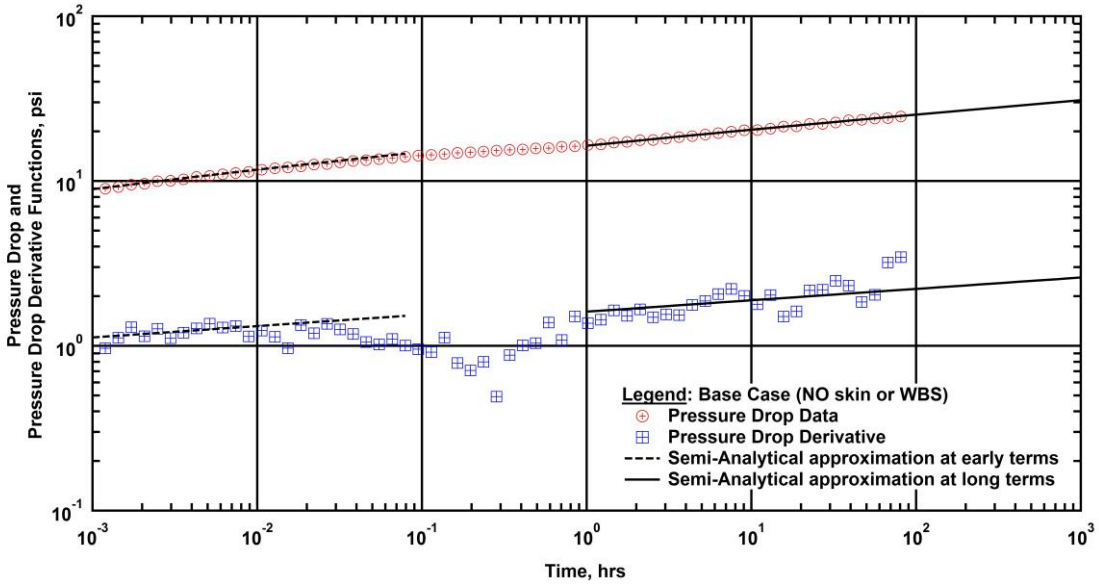

Fig. 47 – Semi-analytical approximation

Case 2: Well Test Data (effects around the wellbore). The same reservoir and well properties are used for this example.

Point	t, hr	Δp, psi	$\Delta p'(t)$, psi
0	0.00028	0.342	0.300
1	0.00033	0.407	0.429
2	0.00040	0.493	0.502
3	0.00048	0.583	0.577
4	0.00058	0.695	0.695
5	0.00069	0.837	0.835
6	0.00083	0.999	0.989
7	0.00100	1.196	1.184
8	0.00119	1.424	1.360
9	0.00143	1.680	1.583
10	0.00172	2.005	1.905
11	0.00206	2.355	2.208
12	0.00248	2.801	2.532
13	0.00297	3.278	2.956
14	0.00357	3.826	3.371
15	0.00428	4.519	3.894
16	0.00514	5.210	4.346
17	0.00616	6.072	4.760
18	0.00740	6.984	5.196
19	0.00887	8.064	5.783
20	0.01065	9.074	6.187
21	0.01278	10.415	6.629
22	0.01534	11.467	6.563
23	0.01840	12.635	6.566
24	0.02208	13.927	6.419
25	0.02650	15.005	5.817
26	0.03180	16.093	5.580
27	0.03816	17.191	4.871
28	0.04579	17.855	4.327
29	0.05495	18.785	3.618
30	0.06594	19.301	2.830
31	0.07913	19.783	2.661
32	0.09495	20.162	1.868
33	0.11394	20.311	1.698
34	0.13673	20.815	1.435
35	0.16407	20.926	1.242
36	0.19689	21.224	1.206
37	0.23627	21.438	1.008
38	0.28352	21.516	1.334
39	0.34022	21.784	0.439
40	0.40827	22.007	0.688
41	0.48992	22.229	0.801
42	0.58791	22.153	0.824
43	0.70549	22.463	1.512
44	0.84659	22.631	1.387
45	1.01591	22.819	1.497
46	1.21909	23.130	1.450
47	1.46290	23.514	1.620
48	1.75549	23.565	1.754
49	2.10658	24.146	1.623
50	2.52790	24.133	1.648
51	3.03348	24.880	1.463
52	3.64018	25.045	1.624

Table 2 — Well test data for case 2 (effects around the wellbore)

Point	t, hr	Δp, psi	$\Delta p'(t)$, psi
53	4.36821	25.446	2.340
54	5.24185	25.682	2.164
55	6.29022	25.985	1.996
56	7.54827	26.503	2.134
57	9.05792	26.482	1.725
58	10.86951	27.107	1.647
59	13.04341	27.471	1.935
60	15.65209	27.764	2.091
61	18.78250	28.034	1.527
62	22.53901	28.734	2.425
63	27.04681	28.815	2.353
64	32.45617	29.472	1.683
65	38.94740	29.750	2.813
66	46.73688	29.858	2.311
67	56.08426	30.175	1.505
68	67.30111	30.995	0.413
69	80.76133	31.077	-1.709

Table 2 continued

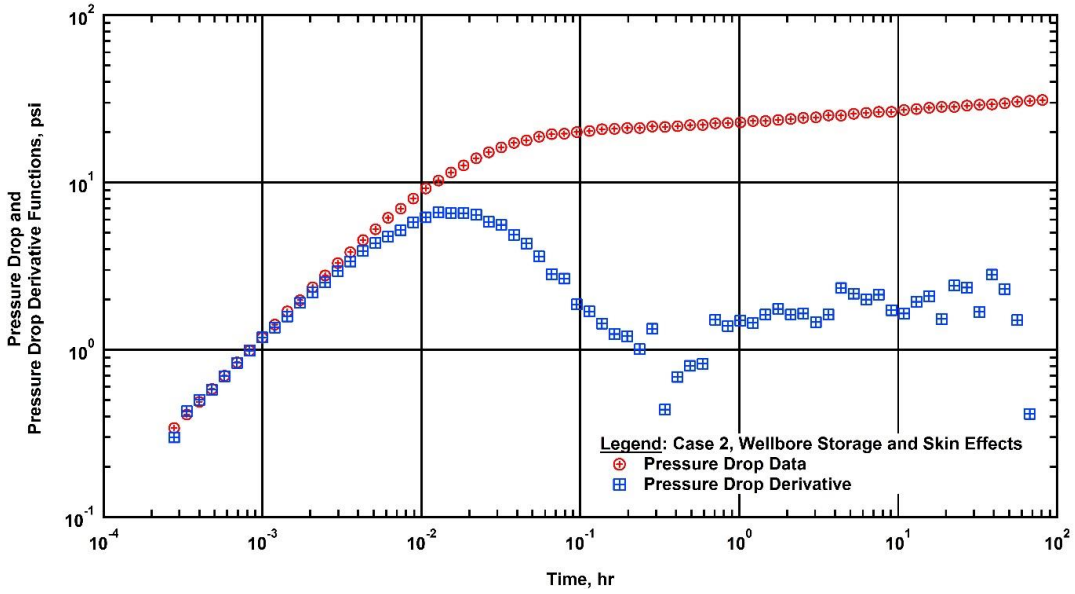

Fig. 48 – Pressure drop data vs time

Solution:

The log-log plot shown in **Fig. 48** depicts a non-Newtonian behavior. Plotting early data for wellbore storage calculations.

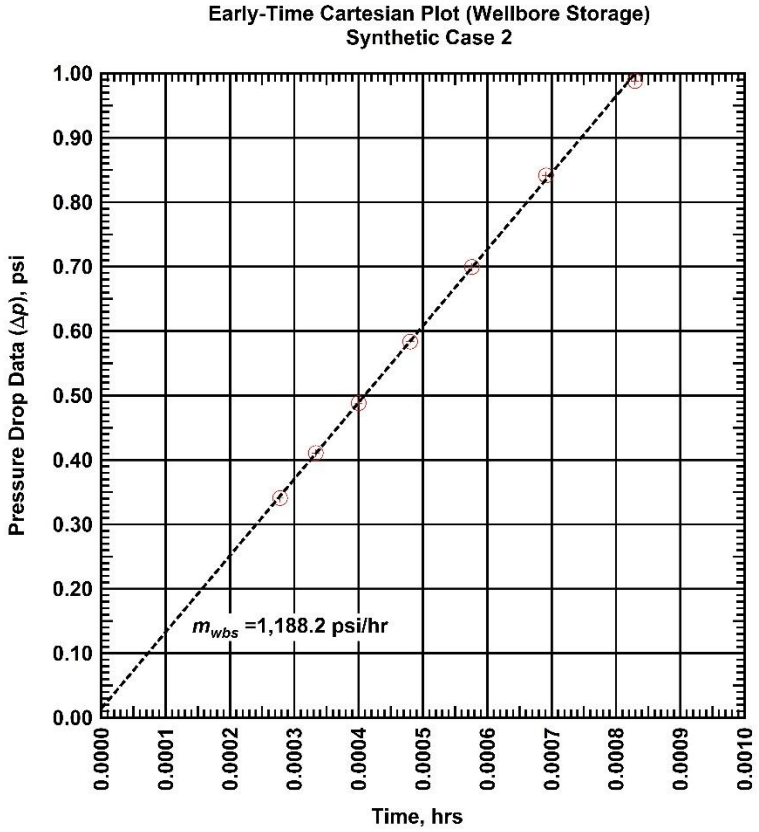

Fig. 49 – Early data- Cartesian plot

From the early data in the Cartesian plot, the slope from the wellbore storage is m_{wbs}=1,188.213 [psi/hr]. Calculating the wellbore storage:

$$C_s = \frac{qB}{24\, m_{wbs}} = \frac{5000\ STB\ /\ D\,(1.19\ RB\ /\ STB)}{24\,(1{,}188.213\ psi\ /\ hr)} = 0.2086\ RB\ /\ psi \quad \text{.....(V.9)}$$

Calculating in field units the dimensionless wellbore storage from the unit slope:

$$C_D = 0.03723\ \frac{qB}{n(\phi c_t)_t\, h\, r_w^2}\left[\frac{\Delta t}{\Delta p}\right]_{usl} \quad \text{.....(V.10)}$$

Substituting the reservoir properties in Eq.V.10

$$C_D = \frac{(0.03723\ )1000\ (STB\ /\ D)(1.19\ RB\ /\ STB)}{0.852\,(0.08)(24.5\times10^{-6}\ psi^{-1})(150\ \ ft)(0.2917\ \ ft)^2}\left[\frac{0.00033\ hr}{0.410\ psi}\right] = 8463.38 \quad \text{.....(V.11)}$$

The slope ν from the straight line observed at late times is equal to 0.0691. Also the slope ν in terms of the flow behavior index is defined by:

$$\nu = \frac{1-n}{3-n}, \quad \text{.....(V.12)}$$

The slope from the pressure drop data at late times in the log-log plot is ν=0.0691 and solving for the flow behavior index gives:

$$n = \frac{1-3\nu}{1-\nu} = \frac{1-3(0.0691)}{1-(0.0691)} = 0.852 \quad \text{.....(V.13)}$$

The next step consists to obtain a relation between the time and the pressure drop. Recalling the approximation at late times Eq. IV.22,

$$p_{Df}(t_D) = \frac{(3-n)^{\frac{2(1-n)}{3-n}}}{\Gamma\left[\frac{2}{3-n}\right](1-n)} t_D^{\frac{1-n}{3-n}} \quad \text{.....(V.14)}$$

Substituting Eq.V.14 by Eq. III.3 and Eq. III.5 gives the next expression:

$$\frac{(2\pi h)^n k_f}{q^n \mu_{eff} r_w^{1-n}}(p_i - p_f) = \frac{(3-n)^{\frac{2(1-n)}{3-n}}}{\Gamma\left(\frac{2}{3-n}\right)(1-n)}\left[\frac{q^{1-n} k_f}{n(\phi c_t)_t (2\pi h)^{1-n} \mu_{eff} r_w^{3-n}} t\right]^{\frac{1-n}{3-n}} \quad \text{.....(V.15)}$$

An slope m_{SL} is obtained from Eq.V.12 as follows:

$$m_{SL} = \frac{(p_i - p_f)}{t^{\frac{1-n}{3-n}}} \quad \text{.....(V.16)}$$

An having known the compressibility and the porosity we may calculate the mobility ratio with this equation:

$$\frac{k_f}{\mu_{eff}} = \left[m_{SL}\,\Gamma\left[\frac{2}{3-n}\right](1-n)\right]^{\frac{n-3}{2}}\left[\frac{(3-n)^2}{n\phi c_t}\right]^{\frac{1-n}{2}}\left[\frac{q}{2\pi h}\right]^{\frac{n+1}{2}} \quad \text{.....(V.17)}$$

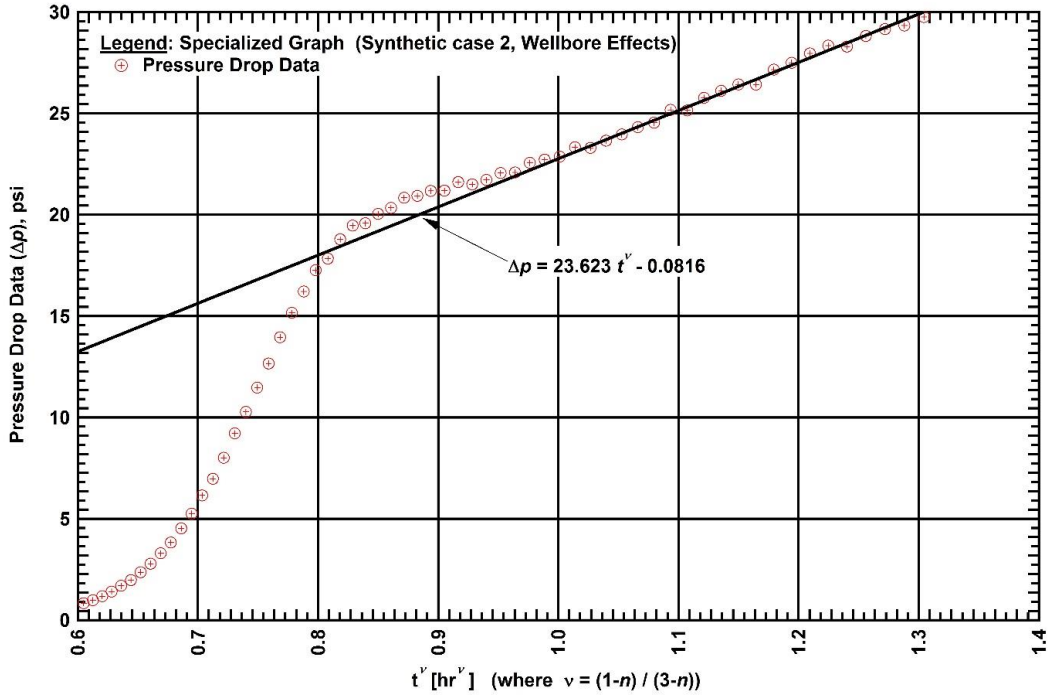

Fig. 50 – Specialized graph

From the specialized graph Δp vs t^{ν} the slope m_{SL} is equal to 23.623 [psi/hr$^{\nu}$] and substituting in Eq.V17 in field units:

$$\frac{k_f}{m_{eff}} = \left[23.623[psi/hr^{0.0691}]\left[\frac{1atm}{14.696psi}\right]\left[\frac{1hr}{3600\sec}\right]^{0.0691}\left[\frac{2}{3-0.852}\right](1-0.852)\right]^{\frac{0.852-3}{2}} \cdot$$

$$\left[\frac{(3-0.852)^2}{0.852(0.08)(24.5\acute{}10^{-6}psi^{-1})(14.696psi)}\right]^{\frac{1-n}{2}} \cdot \qquad \text{....(V.18)}$$

$$\left[\frac{[5000[STB]]\left[\frac{5.615Bbl}{1ft^3}\right]\left[\frac{(30.48ft)^3}{(1cm)^3}\right]\left[\frac{1D}{24hr}\right]\left[\frac{1hr}{3600\sec}\right]1.19\left[\frac{RB}{STB}\right]}{2p(150ft)\frac{30.48ft}{1cm}}\right]^{\frac{0.852+1}{2}} = 8.187\frac{md}{cp}$$

For this synthetic case the effective viscosity is known but in the real field data in order to get the permeability the consistency factor H has to be known. At reservoir conditions this parameter may be very difficult to find. Calculating the permeability in the fracture form the effective mobility in field units is:

$$k_f\left[\frac{1darcy}{1000\ md}\right]=\mu_{eff}\ [cp]\left[8.187\ \frac{md}{cp}\right]=(1000\ md)(0.12\,cp)\left[8.187\ \frac{md}{cp}\right]=983.52\,md \quad \text{.....(V.19)}$$

Also a pressure drop occurred near the wellbore. A skin factor may be calculated using the intercept of the plot Δp vs t^{v}, which is $\Delta p_{(t=0)}$= -0.816[psi].

$$s=\frac{\Delta p_{(t=0)}}{r_w^{1-n}}\left[\frac{2\pi h}{qB}\right]^n\frac{k_f}{\mu_{eff}}+\frac{1}{1-n} \quad \text{.....(V.20)}$$

Using Eq.V.20 and calculating the skin factor s in field units is:

$$s=\frac{-0.816-\left[8.187\frac{md}{cp}\right]^{1-n}}{\left[0.2917\frac{30.48\,ft}{1cm}\right]^{1-n}}\left[\frac{2p\left[150\frac{30.48\,ft}{1cm}\right]}{5000\frac{5.615\,STB}{1ft^3}\frac{(30.48\,ft)^3}{(1cm)^3}\frac{1D}{24hr}\frac{1hr}{3600\,\text{sec}}1.19\,RB/STB}\right]^n \quad \text{.....(V.21)}$$

$$+\frac{1}{1-0.852}=5.97$$

Fig. 51 shows semi-analytical long time approximation in a log-log plot.

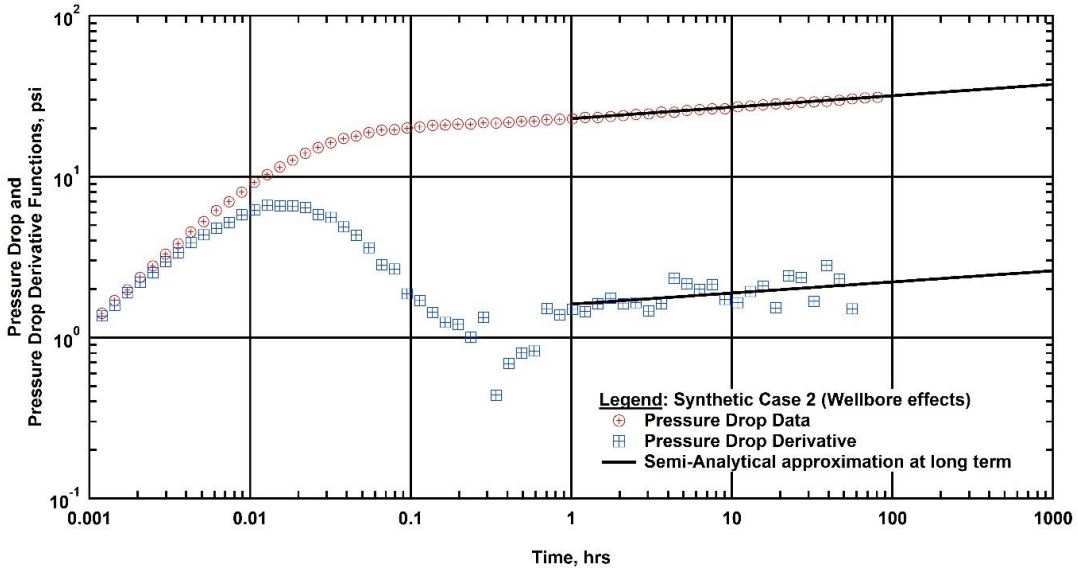

Fig. 51 ─ Semi-analytical approximation

CHAPTER VI

SUMMARY, CONCLUSIONS, AND RECOMMENDATIONS FOR FUTURE WORK

Summary

A consistent reservoir flow model has been developed for the production of a non-Newtonian fluid from a double porosity reservoir. This solution utilizes the concept of the Warren and Root (1963) "pseudosteady-state" interporosity transfer function to develop the interporosity transfer model for the case of a non-Newtonian fluid. This is the base model for this concept, additional models can and should be proposed for the interporosity transfer flow behavior for the case of a non-Newtonian fluid. As a consistency check, our proposed model is confirmed to reduce to the Warren and Root model for the case of a Newtonian fluid (n=1).

In this work we provide a new dimensionless variable (D) which represents the *dimensionless matrix contribution* and is defined as:

$$D = \frac{q_m}{q} \frac{2\pi h r_w}{\Delta L^2}, \quad \text{.....(III.12)}$$

The proposed flow model is presented using various suites of "type curves" (dimensionless solution plots) where the model parameters are varied to show the behavior of different regions of the solution. Early-time and long-time approximations were developed and are validated by comparison to the full solution. The early-time and long-time approximations are used to develop flow diagnostic trends and can be used to estimate the properties of the system using specialized plots.

A workflow is proposed and synthetic examples are generated for non-Newtonian fluid flow in an infinite-acting dual porosity reservoir (with and without wellbore storage and skin effects) to demonstrate the proposed interpretation and analysis workflow.

Conclusions

- The non-Newtonian solution for a dual-porosity reservoir provides a unique performance signature.
- The "early-time" approximation is valid, but may be obscured by wellbore storage and skin effects.
- The "late-time" approximation is valid, and can be used to estimate the mobility ratio and skin factor.

Recommendations

- The analytical solution presented in this work should be validated by a numerical model.
- A complete approximation (for all times) should be pursued for this problem.
- Additional interporosity transfer function models should be proposed for non-Newtonian fluids.

- This work should be exhaustively applied to field cases of heavy oil in double-porosity reservoirs.

REFERENCES

Abramowitz, M. and Stegun, I. A. 1972. *Handbook of Mathematical functions with formulas, graphs and Mathematical Tables*, New York City, Dover Publishing Inc.

Bird, B. R., Stewart, W. E. and Lightfoot, E.N.1960. *Transport Phenomena*. Second Edition., New York City, John Wiley & Sons Inc.

Cinco-Ley, H., & Samaniego V., F. (1982, January 1). Pressure Transient Analysis for Naturally Fractured Reservoirs. Society of Petroleum Engineers. doi:10.2118/11026-MS

Cinco-Ley, H., Samaniego V., F., and Kucuk, F. (1985, January 1). The Pressure Transient Behavior for Naturally Fractured Reservoirs With Multiple Block Size. Society of Petroleum Engineers. doi:10.2118/14168-MS

Chirstopher, R.H and Middleman S., (1965), Power-Law Flow through a Packed Tube. Department of Chemical Engineering, University of Rochester, N.Y.

De Swaan O., A. (1976, June 1). Analytic Solutions for Determining Naturally Fractured Reservoir Properties by Well Testing. Society of Petroleum Engineers. doi:10.2118/5346-PA

Escobar, F. et al. 2011. Pressure and Pressure Derivative Analysis for Non-Newtonian Pseudoplastic Fluids in Double-Porosity Formations. Ciencia-Teconologia. Colombia.

Ikoku, C. U. 1978. *Transient Flow of Non-Newtonian Fluids in Porous Media*, PhD dissertation, Stanford U., Stanford, CA.

Ikoku, C. U., & Ramey, H. J. (1979, June 1). Transient Flow of Non-Newtonian Power-Law Fluids in Porous Media. Society of Petroleum Engineers. doi:10.2118/7139-PA

Liu Ci-qun. 1988. Transient Spherical Flow of Non-Newtonian Power Law Fluids in Porous Media. Applied Mathematics and Mechanics, Published by SUT, Shanghai, China

Moench, A.F. 1984. Double-Porosity Models for a Fissured Groundwater Reservoir with Fracture Skin. Water Resources Research, Vol. 20, No. 7, 831-846.

Najurieta, H. L. (1980, July 1). A Theory for Pressure Transient Analysis in Naturally Fractured Reservoirs. Society of Petroleum Engineers. doi:10.2118/6017-PA

Serra, K., Reynolds, A. C., & Raghavan, R. (1983, December 1). New Pressure Transient Analysis Methods for Naturally Fractured Reservoirs(includes associated papers 12940 and 13014). Society of Petroleum Engineers. doi:10.2118/10780-PA

Stehfest, H. 1970. Algorithm 368 – Numerical Inversion of Laplace Transforms. *Communication, ACM* 13 (1): 47-49

Streltsova, T. D. (1983, October 1). Well Pressure Behavior of a Naturally Fractured Reservoir. Society of Petroleum Engineers. doi:10.2118/10782-PA

Warren, J. E., & Root, P. J. (1963, September 1). The Behavior of Naturally Fractured Reservoirs. Society of Petroleum Engineers. doi:10.2118/426-PA

Olarewaju, J. S. (1992, January 1). A Reservoir Model Of Non-Newtonian Fluid Flow. Society of Petroleum Engineers.

Rondon-Alfonzo, N.J.. 2008. *Determination of Fluid Viscosities from Bioconical-Annular Geometries: Experimental and Modelling Studies.*, PhD. Dissertation, Texas A&M University.

Valdes-Perez Alex. 2013. *Fractal Well Testing Naturally Fractured Reservoirs Double porosity*, MSc Dissertation, U. of Stavanger, Norway.

Valdes-Perez, A.R., Pulido ,H., Cinco-Ley., Larsen, L. 2013. A New Double Porosity Fractal Model for Well Test Analysis with transient interporosity Transference for Petroleum and Geothermal Systems. Proceedings Thirty-Eight Workshop on Geothermal Reservoir Engineering Stanford University, Stanford, California.

Valdes-Perez, A. R., Cinco-Ley, H., Pulido-Bello, H., Hveding, F., & Samaniego, F. (2013, June 10). A new general flow model for Well Test Analysis for fluids used in Enhanced Oil Recovery Projects. Society of Petroleum Engineers. doi:10.2118/164886-MS

Vongvuthipornchai, S., & Raghavan, R. (1987, December 1). Pressure Falloff Behavior in Vertically Fractured Wells: Non-Newtonian Power-Law Fluids. Society of Petroleum Engineers. doi:10.2118/13058-PA

NOMENCLATURE

A = Area, L^2 [m^2] or [ft^2]
$A_{m\text{-}f}$ = Cross-sectional area matrix to fracture, L^2 [m^2] or [ft^2]
A_α = Reservoir area, L^2 [m^2] or [ft^2]
D = Dimensionless Matrix contribution from eq. 39, dimensionless
D_p = Particle Diameter, L [cm] or [in]
E_i = Exponential integral, dimensionless
F = Force, ML/t^2 [Newton] or [lb_f]
H = Variable of consistency [Pa • s^n]
I_0 = Modified Bessel Functions of the first kind, zero order, dimensionless
I_1 = Modified Bessel Functions of the first kind, first order, dimensionless
I_ν = Modified Bessel Functions of the first kind, ν order, dimensionless
K_0 = Modified Bessel Functions of the first kind, zero order, dimensionless
K_1 = Modified Bessel Functions of the first kind, first order, dimensionless
K_ν = Modified Bessel Functions of the first kind, ν order, dimensionless
L = Length, L [m, cm] or [ft, in]
V = Velocity, L/t [m/s] or [ft/s]
V_r = Rock volume, L^3 [m^3] or [ft^3]
Y = Distance, L [m] or [ft]
c_o = Fluid compressibility, $(M/Lt^2)^{-1}$ [Pa^{-1}] or [psi^{-1}]
c_r = Formation compressibility , $(M/Lt^2)^{-1}$ [Pa^{-1}] or [psi^{-1}]
c_t = Total compressibility, $(M/Lt^2)^{-1}$ [Pa^{-1}] or [psi^{-1}]
e = Exponential, 2.71828…
h = Net pay thickness, L [m] or [ft].
k = Permeability, L^2 [mD] or [m^2]
k_f = Fracture permeability, L^2 [mD] or [m^2]
k_m = Matrix permeability, L^2 [mD] or [m^2]
k_r = Radial Permeability, L^2 [mD] or [m^2]
j = Number of fractures, dimensionless
n = Flow behavior index, dimensionless
p = Pressure, M/Lt^2 [Pa] or [psi]
p_f = Pressure in the fracture, M/Lt^2 [Pa] or [psi]
p_i = Initial pressure, M/Lt^2 [Pa] or [psi]
p_m = Pressure in the matrix, M/Lt^2 [Pa] or [psi]
p_D = Dimensionless pressure, dimensionless
p_{DNN} = Dimensionless non-Newtonian pressure, dimensionless
p_{fD} = Dimensionless pressure in the fracture, dimensionless
p_{mD} = Dimensionless pressure in the matrix, dimensionless
p_s = Pressure in the skin zone, M/Lt^2 [Pa] or [psi]
p_{wD} = Dimensionless wellbore pressure, dimensionless
q = Flowrate, L^3/t [m3/sec] or [ft^3/s]
q_m = Matrix flowrate, L^3/t [m3/sec] or [ft^3/s]
r = Radial distance, L [m] or [ft]
r_w = Wellbore radius, L [m] or [ft]

r_{eD} = Dimensionless external radius drainage, dimensionless
r_D = Dimensionless radius, dimensionless
s = Skin factor, dimensionless
t = Time, t [sec]
t_D = Dimensionless time, dimensionless
t_{DNN} = Dimensionless Non-Newtonian time, dimensionless
u_r = Radial velocity, L/t [m/s] or [ft/s]
u, = Laplace transform variable
v_o = Superficial velocity, L/t [m/s] or [ft/s]
v_r = Radial velocity, L/t [m/s] or [ft/s]
ΔL = Length, L [m] or [ft]
Δp = Pressure differential, M/Lt^2 [Pa] or [psi]
α = shape factor, dimensionless
$\dot{\gamma}$ = Shear rate, t^{-1} [s^{-1}]
γ = Euler's constant, 0.577216…
μ = Newtonian Viscosity, M/Lt [cp] or [$lb_m/ft \bullet s$]
μ_{app} = Apparent Viscosity, M/Lt [cp] or [$lb_m/ft \bullet s$]
μ_{eff} = Effective viscosity, M/Lt [cp] or [$lb_m/ft \bullet s$]
λ = Interporosity flow parameter, dimensionless
θ = Ellis model Parameter, dimensionless
ϕ = Porosity, fraction
ϕ_f = Fracture Porosity, fraction
ϕ_m = Matrix Porosity, fraction
ρ = Density, M/L^3 [kg/m^3] or [lb_m/ft^3]
ρ_o = Initial Density, M/L^3 [kg/m^3] or [lb_m/ft^3]
ω = Storativity ratio, dimensionless
$\tau_{0.5}$ = Shear stress when $\mu=\mu_{o0.5}$, M/Lt^2 [N/m^2] or [lb_f/ft^2]
τ = Shear stress M/Lt^2 [N/m^2] or [lb_f/ft^2]
τ = Convolution variable
τ_y = Yield shear stress M/Lt^2 [N/m^2] or [lb_f/ft^2]

APPENDIX A

DERIVATION OF A RADIAL FLOW-DUAL POROSITY MODEL

(PSEUDO-STATE INTERPOROSITY FLOW)

This Appendix presents the derivation of the pseudosteady-state double porosity model proposed by Warren and Root (1963). The continuity equation for a double porosity reservoir is given as:

$$\frac{k_f}{\mu}\nabla^2 p_f = (\phi c_t)_f \frac{\partial p_f}{\partial t} + q^*_{m-f} \quad \text{.....(A.1)}$$

Where q^*_{m-f} is the volumetric flowrate, and is defined by:

$$q^*_{m-f} = \frac{q_{m-f}}{V_r} \quad \text{.....(A.2)}$$

Considering the effects of expansion, q_{m-f} can be expressed as:

$$q_{m-f} = (\phi c_t)_m V_r \frac{\partial p_m}{\partial t} \quad \text{.....(A.3)}$$

Substituting Eq.A.3 into Eq.A.2, the volumetric flowrate becomes:

$$q^*_{m-f} = (\phi c_t)_m \frac{\partial p_m}{\partial t} \quad \text{.....(A.4)}$$

Substituting Eq.A.4 into Eq.A.1, the fracture network diffusivity equation becomes:

$$\frac{k_f}{\mu}\nabla^2 p_f = (\phi c_t)_f \frac{\partial p_f}{\partial t} + (\phi c_t)_m \frac{\partial p_m}{\partial t} \quad \text{.....(A.5)}$$

Based on Darcy's Law, the flow from the matrix to the fractures can be expressed as:

$$q^*_{m-f} = -\frac{k_m}{\mu}\frac{\Delta p_{m-f}}{\Delta L}\left[\frac{A_{m-f}}{\Delta L\, A_\alpha}\right] \quad \text{.....(A.6)}$$

"Lumping" variables, Eq. A.6 can be expressed as:

$$q^*_{m-f} = \alpha \frac{k_m}{\mu}(p_f - p_m), \quad \text{.....(A.7)}$$

Where:

$$\alpha = \frac{A_{m-f}}{(\Delta L)^2 A_\alpha} \quad \text{.....(A.8)}$$

From Warren and Root (1963), assuming uniformly spaced fractures and allowing variations in the fracture width, the shape factor is defined as:

$$\alpha = \frac{1}{l^2} 4 j (j+2), \quad \text{.....(A.9)}$$

where j is the number of sets of fractures and l is the characteristic dimension of heterogeneous region.

Equating Eq.A.4 with Eq.A.7 and solving for $\frac{\partial p_m}{\partial t}$, the interface condition is given by:

$$\frac{\partial p_m}{\partial t} = \alpha \frac{k_m}{\mu} \frac{(p_f - p_m)}{(\phi c_t)_m}. \quad \text{.....(A.10)}$$

In order to transform Eq. A.5 and Eq. A10 to dimensionless form, the following dimensionless variables are used:

Dimensionless pressure in the fracture:

$$p_{fD} = \frac{2\pi k_f h}{q B_o \mu} (p_i - p_f), \quad \text{.....(A.11)}$$

Dimensionless pressure in the matrix:

$$p_{mD} = \frac{2\pi k_f h}{q B_o \mu} (p_i - p_m), \quad \text{.....(A.12)}$$

Dimensionless time:

$$t_D = \frac{\mu r_w^2}{k_f [(\phi c_t)_m + (\phi c_t)_f]} t, \quad \text{.....(A.13)}$$

Dimensionless radius:

$$r_D = \frac{r}{r_w}. \quad \text{.....(A.14)}$$

Substituting Eqs. A.11-A.14 into Eq. A.5 yields:

$$\frac{1}{r_D}\frac{\partial}{\partial r_D}\left[r_D\frac{\partial p_{fD}}{\partial r_D}\right]=\omega\frac{\partial p_{fD}}{\partial t_D}+(1-\omega)\frac{\partial p_{mD}}{\partial t_D}, \quad \text{(A.15)}$$

where ω is the *storativity ratio*, and is given by:

$$\omega=\frac{(\phi c_t)_f}{(\phi c_t)_m+(\phi c_t)_f} \quad \text{(A.16)}$$

Making similar substitutions, Eq. A.10 becomes:

$$\frac{\partial p_{mD}}{\partial t_D}=\frac{\lambda}{(1-\omega)}(p_{fD}-p_{mD}), \quad \text{(A.17)}$$

Where λ is defined as the *interporosity flow coefficient* and is given by:

$$\lambda=\alpha\frac{k_m}{k_f}r_w^2, \quad \text{(A.18)}$$

In order to provide a solution suitable for well test analysis, the following initial and boundary conditions are established in dimensionless form:

Initial Condition: *Uniform pressure distribution*

$$p_{fD}(r_D,t_D=0)=0, \quad \text{(A.19)}$$

Inner Boundary Condition: *Constant Flowrate*

$$\left[r_D\frac{dp_{fD}(r_D,t_D)}{dr_D}\right]_{r_D=1}=-1, \quad \text{(A.20)}$$

Outer Boundary Condition: *Infinite-Acting Reservoir*

$$\lim_{r_D\to\infty}p_{fD}(r_D,t_D)=0 \quad \text{(A.21)}$$

The Laplace transform is applied to solve Eq. A.15 and Eq. A.17. Taking the Laplace transform of Eq. A.17:

$$u\bar{p}_{mD}(r_D,u)-p_{mD}(r_D,0)=\frac{\lambda}{(1-\omega)}(\bar{p}_{fD}(r_D,u)-\bar{p}_{mD}(r_D,u)), \quad \text{(A.22)}$$

Where u is the Laplace transform parameter. Solving for $\bar{p}_{mD}(r_D, u)$, Eq. A.22 becomes:

$$\bar{p}_{mD}(r_D, u) = \frac{\lambda}{u(1-\omega)+\lambda}\,\bar{p}_{fD}(r_D, u) \quad \text{.....(A.23)}$$

Applying the Laplace transform to Eq. A.15 yields:

$$\frac{1}{r_D}\frac{d}{dr_D}\left[r_D\,\frac{d\bar{p}_{fD}(r_D, u)}{dr_D}\right] = \omega\left[u\bar{p}_{fD}(r_D, u) - p_{fD}(r_D, 0)\right] + (1-\omega)\left[u\bar{p}_{mD}(r_D, u) - p_{mD}(r_D, 0)\right] \text{ ..(A.24)}$$

Substituting Eq. A.23 into Eq. A.24, and reducing terms:

$$\frac{1}{r_D}\frac{d}{dr_D}\left[r_D\,\frac{d\bar{p}_{fD}(r_D, u)}{dr_D}\right] = \omega\left[u\bar{p}_{fD}(r_D, u)\right] + (1-\omega)\left[\frac{\lambda}{u(1-\omega)+\lambda}\,u\bar{p}_{fD}(r_D, u)\right], \quad \text{.....(A.25)}$$

Rearranging Eq. A.25, we have:

$$\frac{1}{r_D}\frac{d}{dr_D}\left[r_D\,\frac{d\bar{p}_{fD}(r_D, u)}{dr_D}\right] = u\,f(u)\,\bar{p}_{fD}(r_D, u), \quad \text{.....(A.26)}$$

Where the interporosity flow function given by:

$$f(u) = \frac{\omega(1-\omega)u + \lambda}{(1-\omega)u + \lambda} \quad \text{.....(A.27)}$$

Multiplying Eq.A.26 by r_D^2:

$$r_D\,\frac{d}{dr_D}\left[r_D\,\frac{d\bar{p}_{fD}(r_D, u)}{dr_D}\right] = u\,f(u)\,r_D^2\,\bar{p}_{fD}(r_D, u), \quad \text{.....(A.28)}$$

And defining:

$$a = r_D\sqrt{u\,f(u)}, \quad \text{.....(A.29)}$$

Or:

$$r_D = \frac{a}{\sqrt{u\,f(u)}} \quad \text{.....(A.30)}$$

Eq. A.28 can be expressed as:

$$a^2 \frac{d^2 \bar{p}_{fD}(a)}{da^2} + a \frac{d\bar{p}_{fD}(a)}{da} = a^2 \bar{p}_{fD}(a), \quad \text{(A.31)}$$

Where the general solution of Eq. A.28 is:

$$\bar{p}_{fD}(a) = AI_0(a) + BK_0(a), \quad \text{(A.32)}$$

Or, in terms of r_D and u we have:

$$\bar{p}_{fD}(r_D, u) = AI_0(r_D \sqrt{u\ f(u)}) + BK_0(r_D \sqrt{u\ f(u)}) \quad \text{(A.33)}$$

In order to obtain a particular solution in the Laplace domain, boundary conditions must be transformed to the Laplace domain as well. Therefore, inner boundary condition becomes:

$$\left[r_D \frac{d\bar{p}_{fD}(r_D, u)}{dr_D} \right]_{r_D = 1} = -\frac{1}{u}, \quad \text{(A.34)}$$

And the outer boundary condition is given as:

$$\lim_{r_D \to \infty} \bar{p}_{fD}(r_D, u) = 0 \quad \text{(A.35)}$$

Applying the outer boundary condition to Eq.A.32, we obtain:

$$\lim_{r_D \to \infty} [\bar{p}_{fD}(r_D, u)] = A \lim_{r_D \to \infty} I_0(r_D \sqrt{u\ f(u)}) + B \lim_{r_D \to \infty} K_0(r_D \sqrt{u\ f(u)}) = 0 \quad \text{(A.36)}$$

Analyzing the behavior of Bessel functions for large arguments, it can be concluded that, A=0. Therefore, reduced solution for this case is given by:

$$\bar{p}_{fD}(r_D, u) = BK_0(r_D \sqrt{u\ f(u)}) \quad \text{(A.37)}$$

Taking the derivative $\frac{d\bar{p}_{fD}}{dr_D}$ of Eq. A.37 and multiplying by r_D:

$$r_D \frac{d\bar{p}_{fD}(r_D, u)}{dr_D} = -Br_D \sqrt{u\ f(u)}\, K_1(r_D \sqrt{u\ f(u)}) \quad \text{(A.38)}$$

Applying inner boundary condition to Eq. A.38, we have:

$$\left[r_D \frac{d\bar{p}_{fD}(r_D,u)}{dr_D} \right]_{r_D=1} = -B\sqrt{u\ f(u)}\,K_1(\sqrt{u\ f(u)}) = -\frac{1}{u}, \quad \text{(A.39)}$$

Solving Eq. A.39 for the "*B*" coefficient, we have:

$$B = \frac{1}{u\sqrt{u\ f(u)}} \frac{1}{K_1(\sqrt{u\ f(u)})} \quad \text{(A.40)}$$

Substituting Eq.A.40 into Eq.A.37, the particular solution for this case is:

$$\bar{p}_{fD}(r_D,u) = \frac{1}{u} \frac{K_0(r_D\sqrt{u\ f(u)})}{\sqrt{u\ f(u)}\,K_1(\sqrt{u\ f(u)})} \quad \text{(A.41)}$$

In order to provide a solution in the real domain, we consider the approximation (Abramowitz and Stegun, 1972):

$$K_1(x) = \frac{1}{x} \text{ for } x \to 0 \quad \text{(A.42)}$$

Rearranging Eq. A.42, we obtain:

$$x\,K_1(x) = 1 \quad \text{(A.43)}$$

Substituting Eq. A.43 into Eq. A.41 we obtain the "line source solution" for this case:

$$\bar{p}_{fD}(r_D,u) = \frac{1}{u} K_0(r_D\sqrt{u\ f(u)}) \quad \text{(A.44)}$$

Moreover, for small arguments, we have: (from Abramowitz and Stegun, 1972)

$$K_0(z) \approx \frac{1}{2}\ln\left[\frac{4}{z^2 e^{2\gamma}}\right] \quad \text{(A.45)}$$

Substituting Eq. A.45 into Eq. A.44, we obtain

$$\bar{p}_{fD}(r_D,u) = \frac{1}{2}\left[\frac{1}{2}\ln\left[\frac{4}{r_D^2\,u\ f(u)\,e^{2\gamma}}\right]\right], \quad \text{(A.46)}$$

Using the properties of logarithms and expanding, Eq. A.46 becomes:

$$\overline{p}_{fD}(r_D,u)=\frac{1}{2u}\left[\frac{1}{2}\ln\left[\frac{4}{r_D^2\,e^{2\gamma}}\right]-(\ln(u)+\ln(f(u)))\right], \quad \text{.....(A.47)}$$

For reference, Eq. A.28 can also be expressed as:

$$f(u)=\frac{\frac{\omega(1-\omega)u}{\lambda}+1}{\frac{(1-\omega)u}{\lambda}+1}, \quad \text{.....(A.48)}$$

Therefore, substituting Eq. A.48 into Eq. A.47 yields:

$$\overline{p}_{fD}(r_D,u)=\frac{1}{2u}\ln\left[\frac{4}{r_D^2\,e^{2\gamma}}\right]-\frac{1}{2u}\ln(u)+\frac{1}{2u}\left[\ln\left[1+\frac{(1-\omega)u}{\lambda}\right]-\ln\left[1+\frac{\omega(1-\omega)u}{\lambda}\right]\right] \quad \text{.....(A.49)}$$

Using Laplace transform tables, we find that the inverse of Eq. A.49, which is given as:

$$p_{fD}(r_D,t_D)=\frac{1}{2}\ln\left[\frac{4}{r_D^2\,e^{2\gamma}}\right]+\ln(e^{\gamma}t_D)+\frac{1}{2}E_i\left[\frac{\lambda}{(1-\omega)}t_D\right]-\frac{1}{2}E_i\left[\frac{\lambda}{\omega(1-\omega)}t_D\right], \quad \text{.....(A.50)}$$

Or, in a more compact form, Eq. A.50 becomes:

$$p_{Df}(r_D,t_D)=\frac{1}{2}\ln\left[\frac{4}{r_D^2e^{\gamma}}t_D\right]+\frac{1}{2}E_i\left[\frac{\lambda}{(1-\omega)}t_D\right]-\frac{1}{2}E_i\left[\frac{\lambda}{\omega(1-\omega)}t_D\right]. \quad \text{.....(A.51)}$$

Taking well-testing derivative of the solution (Eq. A.51), we have:

$$p'_D(r_D,t_D)\equiv t_D\,\frac{d\left[p_D(r_D,t_D)\right]}{dt_D}\approx\frac{1}{2}+\frac{1}{2}\exp\left[\frac{-\lambda}{\omega(1-\omega)}t_D\right]-\frac{1}{2}\exp\left[\frac{-\lambda}{(1-\omega)}t_D\right] \quad \text{.....(A.52)}$$

APPENDIX B

DERIVATION OF A RADIAL MODEL FOR NON-NEWTONIAN FLUID THROUGH POROUS MEDIUM

This Appendix presents the derivation of the radial flow model for power law fluids in homogeneous reservoirs, proposed by Ikoku and Ramey (1979). The main assumptions for the model are:

- Well penetrates the entire thickness of the formation.
- Uniform thickness.
- Permeability is constant throughout the entire porous medium.
- Compressibility of the fluid is small.
- Effects of gravity are negligible.
- Pressure gradients are small.
- Non-Newtonian fluids obey the Oastwald de Waele (power law) relationship.
- The fluid is considered to be pseudoplastic.

The continuity equation in radial coordinates for a homogeneous reservoir is:

$$\frac{1}{r}\frac{\partial}{\partial r}(r\rho v_r) = -\frac{\partial}{\partial t}(\phi\rho), \quad \text{.....(B.1)}$$

According to Christopher et al. (1965);

$$v_r^n = \frac{k_r}{\mu_{eff}}\frac{\partial p}{\partial r} \quad \text{..... (B.2)}$$

Substituting Eq. B.2 in Eq. B.1 we have:

$$\frac{1}{r}\frac{\partial}{\partial r}\left[r\rho\left[\frac{k_r}{\mu_{eff}}\frac{\partial p}{\partial r}\right]^{\frac{1}{n}}\right] = -\frac{\partial}{\partial t}(\phi\rho), \quad \text{.....(B.3)}$$

The definition of fluid compressibility is:

$$c_o = -\frac{1}{\rho}\frac{d\rho}{dp}, \quad \text{.....(B.4)}$$

Integrating this definition (Eq. B.4), the equation of state for a slightly compressible fluid is obtained:

$$\rho = \rho_0 e^{c(p-p_0)}. \quad \text{.....(B.5)}$$

Assuming that the compressibility is small, then c_o and ρ may be treated as constants. Expanding Eq. B.5:

$$\frac{\rho}{r}\frac{\partial}{\partial r}\left[r\left[-\frac{k_r}{\mu_{eff}}\frac{\partial p}{\partial r}\right]^{\frac{1}{n}}\right]-c_o\rho\left[\frac{k_r}{\mu_{eff}}\right]^{\frac{1}{n}}\left[-\frac{\partial p}{\partial r}\right]^{\frac{1}{n}}\left[\frac{\partial p}{\partial r}\right]=\phi\, c_o\rho\frac{\partial\rho}{\partial t}-\rho\frac{\partial\phi}{\partial t}, \quad \text{.....(B.6)}$$

Eq. B.6 can be reduced to:

$$\frac{1}{r}\frac{\partial}{\partial r}\left[r\left[-\frac{k_r}{\mu_{eff}}\frac{\partial p}{\partial r}\right]^{\frac{1}{n}}\right]-c_o\left[\frac{k_r}{\mu_{eff}}\right]^{\frac{1}{n}}\left[-\frac{\partial p}{\partial r}\right]^{\frac{1+n}{n}}=\phi\, c_o\frac{\partial\rho}{\partial t}-\frac{\partial\phi}{\partial t}, \quad \text{.....(B.7)}$$

Applying the chain rule to the last term on RHS of Eq. B.7:

$$\frac{1}{r}\frac{\partial}{\partial r}\left[r\left[\frac{\partial p}{\partial r}\right]^{\frac{1}{n}}\right]-c_o\left[-\frac{\partial p}{\partial r}\right]^{\frac{1+n}{n}}=-\left[\frac{\mu_{eff}}{k_r}\right]^{\frac{1}{n}}\phi\, c_t\frac{\partial p}{\partial t}, \quad \text{.....(B.8)}$$

Where the total compressibility is:

$$c_t=c_o+c_r, \quad \text{.....(B.9)}$$

Expanding Eq. B.8:

$$\frac{1}{r}\left[-\frac{\partial p}{\partial r}\right]^{\frac{1}{n}}+\frac{1}{n}\left[-\frac{\partial p}{\partial r}\right]^{\frac{1-n}{n}}\left[-\frac{\partial^2 p}{\partial r^2}\right]-c_o\left[-\frac{\partial p}{\partial r}\right]^{\frac{1+n}{n}}=-\left[\frac{\mu_{eff}}{k_r}\right]^{\frac{1}{n}}\phi\, c_t\frac{\partial p}{\partial t}, \quad \text{.....(B.10)}$$

Multiplying Eq. B.10 by $\left[-\frac{\partial p}{\partial r}\right]^{\frac{n-1}{n}}$:

$$\frac{1}{r}\left[-\frac{\partial p}{\partial r}\right]+\frac{1}{n}\left[-\frac{\partial^2 p}{\partial r^2}\right]-c_o\left[-\frac{\partial p}{\partial r}\right]^2=-\left(\frac{\mu_{eff}}{k_r}\right)^{\frac{1}{n}}\phi\, c_t\left[-\frac{\partial p}{\partial r}\right]^{\frac{n-1}{n}}\frac{\partial p}{\partial t} \quad \text{.....(B.11)}$$

Assuming small and constant compressibility, and small pressure gradients, multiplying Eq. B.11 by (-*n*):

$$\frac{\partial^2 p}{\partial r^2}+\frac{n}{r}\frac{\partial p}{\partial r}=\phi\, c_t\, n\left[\frac{\mu_{eff}}{k_r}\right]^{\frac{1}{n}}\left[-\frac{\partial p}{\partial r}\right]^{\frac{n-1}{n}}\frac{\partial p}{\partial t} \quad \text{.....(B.12)}$$

Ikoku and Ramey (1979) proposed a linearization form as follows:

$$\left[-\frac{\partial p}{\partial r}\right]^{\frac{1}{n}} = \left[\frac{\mu_{eff}}{k_r}\right]^{\frac{1}{n}} v_r \approx \left[\frac{\mu_{eff}}{k_r}\right]^{\frac{1}{n}} \frac{q}{2\pi hr}, \quad \text{.....(B.13)}$$

Or

$$\left[-\frac{\partial p}{\partial r}\right] = \frac{\mu_{eff}}{k_r}\left[\frac{q}{2\pi hr}\right]^{n}, \quad \text{.....(B.14)}$$

Substituting Eq. B.14 into Eq. B.12 and simplifying terms gives:

$$\frac{\partial^2 p}{\partial r^2} + \frac{n}{r}\frac{\partial p}{\partial r} = G\, r^{1-n}\, \frac{\partial p}{\partial t} \quad \text{.....(B.15)}$$

Where the apparent hydraulic diffusivity coefficient is defined as:

$$G = \frac{\phi\, \mu_{eff}\, c_t\, n}{k_r}\left[\frac{2\pi h}{q}\right]^{1-n}, \quad \text{.....(B.16)}$$

In order to transform Eq. B.15 to dimensionless form, following dimensionless variables are used.

Dimensionless Pressure:

$$p_{DNN} = \frac{p - p_i}{\left[\frac{q}{2\pi h}\right]^{n} \frac{\mu_{eff}\, r_w^{1-n}}{k_r}}, \quad \text{.....(B.17)}$$

Dimensionless Time:

$$t_{DNN} = \frac{t}{G\, r_w^{3-n}}, \quad \text{.....(B.18)}$$

Dimensionless Radius:

$$r_D = \frac{r}{r_w} \quad \text{.....(B.19)}$$

Based on Eqs. B.17-B.19, the dimensionless form of Eq. B.15 becomes:

$$\frac{\partial^2 p_{DNN}}{\partial r_D^2} + \frac{n}{r_D}\frac{\partial p_{DNN}}{\partial r_D} = r_D^{1-n}\frac{\partial p_{DNN}}{\partial t_{DNN}} \quad \text{.....(B.20)}$$

In order to provide a solution suitable for well test analysis the following initial and boundary conditions are established:

Initial Condition: *Uniform pressure distribution*

$$p_{DNN}\ (r_D, t_D = 0) = 0\ , \quad \text{.....(B.21)}$$

Inner Boundary Condition: *Constant Flowrate*

$$\left[r_D \frac{dp_{DNN}\ (r_D, t_D)}{r_D} \right]_{r_D = 1} = -1\ , \quad \text{.....(B.22)}$$

Outer Boundary Condition: *Infinite-Acting Reservoir*

$$\lim_{r_D \to \infty} p_{DNN}\ (r_D, t_D) = 0 \quad \text{.....(B.23)}$$

Applying the Laplace Transform to Eq. B.20:

$$\frac{d^2 \bar{p}_{DNN}\ (r_D, u)}{dr_D^2} + \frac{n}{r_D}\frac{d\bar{p}_{DNN}\ (r_D, u)}{dr_D} = r_D^{1-n}\, u\, \bar{p}_{DNN}\ (r_D, u)\ , \quad \text{.....(B.24)}$$

In order to obtain a particular solution in the Laplace domain, the Laplace transform of the boundary conditions are required. The Laplace transform of the inner boundary condition is:

$$\left[r_D \frac{d\bar{p}_{DNN}\ (r_D, u)}{dr_D} \right]_{r_D = 1} = -\frac{1}{u}\ , \quad \text{.....(B.25)}$$

The Laplace transform of the outer boundary condition is:

$$\lim_{r_D \to \infty} \bar{p}_{DNN}\ (r_D, u) = 0 \quad \text{.....(B.26)}$$

Multiplying Eq. B.24 by r_D^2 :

$$r_D^2 \frac{d^2 \overline{p}_{DNN}(r_D,u)}{dr_D^2} + r_D n \frac{d\overline{p}_{DNN}(r_D,u)}{dr_D} = r_D^{3-n} u \overline{p}_{DNN}(r_D,u). \quad \text{(B.27)}$$

The parameter δ is defined as:

$$\delta = \frac{1-n}{2}, \quad \text{(B.28)}$$

Therefore, Eq. B.27 can be expressed as:

$$r_D^2 \frac{d^2 \overline{p}_{DNN}(r_D,u)}{dr_D^2} + (1-2\delta) r_D \frac{d\overline{p}_{DNN}(r_D,u)}{dr_D} = r_D^{3-n} u \overline{p}_{DNN}(r_D,u) \quad \text{(B.29)}$$

The following transform function is defined:

$$\overline{p}_{DNN}(r_D,u) = \overline{G}_D(z), \quad \text{(B.30)}$$

Where the transform variable is defined as:

$$z = \frac{2\sqrt{u}}{3-n} r_D^{\frac{3-n}{2}}, \quad \text{(B.31)}$$

Substituting Eqs. B.30 and B.31 into Eq. B29, we have:

$$z^2 \frac{d^2 \overline{G}_D(z)}{dz^2} + (1-2\nu) z \frac{d\overline{G}_D(z)}{dz} = z^2 \overline{G}_D(z), \quad \text{(B.32)}$$

Where the ν parameter is defined as:

$$\nu = \frac{1-n}{3-n} \quad \text{(B.33)}$$

To set the coefficient of first derivative term in Eq. B.32 to one, the following equation is proposed:

$$\overline{G}_D(z) = \frac{z^\nu}{\psi} B_D(z), \quad \text{(B.34)}$$

where:

$$\psi = \left[\frac{2\sqrt{u}}{3-n} \, r_D^{\frac{3-n}{2}} \right]^{\frac{1-n}{3-n}} \quad \text{.....(B.35)}$$

Applying the transformation given by Eqs. B.34 and B.35 to Eq.B.32, we obtain the form:

$$z^2 \frac{d^2 B_D(z)}{dz^2} + z \frac{dB_D(z)}{dz} = (\nu^2 + z^2) B_D(z) \text{ , ...(B.36)}$$

Where the general solution of Eq. B.36 is:

$$B_D(z) = C_1 I_\nu(z) + C_2 K_\nu(z) \text{ . .....(B.37)}$$

Using the transform definition (*i.e.*, Eq.B.34), Eq. B.37 becomes:

$$\overline{G}_D(z) = \frac{z^\nu}{\psi} \left[C_1 I_\nu(z) + C_2 K_\nu(z) \right] \text{ , ...(B.38)}$$

Therefore in terms of forms given by Eq.B.27, we have:

$$\overline{p}_{DNN}(r_D, u) = r_D^{\frac{1-n}{2}} \left[C_1 \, I_{\frac{1-n}{3-n}} \left[r_D^{\frac{3-n}{2}} \frac{2\sqrt{u}}{3-n} \right] + C_2 \, K_{\frac{1-n}{3-n}} \left[r_D^{\frac{3-n}{2}} \frac{2\sqrt{u}}{3-n} \right] \right] \text{ .....(B.39)}$$

Applying the infinite-acting outer boundary condition to Eq.B.39, we have:

$$\lim_{r_D \to \infty} \overline{p}_{DNN}(r_D, u) = r_D^{\frac{1-n}{2}} \left[C_1 \lim_{r_D \to \infty} I_{\frac{1-n}{3-n}} \left[r_D^{\frac{3-n}{2}} \frac{2\sqrt{u}}{3-n} \right] + C_2 \lim_{r_D \to \infty} K_{\frac{1-n}{3-n}} \left[r_D^{\frac{3-n}{2}} \frac{2\sqrt{u}}{3-n} \right] \right] = 0 \text{ . (B.40)}$$

Considering the behavior of Bessel functions for large arguments, we conclude that $C_1 = 0$. As such, Eq.B.39 reduces to:

$$\overline{p}_{DNN}(r_D, u) = r_D^{\frac{1-n}{2}} \left[C_2 K_{\frac{1-n}{3-n}} \left[r_D^{\frac{3-n}{2}} \frac{2\sqrt{u}}{3-n} \right] \right] \text{ .....(B.41)}$$

Taking the derivative of Eq. B.41 with respect to r_D, and applying the inner boundary condition:

$$\left[r_D \frac{d\,\bar{p}_{DNN}\ (r_D,u)}{dr_D} \right]_{r_D=1} = -\frac{1}{u} = C_2 \left[\frac{1-n}{2} K_{\frac{1-n}{3-n}}\left[\frac{2\sqrt{u}}{3-n} \right] + K'_{\frac{1-n}{3-n}}\left[\frac{2\sqrt{u}}{3-n} \right] \sqrt{u} \right] \quad \text{.....(B.42)}$$

Or, in a more compact form, we have:

$$-\frac{1}{u} = C_2 \left[-\sqrt{u} K_{\frac{2}{3-n}}\left[\frac{2\sqrt{u}}{3-n} \right] \right], \quad \text{.....(B.43)}$$

Using Eq. B.43 and solving for the coefficient, C_2, we obtain:

$$C_2 = \frac{1}{u} \frac{1}{\sqrt{u}\, K_{\frac{2}{3-n}}\left[\frac{2\sqrt{u}}{3-n} \right]}. \quad \text{.....(B.44)}$$

Substituting Eq. B.44 into Eq. B.41 yields the solution for this case in the Laplace domain.

$$\bar{p}_{DNN}\ (r_D,u) = r_D^{\frac{1-n}{2}} \frac{K_{\frac{1-n}{3-n}}\left[r_D^{\frac{3-n}{2}} \frac{2\sqrt{u}}{3-n} \right]}{u^{\frac{3}{2}} K_{\frac{2}{3-n}}\left[\frac{2\sqrt{u}}{3-n} \right]} \quad \text{.....(B.45)}$$

APPENDIX C

PROPOSED DUAL POROSITY MODELINCLUDING NON-NEWTONIAN FLUID FLOW

(PSEUDOSTEADY-STATE INTERPOROSITY FLOW)

This Appendix presents the proposed model for a Non-Newtonian fluid through a Double Porosity Medium taking into account the interporosity transfer conditions under pseudosteady-state.

The continuity equation for a double porosity reservoir is:

$$\frac{1}{r}\frac{\partial}{\partial r}(r\rho v_r) = -\left[\frac{\partial}{\partial t}(\rho\phi_f) + \frac{\partial}{\partial t}(\rho\phi_m)\right], \quad \text{.....(C.1)}$$

According to Christopher et al. (1965);

$$v_r^n = \frac{k_r}{\mu_{eff}}\frac{\partial p}{\partial r}, \quad \text{.....(C.2)}$$

Substituting Eq.C.2 into Eq.C.1 yields:

$$\frac{1}{r}\frac{\partial}{\partial r}\left[r\rho\left[-\frac{k_f}{\mu_{eff}}\frac{\partial p_f}{\partial r}\right]^{\frac{1}{n}}\right] = -\left[\frac{\partial}{\partial t}(\rho\phi_f) + \frac{\partial}{\partial t}(\rho\phi_m)\right] \quad \text{.....(C.3)}$$

As permeability and viscosity are constant, expansion of Eq.C.3 yields the form:

$$\left[-\frac{k_f}{\mu_{eff}}\right]^{\frac{1}{n}}\left[\frac{\rho}{r}\left[\frac{\partial p_f}{\partial r}\right]^{\frac{1}{n}} + \left[\frac{\partial p_f}{\partial r}\right]^{\frac{1}{n}}\left[\frac{\partial \rho}{\partial r}\right] + \frac{\rho}{n}\left[\frac{\partial p_f}{\partial r}\right]^{\frac{1-n}{n}}\left[\frac{\partial^2 p_f}{\partial r^2}\right]\right] = \quad \text{.....(C.4)}$$

$$-\left[\frac{\partial}{\partial t}(\rho\phi_f) + \frac{\partial}{\partial t}(\rho\phi_m)\right]$$

Eq. C.4 will be handled in two parts, first the left-hand-side (LHS) and second the right-hand-side (RHS). Applying the chain rule to the LHS yields:

$$\left[-\frac{k_f}{\mu_{eff}}\right]^{\frac{1}{n}}\left[\frac{\rho}{r}\left[\frac{\partial p_f}{\partial r}\right]^{\frac{1}{n}} + \left[\frac{\partial p_f}{\partial r}\right]^{\frac{1}{n}}\left[\frac{\partial \rho}{\partial p_f}\right]\left[\frac{\partial p_f}{\partial r}\right] + \frac{\rho}{n}\left[\frac{\partial p_f}{\partial r}\right]^{\frac{1-n}{n}}\left[\frac{\partial^2 p_f}{\partial r^2}\right]\right], \quad \text{.....(C.5)}$$

Multiplying Eq.C.5 by $\frac{\rho}{\rho}$ gives us the following form:

$$\rho\left[-\frac{k_f}{\mu_{eff}}\right]^{\frac{1}{n}}\left[\frac{1}{r}\left[\frac{\partial p_f}{\partial r}\right]^{\frac{1}{n}}+\left[\frac{\partial p_f}{\partial r}\right]^{\frac{n+1}{n}}\frac{1}{\rho}\left[\frac{\partial \rho}{\partial p_f}\right]+\frac{1}{n}\left[\frac{\partial p_f}{\partial r}\right]^{\frac{1-n}{n}}\left[\frac{\partial^2 p_f}{\partial r^2}\right]\right] \quad \text{.....(C.6)}$$

Assuming compressibility and pressure gradients are small, Eq.C.6 becomes:

$$\rho\left[-\frac{k_f}{\mu_{eff}}\right]^{\frac{1}{n}}\left[\frac{\partial p_f}{\partial r}\right]^{\frac{1-n}{n}}\left[\frac{1}{n}\left[\frac{\partial^2 p_f}{\partial r^2}\right]+\frac{1}{r}\left[\frac{\partial p_f}{\partial r}\right]\right] \quad \text{.....(C.7)}$$

Expanding the RHS of Eq.C.4 we have:

$$\left[\rho\frac{\partial \phi_f}{\partial t}+\phi_f\frac{\partial \rho}{\partial t}+\rho\frac{\partial \phi_m}{\partial t}+\phi_m\frac{\partial \rho}{\partial t}\right], \quad \text{.....(C.8)}$$

Applying the chain rule to Eq.C.8:

$$\left[\rho\frac{\partial \phi_f}{\partial p_f}\frac{\partial p_f}{\partial t}+\phi_f\frac{\partial \rho}{\partial p_f}\frac{\partial p_f}{\partial t}+\rho\frac{\partial \phi_m}{\partial p_m}\frac{\partial p_m}{\partial t}+\phi_m\frac{\partial \rho}{\partial p_m}\frac{\partial p_m}{\partial t}\right], \quad \text{.....(C.9)}$$

Factoring the $\rho\phi$-product for the fracture and matrix, respectively in Eq.C.9, we have:

$$\rho\phi_f\left[\frac{1}{\phi_f}\frac{\partial \phi_f}{\partial p_f}\frac{\partial p_f}{\partial t}+\frac{1}{\rho}\frac{\partial \rho}{\partial p_f}\frac{\partial p_f}{\partial t}\right]+\rho\phi_m\left[\frac{1}{\phi_m}\frac{\partial \phi_m}{\partial p_m}\frac{\partial p_m}{\partial t}+\frac{1}{\rho}\frac{\partial \rho}{\partial p_m}\frac{\partial p_m}{\partial t}\right] \quad \text{.....(C.10)}$$

Collecting terms, Eq.C.10 becomes:

$$\rho\left[(\phi c_t)_f\frac{\partial p_f}{\partial t}+(\phi c_t)_m\frac{\partial p_m}{\partial t}\right] \quad \text{.....(C.11)}$$

Where:

$$c_t = c_o + c_r \text{ .} \quad \text{.....(C.12)}$$

Equating the LHS of Eq. C.7 and the RHS of Eq. C.11, we have:

$$\rho\left[-\frac{k_f}{\mu_{eff}}\right]^{\frac{1}{n}}\left[\frac{\partial p_f}{\partial r}\right]^{\frac{1-n}{n}}\left[\frac{1}{n}\left[\frac{\partial^2 p_f}{\partial r^2}\right]^{\frac{1}{n}}+\frac{1}{r}\left[\frac{\partial p_f}{\partial r}\right]\right]=\rho\left[(\phi c_t)_f\ \frac{\partial p_f}{\partial t}+(\phi c_t)_m\ \frac{\partial p_m}{\partial t}\right] \quad \text{.....(C.13)}$$

Re-arranging Eq. C.13 gives us:

$$\frac{1}{n}\left[\frac{\partial^2 p_f}{\partial r^2}\right]+\frac{1}{r}\left[\frac{\partial p_f}{\partial r}\right]=\left[-\frac{\mu_{eff}}{k_f}\right]^{\frac{1}{n}}\left[\frac{\partial p_f}{\partial r}\right]^{\frac{n-1}{n}}\left[(\phi c_t)_f\ \frac{\partial p_f}{\partial t}+(\phi c_t)_m\ \frac{\partial p_m}{\partial t}\right] \quad \text{.....(C.14)}$$

Ikoku and Ramey (1979) proposed the following linearization:

$$\frac{\partial p_f}{\partial r}=-\frac{\mu_{eff}}{k_f}v_r^n\approx-\frac{\mu_{eff}}{k_r}\left[\frac{q}{2\pi hr}\right]^n \quad \text{.....(C.15)}$$

Substituting Eq. C.15 into Eq. C.14 yields:

$$\frac{1}{n}\left[\frac{\partial^2 p_f}{\partial r^2}\right]+\frac{1}{r}\left[\frac{\partial p_f}{\partial r}\right]= \left[-\frac{\mu_{eff}}{k_f}\right]^{\frac{1}{n}}\left[-\frac{\mu_{eff}}{k_f}\left[\frac{q}{2\pi hr}\right]^n\right]^{\frac{n-1}{n}}\left[(\phi c_t)_f\ \frac{\partial p_f}{\partial t}+(\phi c_t)_m\ \frac{\partial p_m}{\partial t}\right] \quad \text{.....(C.16)}$$

Reduction of Eq.C.16 yields:

$$\frac{\partial^2 p_f}{\partial r^2}+\frac{n}{r}\left[\frac{\partial p_f}{\partial r}\right]=\frac{n\mu_{eff}}{k_f}\left[\frac{q}{2\pi hr}\right]^{n-1}\left[(\phi c_t)_f\ \frac{\partial p_f}{\partial t}+(\phi c_t)_m\ \frac{\partial p_m}{\partial t}\right] \quad \text{.....(C.17)}$$

The volumetric flow from the matrix (source term) may be defined as follows:

$$q^*_{m-f}=\frac{q}{V_r}, \quad \text{.....(C.18)}$$

Recalling the Blake and Kozeny modified velocity power law (Christopher et al. 1965):

$$v_r^n=-\frac{k_m}{\mu_{eff}}\frac{\Delta p_{m-f}}{\Delta L}, \quad \text{.....(C.19)}$$

Considering the effects of expansion, the flowrate (q) can be expressed as:

$$q = (\phi c_t)_m V_r \frac{\partial p_m}{\partial t}. \quad \text{(C.20)}$$

As an analog with Darcy's Law, Eq. C.19 is substituted into Eq. C.18 to yield:

$$q^*_{m-f} = \left[-\frac{k_m}{\mu_{eff}} \right]^{\frac{1}{n}} \left[\frac{\Delta p_{m-f}}{\Delta L} \right]^{\frac{1}{n}} \frac{A_{m-f}}{\Delta L\, A_\alpha}, \quad \text{(C.21)}$$

Where:

$$V_r = \Delta L\, A_\alpha, \quad \text{(C.22)}$$

Eq. C.21 can be expressed as:

$$q^*_{m-f} = \left[-\frac{k_m}{\mu_{eff}} \right]^{\frac{1}{n}} (p_m - p_f)^{\frac{1}{n}} \frac{A_{m-f}}{\Delta L^{\frac{1+n}{n}} A_\alpha}, \quad \text{(C.23)}$$

Multiplying Eq.C.23 by $\frac{\Delta L^2}{\Delta L^2}$:

$$q^*_{m-f} = \left[\frac{k_m}{\mu_{eff}} (p_f - p_m) \right]^{\frac{1}{n}} \alpha\, \Delta L^{\frac{n-1}{n}}, \quad \text{(C.24)}$$

Where:

$$\alpha = \frac{A_{m-f}}{\Delta L^2\, A_\alpha} \quad \text{(C.25)}$$

Substituting Eq. C.20 into Eq. C.18 and equating this result with Eq.C.24, we have:

$$(\phi c_t)_m \frac{\partial p_m}{\partial t} = \left[\frac{k_m}{\mu_{eff}} (p_f - p_m) \right]^{\frac{1}{n}} \alpha\, \Delta L^{\frac{n-1}{n}}, \quad \text{(C.26)}$$

Solving Eq. C.26 for the $\frac{\partial p_m}{\partial t}$ term, we have:

$$\frac{\partial p_m}{\partial t} = \frac{\alpha}{(\phi c_t)_m}\left[\frac{k_m}{\mu_{eff}}\right]^{\frac{1}{n}} \Delta L^{\frac{n-1}{n}} (p_f - p_m)^{\frac{1}{n}}, \quad \text{(C.27)}$$

We immediately note that Eq.C.27 has a pressure difference elevated to a power, which will present a very significant challenge in our quest to find a solution. In order to eliminate this situation, the following linearization is presented:

$$\frac{(p_f - p_m)}{\Delta L} = -\frac{\mu_{eff}}{k_m}\left[\frac{q_m}{\Delta L^2}\right]^n, \quad \text{(C.28)}$$

Solving for $p_f - p_m$ in Eq. C.28

$$p_f - p_m = -\frac{\mu_{eff}}{k_m}\frac{q_m^n}{\Delta L^{2n-1}}, \quad \text{(C.29)}$$

Multiplying Eq. C.27 by $\frac{p_f - p_m}{p_f - p_m}$:

$$\frac{\partial p_m}{\partial t} = \frac{\alpha}{(\phi c_t)_m}\left[\frac{k_m}{\mu_{eff}}\right]^{\frac{1}{n}} (p_f - p_m)\left[\frac{p_f - p_m}{\Delta L}\right]^{\frac{1-n}{n}}, \quad \text{(C.30)}$$

Substituting Eq.C.29 into Eq.C.30, we obtain:

$$\frac{\partial p_m}{\partial t} = \frac{\alpha}{(\phi c_t)_m}\left[\frac{k_m}{\mu_{eff}}\right]^{\frac{1}{n}} (p_f - p_m)\left[-\frac{\mu_{eff}}{k_m}\frac{q_m^n}{\Delta L^{2n-1}}\right]^{\frac{1-n}{n}}, \quad \text{(C.31)}$$

Reducing terms and simplifying Eq.C.31 yields the dimensionless non-Newtonian interface condition:

$$\frac{\partial p_m}{\partial t} = \frac{\alpha}{(\phi c_t)_m}\frac{k_m}{\mu_{eff}}\left[\frac{q_m}{\Delta L^2}\right]^{1-n} (p_f - p_m) \quad \text{(C.32)}$$

In order to transform Eq. C.17 and Eq. C.32 into dimensionless forms, the following dimensionless variables are used.

Dimensionless Pressure: *Fracture network*

$$p_{fD} = \frac{(2\pi h)^n k_f}{q^n \mu_{eff} r_w^{1-n}} (p_i - p_f), \quad \text{(C.33)}$$

Dimensionless Pressure: *Matrix system*

$$p_{mD} = \frac{(2\pi h)^n k_f}{q^n \mu_{eff} r_w^{1-n}} (p_i - p_m), \quad \text{(C.34)}$$

Dimensionless Time:

$$t_D = \frac{q^{1-n} k_f}{n(\phi c_t)_t (2\pi h)^{1-n} \mu_{eff} r_w^{3-n}} t, \quad \text{(C.35)}$$

Where the *total expansion* term for the reservoir is given as:

$$(\phi c_t)_t = (\phi c_t)_f + (\phi c_t)_m, \quad \text{(C.36)}$$

Dimensionless Radius:

$$r_D = \frac{r}{r_w}, \quad \text{(C.37)}$$

Solving p_f, p_m, t and r respectively in order to transform Eqs. C.17 and C.32:

$$p_f = p_i - \frac{q^n \mu_{eff} r_w^{1-n}}{(2\pi h)^n k_f} p_{fD} \quad \text{(C.38)}$$

$$p_m = p_i - \frac{q^n \mu_{eff} r_w^{1-n}}{(2\pi h)^n k_f} p_{mD} \quad \text{(C.39)}$$

$$t = \frac{n(\phi c_t)_t (2\pi h)^{1-n} r_w^{3-n} \mu_{eff}}{q^{1-n} k_f} t_D \quad \text{(C.40)}$$

$$r = r_D r_w \quad \text{(C.41)}$$

Eqs.C.38-C.41 are substituted into the LHS of Eq. C.17 to yield:

$$\frac{1}{r_w^2}\frac{\partial^2\left[p_i-\frac{q^n\mu_{eff}\,r_w^{1-n}}{(2\pi h)^n k_f}p_{fD}\right]}{\partial r^2}+\frac{n}{r_D r_w}\frac{\partial\left[p_i-\frac{q^n\mu_{eff}\,r_w^{1-n}}{(2\pi h)^n k_f}p_{fD}\right]}{\partial(r_D r_w)}, \quad \text{.....(C.42)}$$

Simplifying Eq. C.42, we have:

$$-\frac{q^n\mu_{eff}\,r_w^{1-n}}{(2\pi h)^n k_f}\left[\frac{1}{r_w^2}\frac{\partial^2 p_{fD}}{\partial r_D^2}+\frac{1}{r_D r_w^2}\frac{\partial p_{fD}}{\partial r_D}\right], \quad \text{.....(C.43)}$$

Eqs.C.38-C.41 are substituted into the RHS of Eq. C.17 to yield:

$$\frac{n\,\mu_{eff}}{k_f}\left[\frac{q}{2\pi h\, r_D r_w}\right]^{n-1}\left[(\phi c_t)_f\frac{\partial\left[p_i-\frac{q^n\mu_{eff}\,r_w^{1-n}}{(2\pi h)^n k_f}p_{fD}\right]}{\partial\left[\frac{n(\phi c_t)_t(2\pi h)^{1-n}\,r_w^{3-n}\mu_{eff}}{q^{1-n}k_f}t_D\right]}+(\phi c_t)_m\frac{\partial\left[p_i-\frac{q^n\mu_{eff}\,r_w^{1-n}}{(2\pi h)^n k_f}p_{mD}\right]}{\partial\left[\frac{n(\phi c_t)_t(2\pi h)^{1-n}\,r_w^{3-n}\mu_{eff}}{q^{1-n}k_f}t_D\right]}\right]$$

, ...(C.44)

Simplifying Eq. C.44, we have:

$$\frac{\mu_{eff}}{k_f}\frac{q^n}{(2\pi h)^n r_w^{n-1}}\frac{1}{r_D^{n-1}r_w^2}\left[\omega\frac{\partial p_{fD}}{\partial t_D}+(1-\omega)\frac{\partial p_{mD}}{\partial t_D}\right], \quad \text{.....(C.45)}$$

Equating the forms given by Eq.C.43 Eq.C.45, we obtain:

$$-\frac{q^n\mu_{eff}\,r_w^{1-n}}{(2\pi h)^n k_f}\left[\frac{1}{r_w^2}\frac{\partial^2 p_{Df}}{\partial r_D^2}+\frac{1}{r_D r_w^2}\frac{\partial p_{Df}}{\partial r_D}\right]=$$

, ...(C.46)

$$\frac{\mu_{eff}}{k_f}\frac{q^n}{(2\pi h)^n r_w^{n-1}}\frac{1}{r_D^{n-1}r_w^2}\left[\omega\frac{\partial p_{Df}}{\partial t_D}+(1-\omega)\frac{\partial p_{mD}}{\partial t_D}\right]$$

Rearranging Eq.C.45, we have:

$$\frac{\partial^2 p_{fD}}{\partial r_D^2}+\frac{n}{r_D}\frac{\partial p_{fD}}{\partial r_D}=r_D^{1-n}\left[\omega\frac{\partial p_{fD}}{\partial t_D}+(1-\omega)\frac{\partial p_{mD}}{\partial t_D}\right] \quad \text{.....(C.47)}$$

Where the storativity ratio (ω) is defined as:

$$\omega = \frac{(\phi c_t)_f}{(\phi c_t)_t}, \quad \text{(C.48)}$$

In order to transform the interface condition into dimensionless form the interface condition, we recall the LHS of Eq. C.32 and substitute Eqs. C.39 and C.40 to obtain:

$$\frac{\partial\left[p_i - \frac{q^n \mu_{eff}\, r_w^{1-n}}{(2\pi h)^n k_f} p_{mD}\right]}{\partial\left[\frac{n(\phi c_t)_t (2\pi h)^{1-n} r_w^{3-n} \mu_{eff}}{q^{1-n} k_f} t_D\right]}, \quad \text{(C.49)}$$

Simplifying Eq. C.49, we have:

$$-\frac{q}{n(\phi c_t)_t (2\pi h) r_w^2}\left[\frac{\partial p_{mD}}{\partial t_D}\right], \quad \text{(C.50)}$$

Substituting Eq.C.38 and C.39 into the RHS of Eq. C.32, we have:

$$\frac{\alpha}{(\phi c_t)_m}\frac{k_m}{\mu_{eff}}\left[\frac{q_m}{\Delta L^2}\right]^{1-n}\left[p_i - \frac{q^n \mu_{eff}\, r_w^{1-n}}{(2\pi h)^n k_f} p_{fD} - p_i + \frac{q^n \mu_{eff}\, r_w^{1-n}}{(2\pi h)^n k_f} p_{mD}\right], \quad \text{(C.51)}$$

Simplifying Eq. C.51, we have:

$$\frac{\alpha}{(\phi c_t)_m}\frac{k_m}{k_f}\left[\frac{q_m}{\Delta L^2}\right]^{1-n}\left[-\frac{q^n r_w^{1-n}}{(2\pi h)^n}\right](p_{fD} - p_{mD}) \quad \text{(C.52)}$$

Equating Eqs. C.50 and C.52, we obtain:

$$-\frac{q}{n(\phi c_t)_t (2\pi h) r_w^2}\left[\frac{\partial p_{mD}}{\partial t_D}\right] = \frac{\alpha}{(\phi c_t)_m}\frac{k_m}{k_f}\left[\frac{q_m}{\Delta L^2}\right]^{1-n}\left[-\frac{q^n r_w^{1-n}}{(2\pi h)^n}\right](p_{fD} - p_{mD}), \quad \text{(C.53)}$$

Solving for Eq. C.53 for $\frac{\partial p_{mD}}{\partial t_D}$ yields:

$$\frac{\partial p_{mD}}{\partial t_D} = n\frac{(\phi c_t)_t}{(\phi c_t)_m}\alpha\frac{k_m}{k_f} r_w^2\left[\frac{q_m}{\Delta L^2}\right]^{1-n}(q^{n-1}(2\pi h)^{1-n} r_w^{1-n})(p_{fD} - p_{mD}), \quad \text{(C.54)}$$

Where λ, the interface interporosity flow coefficient is defined as:

$$\lambda = \alpha \frac{k_m}{k_f} r_w^2 , \quad \text{(C.55)}$$

Substituting Eqs. C.53 and C.54 into Eq. C.52 yields:

$$\frac{\partial p_{mD}}{\partial t_D} = \frac{n\lambda}{(1-\omega)} \left[\frac{q_m}{q} \frac{2\pi h r_w}{\Delta L^2} \right]^{1-n} (p_{fD} - p_{mD}) \quad \text{(C.56)}$$

Where the dimensionless interporosity flowrate is:

$$\frac{q_m}{q} , \quad \text{(C.57)}$$

And the dimensionless interporosity term is:

$$\frac{2\pi h r_w}{\Delta L^2} \quad \text{(C.58)}$$

Defining a dimensionless variable which we term the *dimensionless matrix contribution*, we combine Eq. C.57 and Eq. C.58 to yield:

$$D = \frac{q_m}{q} \frac{2\pi h r_w}{\Delta L^2} , \quad \text{(C.59)}$$

Using the definition given by Eq. C.59, then Eq.C.56 becomes:

$$\frac{\partial p_{Dm}}{\partial t_D} = \frac{n\lambda}{(1-\omega)} D^{1-n} (p_{fD} - p_{mD}) \quad \text{(C.60)}$$

In order to provide a solution suitable for well test analysis the following initial and boundary conditions are established in dimensionless variables:

Initial Condition: *Uniform pressure distribution*

$$p_{fD}(r_D, t_D = 0) = 0 , \quad \text{(C.61)}$$

Inner Boundary Condition: *Constant flowrate*

$$\left[r_D \frac{dp_{fD}(r_D, t_D)}{dr_D} \right]_{r_D = 1} = -1 , \quad \text{(C.62)}$$

Outer Boundary Condition: *Infinite acting reservoir*

$$\lim_{r_D \to \infty} p_{fD}(r_D, t_D) = 0 \quad \text{.....(C.63)}$$

The Laplace Transform is used to solve Eq.C.46 and Eq. C.60. Taking the Laplace transform of Eq.A.46:

$$\frac{d^2 \bar{p}_{fD}(r_D, u)}{dr_D^2} + \frac{n}{r_D} \frac{d \bar{p}_{fD}(r_D, u)}{dr_D} = r_D^{1-n} \left[\omega (u \bar{p}_{fD}(r_D, u)) + (1-\omega)(u \bar{p}_{mD}(r_D, u)) \right], \text{.....(C.64)}$$

Substituting Eq. C.60 into Eq. C.64:

$$\frac{d^2 \bar{p}_{fD}(r_D, u)}{dr_D^2} + \frac{n}{r_D} \frac{d \bar{p}_{fD}(r_D, u)}{dr_D} = r_D^{1-n} \left[\omega (u \bar{p}_{fD}(r_D, u)) + (1-\omega) \left[u \frac{n \lambda D^{1-n}}{u(1-\omega) + n \lambda D^{1-n}} \bar{p}_{fD}(r_D, u) \right] \right], \text{.....(C.65)}$$

Factoring the $u \bar{p}_{fD}(u)$ term from Eq.C.65 yields

$$\frac{d^2 \bar{p}_{fD}(r_D, u)}{dr_D^2} + \frac{n}{r_D} \frac{d \bar{p}_{fD}(r_D, u)}{dr_D} = r_D^{1-n} \left[u \bar{p}_{fD}(r_D u) \frac{u(1-\omega)\omega + n \lambda D^{1-n}}{u(1-\omega) + n \lambda D^{1-n}} \right], \text{.....(C.66)}$$

Where the interporosity flow function for this case is given by:

$$g(u) = \frac{u(1-\omega)\omega + n \lambda D^{1-n}}{u(1-\omega) + n \lambda D^{1-n}}, \text{.....(C.67)}$$

Substitution of Eq. C.67 into Eq.C.66, we have:

$$\frac{d^2 \bar{p}_{fD}(r_D, u)}{dr_D^2} + \frac{n}{r_D} \frac{d \bar{p}_{fD}(r_D, u)}{dr_D} = r_D^{1-n} \left[u g(u) \bar{p}_{fD}(r_D, u) \right], \text{.....(C.68)}$$

Multiplying Eq. C.68 by r_D^2 gives us:

$$r_D^2 \frac{d^2 \bar{p}_{fD}(r_D, u)}{dr_D^2} + n r_D \frac{d \bar{p}_{fD}(r_D, u)}{dr_D} = r_D^{3-n} \left[u g(u) \bar{p}_{fD}(r_D, u) \right] \text{.....(C.69)}$$

Taking the Laplace transform of Eq. C.60:

$$u\,\bar{p}_{mD}(r_D,u) - p_{mD}(r_D,0) = \frac{n\lambda}{(1-\omega)} D^{1-n}\left(\bar{p}_{fD}(r_D,u) - \bar{p}_{mD}(r_D,u)\right), \quad \text{.....(C.70)}$$

Solving for the $\bar{p}_{mD}(u)$ function in Eq. C.70 we have:

$$\bar{p}_{mD}(r_D,u) = \frac{n\,\lambda\,D^{1-n}}{u(1-\omega) + n\,\lambda\,D^{1-n}}\,\bar{p}_{fD}(r_D,u) \quad \text{.....(C.71)}$$

In order to solve Eq. C.69 the δ parameter is defined as:

$$\delta = \frac{1-n}{2}, \quad \text{.....(C.72)}$$

Using the δ parameter, Eq. C.69 can be expressed as:

$$r_D^2\,\frac{d^2\bar{p}_{DNN}(r_D,u)}{dr_D^2} + (1-2\delta)\,r_D\,\frac{d\,\bar{p}_{DNN}(r_D,u)}{dr_D} = r_D^{3-n}u\,\bar{p}_{DNN}(r_D,u), \quad \text{.....(C.73)}$$

Similar to Ikoku and Ramey (1979), we define the following transform function:

$$\bar{p}_{fD}(r_D,u) = \bar{H}_D(z), \quad \text{.....(C.74)}$$

Where this form uses the transformation variable (z):

$$z = \frac{2\sqrt{ug(u)}}{3-n} r_D^{\frac{3-n}{2}}, \quad \text{.....(C.75)}$$

Using the definitions prescribed by Eqs. C.74 and C.75, we obtain:

$$z^2\,\frac{d^2\bar{H}_D(z)}{dz^2} + (1-2\nu)z\,\frac{d\bar{H}_D(z)}{dz} = z^2\bar{H}_D(z), \quad \text{.....(C.76)}$$

Where, as in the case of Ikoku and Ramey (1979), we obtain:

$$\nu = \frac{1-n}{3-n}, \quad \text{.....(C.77)}$$

To set the coefficient of first derivative term in Eq. C.73 to one, the following equation is proposed:

$$\overline{H}_D(z) = \frac{z^{\nu}}{\psi}\overline{B}_D(z)\,, \quad \text{.....(C.78)}$$

Where:

$$\psi = \left[\frac{2\sqrt{ug(u)}}{3-n}\right]^{\frac{1-n}{3-n}}\,, \quad \text{.....(C.79)}$$

Therefore Eq. C.76 can be expressed in terms of Eq. C.78 as:

$$z^2\frac{d^2\overline{B}_D(z)}{dz^2} + z\frac{d\overline{B}_D(z)}{dz} = (\nu^2 + z^2)\overline{B}_D(z)\,, \quad \text{.....(C.80)}$$

Where the solution is given by:

$$\overline{B}_D(z) = C_1 I_{\nu}(z) + C_2 K_{\nu}(z) \quad \text{.....(C.81)}$$

Recalling the change of variable from Eq. C.78 and Eq. C.80, we have:

$$\overline{H}_D(z) = r_D^{\frac{1-n}{2}}\left[C_1 I_{\nu}(z) + C_2 K_{\nu}(z)\right], \quad \text{.....(C.82)}$$

And Eq. C.82 may be written as:

$$\overline{p}_{fD}(r_D, u) = r_D^{\frac{1-n}{2}}\left[C_1 I_{\frac{1-n}{3-n}}\left[r_D^{\frac{3-n}{2}}\frac{2\sqrt{ug(u)}}{3-n}\right] + C_2 K_{\frac{1-n}{3-n}} r_D^{\frac{3-n}{2}}\frac{2\sqrt{ug(u)}}{3-n}\right] \quad \text{.....(C.83)}$$

In order to solve for the coefficinrEq. C.83 it is necessary to use initial and boundary conditions.

Initial Condition: *Uniform pressure distribution*

$$\overline{p}_{fD}(r_D, u=0) = 0\,, \quad \text{.....(C.84)}$$

Inner Boundary Condition: *Constant flowrate*

$$\left[r_D\frac{d\,\overline{p}_{fD}(r_D,u)}{dr_D}\right]_{r_D=1} = -\frac{1}{u}\,, \quad \text{.....(C.85)}$$

Outer Boundary Condition: *Infinite-acting reservoir system*

$$\lim_{r_D \to \infty} \bar{p}_{Df}(r_D, u) = 0 \,, \quad \text{.....(C.86)}$$

Applying the outer boundary condition to Eq.C.83 we conclude that $C_1 = 0$ to assure "bounded-ness" of the solution. Simultaneously, applying the inner boundary condition (constant flowrate), we have:

$$-\frac{1}{u} = C_2 \left[\frac{1-n}{2} K_{\frac{1-n}{3-n}} \left[r_D^{\frac{3-n}{2}} \frac{2\sqrt{ug(u)}}{3-n} \right] + K'_{\frac{1-n}{3-n}} \left[r_D^{\frac{3-n}{2}} \frac{2\sqrt{ug(u)}}{3-n} \right] \sqrt{ug(u)} \right], \quad \text{.....(C.87)}$$

Using the properties of Bessel functions to reduce Eq.C.87:

$$-\frac{1}{u} = C_2 \left[-\sqrt{ug(u)} K_{\frac{2}{3-n}} \left[\frac{2\sqrt{ug(u)}}{3-n} \right] \right], \quad \text{.....(C.88)}$$

Solving for C_2:

$$C_2 = \frac{1}{u} \frac{1}{\sqrt{u\, g(u)} K_{\frac{2}{3-n}} \left[\frac{2\sqrt{ug(u)}}{3-n} \right]}, \quad \text{.....(C.89)}$$

Substituting Eq.C.89 into Eq.C.83 yields the particular solution in the Laplace domain:

$$\bar{p}_{fD}(r_D, u) = \frac{r_D^{\frac{1-n}{2}} K_{\frac{1-n}{3-n}} \left[r_D^{\frac{3-n}{2}} \frac{2\sqrt{ug(u)}}{3-n} \right]}{u\sqrt{ug(u)} K_{\frac{2}{3-n}} \left[\frac{2\sqrt{ug(u)}}{3-n} \right]} \quad \text{.....(C.90)}$$

As validation, we note that when note that when n=1, Eq. C.90 reduces to the general solution for pesudosteady-state double porosity model (*i.e.*, the Warrant and Root case).

APPENDIX D

CLOSED RESERVOIR AT THE OUTER BOUNDARY AND

CONSTANT RATE AT THE WELLBORE

This appendix presents the outer boundary case referred as constant pressure at the reservoir boundary. Recalling the general solution obtained for the double porosity model including non-Newtonian fluid flow (pseudosteady-state interporosity flow):

$$\bar{p}_{fD}(r_D,u) = r_D^{\frac{1-n}{2}}\left[C_1 I_\nu(r_D^{\varepsilon}h(u)) + C_2 K_\nu(r_D^{\varepsilon}h(u))\right], \quad \text{(D.1)}$$

Where:

$$g(u) = \frac{u(1-\omega)\omega + n\lambda\, D^{1-n}}{u(1-\omega)\omega + n\lambda\, D^{1-n}}, \quad \text{(D.2)}$$

$$\nu = \frac{1-n}{3-n}, \quad \text{(D.3)}$$

$$\varepsilon = \frac{3-n}{2}, \quad \text{(D.4)}$$

And

$$h(u) = \frac{2\sqrt{u\, g(u)}}{3-n}. \quad \text{(D.5)}$$

In order to obtain the constants from Eq.D.1, it is necessary to use boundary conditions.

Inner boundary condition, constant flowrate;

$$r_D \left.\frac{d\,\bar{p}_{fD}(r_D,u)}{dr_D}\right|_{r_D=1} = -\frac{1}{u}, \quad \text{(D.6)}$$

And outer boundary condition, closed reservoir

$$\left.\frac{d\,\bar{p}_{fD}(r_D,u)}{dr_D}\right|_{r_D=r_{eD}} = 0 \quad \text{(D.7)}$$

Deriving Eq.D.1

$$\frac{d\bar{p}_{fD}(r_D,u)}{dr_D} = C_1 r_D^{\frac{-1-n}{2}}\left[h(u)\varepsilon\, r_D^{\varepsilon}\, I_{\nu-1}(h(u)r_D^{\varepsilon})\right] - C_2 r_D^{\frac{-1-n}{2}}\left[h(u)\varepsilon\, r_D^{\varepsilon}\, K_{\nu-1}(h(u)r_D^{\varepsilon})\right], \quad \text{.....(D.8)}$$

Applying inner boundary condition, constant flowrate,

$$C_1\left[h(u)\varepsilon\; I_{\nu-1}(h(u)r_D^{\varepsilon})\right] - C_2\left[h(u)\varepsilon\, K_{\nu-1}(h(u)r_D^{\varepsilon})\right] = -\frac{1}{u} \quad \text{.....(D.9)}$$

Applying outer boundary condition, closed reservoir, $r_D=r_{eD}$;

$$C_1 r_{eD}^{\frac{-1-n}{2}}\left[h(u)\varepsilon\, r_{eD}^{\varepsilon}\; I_{\nu-1}(h(u)r_{eD}^{\varepsilon})\right] - C_2 r_{eD}^{\frac{-1-n}{2}}\left[h(u)\varepsilon\, r_{eD}^{\varepsilon}\; K_{\nu-1}(h(u)r_{eD}^{\varepsilon})\right] = 0\,, \quad \text{.....(D.10)}$$

Solving for C_1;

$$C_1 = C_2\,\frac{K_{\nu-1}(r_{eD}^{\varepsilon}\,h(u))}{I_{\nu-1}(r_{eD}^{\varepsilon}\,h(u))}\,. \quad \text{.....(D.11)}$$

Substituting Eq.D.11 in Eq.D.9, r_D=1

$$C_2\,\frac{K_{\nu-1}(r_{eD}^{\varepsilon}\,h(u))}{I_{\nu-1}(r_{eD}^{\varepsilon}\,h(u))}\left[h(u)\varepsilon\; I_{\nu-1}(h(u))\right] - C_2\left[h(u)\varepsilon\, K_{\nu-1}(h(u))\right] = -\frac{1}{u}, \quad \text{.....(D.12)}$$

Arranging and factorizing terms:

$$C_2\left[\frac{K_{\nu-1}(r_{eD}^{\varepsilon}\,h(u))\; I_{\nu-1}(h(u)) - K_{\nu-1}(h(u))\; I_{\nu-1}(h(u)r_D^{\varepsilon})}{I_{\nu-1}(r_{eD}^{\varepsilon}\,h(u))}\right] = -\frac{1}{u\,h(u)\,\varepsilon}\,, \quad \text{.....(D.13)}$$

Solving for C_2

$$C_2 = \frac{1}{u\,h(u)\,\varepsilon}\left[\frac{I_{\nu-1}(r_{eD}^{\varepsilon}\,h(u))}{K_{\nu-1}(h(u))\; I_{\nu-1}(h(u)r_D^{\varepsilon}) - K_{\nu-1}(h(u)\,r_D^{\varepsilon})\; I_{\nu-1}(h(u))}\right]. \quad \text{.....(D.14)}$$

Hence substituting Eq.D.14 in Eq.D.11 gets

$$C_1 = \frac{1}{u\, h(u)\, \varepsilon}\left[\frac{K_{\nu-1}(r_{eD}^{\varepsilon} h(u))}{K_{\nu-1}(h(u))\, I_{\nu-1}(h(u) r_D^{\varepsilon}) - K_{\nu-1}(h(u)\, r_D^{\varepsilon})\, I_{\nu-1}(h(u))}\right] \quad \text{.....(D.15)}$$

Therefore substituting C_1 and C_2 into Eq. D.1, we obtain the solution in the Laplace domain:

$$\overline{p}_{fD}(r_D, u) = r_D^{\frac{1-n}{2}}\, \frac{1}{u\, h(u)\, \varepsilon}\left[\frac{K_{\nu-1}(r_{eD}^{\varepsilon} h(u)) I_{\nu}(h(u) r_D^{\varepsilon}) + I_{\nu-1}(r_{eD}^{\varepsilon} h(u)) K_{\nu}(h(u) r_D^{\varepsilon})}{K_{\nu-1}(h(u))\, I_{\nu-1}(h(u) r_D^{\varepsilon}) - K_{\nu-1}(h(u)\, r_D^{\varepsilon})\, I_{\nu-1}(h(u))}\right] \quad \text{.....(D.16)}$$

APPENDIX E

CONSTANT PRESSURE AT THE OUTER BOUNDARY AND

CONSTANT RATE AT THE WELLBORE

This appendix presents the outer boundary case referred as constant pressure at the reservoir boundary. Recalling the general solution obtained for the double porosity model including non-Newtonian fluid flow (pseudosteady-state interporosity flow):

$$\bar{p}_{fD}(r_D,u) = r_D^{\frac{1-n}{2}}\left[C_1 I_\nu(r_D^{\varepsilon}h(u)) + C_2 K_\nu(r_D^{\varepsilon}h(u))\right], \quad \text{(E.1)}$$

Where:

$$g(u) = \frac{u(1-\omega)\omega + n\lambda D^{1-n}}{u(1-\omega) + n\lambda D^{1-n}}, \quad \text{(E.2)}$$

$$\nu = \frac{1-n}{3-n}, \quad \text{(E.3)}$$

$$\varepsilon = \frac{3-n}{2}, \quad \text{(E.4)}$$

And

$$h(u) = \frac{2\sqrt{ug(u)}}{3-n}. \quad \text{(E.5)}$$

In order to obtain the constants from Eq.E.1, it is necessary to use boundary conditions.

Inner Boundary Condition: Constant flowrate

$$r_D \left.\frac{d\,\bar{p}_{fD}(r_D,u)}{dr_D}\right|_{r_D=1} = -\frac{1}{u}, \quad \text{(E.6)}$$

Outer Boundary Condition: Constant pressure at the reservoir boundary

$$\bar{p}_{fD}(r_{eD},u) = 0. \quad \text{(E.7)}$$

Applying the outer boundary condition to Eq.E.1

$$\bar{p}_{fD}(r_D = r_{eD}, u) = r_{eD}^{\frac{1-n}{2}}\left[C_1 I_\nu(r_{eD}^{\varepsilon} h(u)) + C_2 K_\nu(r_{eD}^{\varepsilon} h(u))\right] = 0 \text{ , ...(E.8)}$$

Solving for C_1

$$C_1 = -C_2 \frac{K_\nu(r_{eD}^{\varepsilon} h(u))}{I_\nu(r_{eD}^{\varepsilon} h(u))} \text{ . .....(E.9)}$$

Taking the derivative of Eq. E.1 with respect to r_D, we have:

$$\frac{d\bar{p}_{fD}(r_D, u)}{dr_D} = C_1 r_D^{\frac{-1-n}{2}}\left[h(u)\varepsilon\, r_D^{\varepsilon}\, I_{\nu-1}(h(u) r_D^{\varepsilon})\right] - C_2 r_D^{\frac{-1-n}{2}}\left[h(u)\varepsilon\, r_D^{\varepsilon}\, K_{\nu-1}(h(u) r_D^{\varepsilon})\right], \text{.....(E.10)}$$

Hence applying inner boundary condition to Eq.E.10:

$$r_D^n \frac{d\bar{p}_{fD}(r_D = 1, u)}{dr_D} = C_1\left[h(u)\varepsilon\, I_{\nu-1}(h(u))\right] - C_2\left[h(u)\varepsilon\, K_{\nu-1}(h(u))\right] = -\frac{1}{u} \text{ , ...(E.11)}$$

Reduction of Eq.E.11 yields:

$$C_1 I_{\nu-1}(h(u)) - C_2 K_{\nu-1}(h(u)) = -\frac{1}{uh(u)\varepsilon} \text{ ,.....(E.12)}$$

Substituting Eq. E.9 into Eq. E.12:

$$-C_2 \frac{K_\nu(r_{eD}^{\varepsilon} h(u))}{I_\nu(r_{eD}^{\varepsilon} h(u))} I_{\nu-1}(h(u)) - C_2 K_{\nu-1}(h(u)) = -\frac{1}{uh(u)\varepsilon} \text{ , ...(E.13)}$$

Factoring for C_2, we have:

$$C_2\left[\frac{K_\nu(r_{eD}^{\varepsilon} h(u)) I_{\nu-1}(h(u)) + K_{\nu-1}(h(u)) I_\nu(r_{eD}^{\varepsilon} h(u))}{I_\nu(r_{eD}^{\varepsilon} h(u))}\right] = \frac{1}{uh(u)\varepsilon} \text{ ,.....(E.14)}$$

Solving for C_2, we have:

$$C_2 = \frac{1}{uh(u)\varepsilon}\left[\frac{I_\nu(r_{eD}^{\varepsilon} h(u))}{K_\nu(r_{eD}^{\varepsilon} h(u)) I_{\nu-1}(h(u)) + K_{\nu-1}(h(u)) I_\nu(r_{eD}^{\varepsilon} h(u))}\right] \text{ . .....(E.15)}$$

Substituting Eq. E.14 into Eq. E.9 yields

$$C_1 = -\frac{1}{uh(u)\varepsilon}\left[\frac{K_\nu(r_{eD}^{\varepsilon}h(u))}{K_\nu(r_{eD}^{\varepsilon}h(u))I_{\nu-1}(h(u)) + K_{\nu-1}(h(u))I_\nu(r_{eD}^{\varepsilon}h(u))}\right] \quad \text{.....(E.16)}$$

Therefore substituting C_1 and C_2 into Eq. E.1, we obtain the solution in the Laplace domain:

$$\overline{p}_{fD}(r_D, u) = r_D^{\frac{1-n}{2}}\frac{1}{u\,h(u)\varepsilon}\left[\frac{I_\nu(r_{eD}^{\varepsilon}h(u))K_\nu(h(u)r_D^{\varepsilon}) - K_\nu(r_{eD}^{\varepsilon}h(u))I_\nu(h(u)r_D^{\varepsilon})}{K_\nu(r_{eD}^{\varepsilon}h(u))I_{\nu-1}(h(u)) + K_{\nu-1}(h(u))I_\nu(r_{eD}^{\varepsilon}h(u))}\right] \quad \text{.....(E.17)}$$

APPENDIX F

WELLBORE STORAGE

This appendix adds the wellbore storage for a Dual Porosity with PSS Interporosity Transfer Non-Newtonian Model. The total flowrate is given by:

$$q = q_{wb} + q_{sf} \quad , \qquad \text{(F.1)}$$

Where $q_{wb}(t)$ is the rate in the wellbore and $q_{sf}(t)$ is the sandface rate. Multiplying Eq. F.1 by B_o:

$$qB_o = q_{wb} B_o + q_{sf} B_o \qquad \text{(F.2)}$$

The rate in the wellbore is given by:

$$q_{wb} B_o = -24 C B_o \frac{dp_f}{dt} , \qquad \text{(F.3)}$$

Where C is the storage coefficient defined as:

$$C = -c_{wb} V_{wb} \qquad \text{(F.4)}$$

On the other hand, the sandface rate (in the main flowpath which is the fracture) is expressed as:

$$q_{sf} B_o = 2\pi h \left[-\frac{k_f}{\mu_{eff}} r^n \frac{\partial p_f}{\partial r} \right]^{\frac{1}{n}} B_o \qquad \text{(F.5)}$$

Therefore, substituting Eq.F.3 and Eq.F.5 in Eq.F.2:

$$qB_o = -24 C B_o \frac{dp_f}{dt} + 2\pi h \left[-\frac{k_f}{\mu_{eff}} r^n \frac{\partial p_f}{\partial r} \right]^{\frac{1}{n}} B_o \qquad \text{(F.6)}$$

In order to obtain an expression in dimensionless form for Eq.F.6 we recall dimensionless variables.

Dimensionless Time:

$$t_D = \frac{q^{1-n} k_f}{n(\phi c_t)_t (2\pi h)^{1-n} \mu_{eff} r_w^{3-n}} t \qquad \text{(F.7)}$$

Dimensionless Pressure: *Fracture system*

$$p_{fD} = \frac{(2\pi h)^n k_f}{q^n \mu_{eff} r_w^{1-n}} (p_i - p_f) \quad \text{.....(F.8)}$$

Dimensionless Radius:

$$r_D = \frac{r}{r_w} \quad \text{.....(F.9)}$$

Solving for t and p_f, respectively;

$$t = \frac{n(\phi c_t)_t (2\pi h)^{1-n} r_w^{3-n} \mu_{eff}}{q^{1-n} k_f} t_D \quad \text{,.....(F.10)}$$

$$p_f = p_i - \frac{q^n \mu_{eff} r_w^{1-n}}{(2\pi h)^n k_f} p_{fD} \quad \text{, ...(F.11)}$$

$$r = r_D r_w \quad \text{. .....(F.12)}$$

Substituting Eqs. F.10 and F.11 into Eq. F.3;

$$q_{wb} B_o = -24 C B_o \frac{d\left[p_i - \frac{q^n \mu_{eff} r_w^{1-n}}{(2\pi h)^n k_f} p_{fD}\right]}{d\left[\frac{n(\phi c_t)_t (2\pi h)^{1-n} r_w^{3-n} \mu_{eff}}{q^{1-n} k_f} t_D\right]} \quad \text{,.....(F.13)}$$

Arranging terms in Eq.F.11:

$$q_{wb} B_o = 24 C B_o \frac{q}{n(\phi c_t)_t (2\pi h) r_w^2} \frac{dp_{fD}}{dt_D} \quad \text{.....(F.14)}$$

Substituting Eq. F.11 and Eq. F.13 into the sandface rate relation, Eq. F.5, we obtain:

$$q_{sf}\,B_o = 2\pi h\left[-\frac{k_f}{\mu_{eff}}\right]\left[\frac{r_w^n r_D^n\, d\left[p_i - \dfrac{q^n \mu_{eff}\, r_w^{1-n}}{(2\pi h)^n\, k_f}\, p_{fD}\right]}{d\,(r_w r_D)}\right]^{\frac{1}{n}} B_o \quad \text{.....(F.15)}$$

Arranging terms in Eq.F.15:

$$q_{sf}\,B_o = qB_o\left[r_D^n\,\frac{dp_{fD}}{d\,r_D}\right]^{\frac{1}{n}} \quad \text{.....(F.16)}$$

Substituting Eq.F.14 and 16 in Eq.F.6 gives:

$$qB_o = -24C\,B_o\,\frac{q}{n(\phi c_t)_t\,(2\pi h) r_w^2}\,\frac{dp_{fD}}{dt_D} + qB_o\left[r_D^n\,\frac{dp_{fD}}{d\,r_D}\right]^{\frac{1}{n}} \quad \text{.....(F.17)}$$

Finally the equation Eq.F.17 may be written as:

$$C_D\,\frac{dp_{fD}\,(t_D)}{dt_D} + \left[r_D^n\,\frac{dp_{fD}\,(t_D)}{d\,r_D}\right]^{\frac{1}{n}} = 1\,, \quad \text{.....(F.18)}$$

Where

$$C_D = \frac{24\,C}{n(\phi c_t)_t\,(2\pi h) r_w^2} \quad \text{.....(F.19)}$$

APPENDIX G

SKIN FACTOR

This appendix shows the derivation of the skin factor effect. Around the wellbore there is a zone called the *skin zone*, which means that there is a pressure drop Δp_s near the wellbore. This pressure drop is due to adverse drilling and completion conditions. The pressure drop is defined by:

$$\Delta p_s = \Delta p_1 - \Delta p_2 \,, \quad \text{..... (1)}$$

Where

$$\Delta p_1 = \left[\frac{q}{2\pi h}\right]^n \frac{\mu_{eff}}{k_s} r^{w-1} \ln\left[\frac{r_s}{r_w}\right], \quad \text{..... (2)}$$

And

$$\Delta p_2 = \left[\frac{q}{2\pi h}\right]^n \frac{\mu_{eff}}{k_f} r^{w-1} \ln\left[\frac{r_s}{r_w}\right] \quad \text{..... (3)}$$

Δp_1 pressure drop from a radius r_s to the wellbore radius r_w, which would normally occur because of flow through the altered zone. Δp_2 pressure drop from a radius r_s to the wellbore radius r_w, which would have occurred had there been no change in permeability in the altered zone. Substituting 2 and 3 into 1 gives:

$$\Delta p_s = \left[\frac{q}{2\pi h}\right]^n \frac{\mu_{eff}}{k_s} r^{w-1} \ln\left[\frac{r_s}{r_w}\right] - \left[\frac{q}{2\pi h}\right]^n \frac{\mu_{eff}}{k_f} r^{w-1} \ln\left[\frac{r_s}{r_w}\right]. \quad \text{..... (4)}$$

Factorizing and arranging terms in 4 we get the expression as follows:

$$\Delta p_s = \left[\frac{q}{2\pi h}\right]^n \frac{\mu_{eff}}{k_f} r^{w-1} \left[\frac{k_f}{k_s} - 1\right] \ln\left[\frac{r_s}{r_w}\right] \quad \text{..... (5)}$$

Defining a skin factor from the properties of the altered zone:

$$s = \left[\frac{k_f}{k_s} - 1\right] \ln\left[\frac{r_s}{r_w}\right] \quad \text{..... (6)}$$

Combining Eq.5 and Eq.6, and solving for *s*

$$s = \Delta p_s \left[\frac{2\pi h}{q} \right]^n \frac{k_f}{\mu_{eff}} r^{w-1} \quad \text{..... (7)}$$

Eq.7 is the definition of skin factor for this .

APPENDIX H

EARLY-TIME APPROXIMATIONS

This appendix presents the "early-time" approximation for the dual porosity, non-Newtonian model.

Recalling the General Solution in the Laplace Domain:

$$\overline{p}_{fD}(r_D,u)=\frac{r_D^{\frac{1-n}{2}}K_{\frac{1-n}{3-n}}\left[\frac{2\sqrt{ug(u)}}{3-n}r_D^{\frac{3-n}{2}}\right]}{u\sqrt{u\,g(u)}K_{\frac{2}{3-n}}\left[\frac{2\sqrt{ug(u)}}{3-n}\right]}, \quad \text{.....(H.1)}$$

Where:

$$g(u)=\frac{u(1-\omega)\omega+n\lambda D^{1-n}}{u(1-\omega)+n\lambda D^{1-n}} \quad \text{.....(H.2)}$$

When r_D=1 Eq.H.1 reduces to:

$$\overline{p}_{fD}(u)=\frac{K_{\frac{1-n}{3-n}}\left[\frac{2\sqrt{u\,g(u)}}{3-n}\right]}{u\sqrt{u\,g(u)}K_{\frac{2}{3-n}}\left[\frac{2\sqrt{ug(u)}}{3-n}\right]} \quad \text{.....(H.3)}$$

Eq.H.2 can be rearranged as follows:

$$g(u)=\omega+(1-\omega)\frac{n\lambda D^{1-n}}{u(1-\omega)+n\lambda D^{1-n}} \quad \text{.....(H.4)}$$

Considering Eq. H.4, as $u\rightarrow\infty$ (short times), we have:

$$g(u\rightarrow\infty)=\omega+(1-\omega)\frac{n\lambda D^{1-n}}{\infty(1-\omega)+n\lambda D^{1-n}} \quad \text{.....(H.5)}$$

The second term of Eq.H.5 goes to zero and the result of the limit is:

$$g(u\rightarrow\infty)=\omega \quad \text{.....(H.6)}$$

Eq.H.6 is then substituted into Eq. H.3, which yields:

$$\overline{p}_{fD}(u) = \frac{K_{\frac{1-n}{3-n}}\left[\frac{2\sqrt{u\omega}}{3-n}\right]}{u\sqrt{u\omega}\,K_{\frac{2}{3-n}}\left[\frac{2\sqrt{u\omega}}{3-n}\right]} \quad \text{.....(H.7)}$$

The approximation for the Bessel function is defined as:

$$K_{\nu}(z) = \frac{1}{2}\Gamma(\nu)\left[\frac{1}{2}z\right]^{-\nu} \quad \text{.....(H.8)}$$

Eq.H.7 may be rewritten as:

$$\overline{p}_{fD}(u) \approx \frac{\frac{1}{2}\Gamma\left[\frac{1-n}{3-n}\right]\left[\frac{1}{2}\frac{2\sqrt{u\omega}}{3-n}\right]^{\frac{n-1}{3-n}}}{u\sqrt{u\omega}\,\frac{1}{2}\Gamma\left[\frac{2}{3-n}\right]\left[\frac{1}{2}\frac{2\sqrt{u\omega}}{3-n}\right]^{\frac{-2}{3-n}}}, \quad \text{.....(H.9)}$$

Rearranging Eq.H.9, we obtain:

$$\overline{p}_{fD}(u) \approx \frac{\Gamma\left[\frac{1-n}{3-n}\right]\left[\frac{1}{3-n}\right]^{\frac{n+1}{3-n}}(\sqrt{u\omega})^{\frac{n+1}{3-n}}}{u\sqrt{u\omega}\,\Gamma\left[\frac{2}{3-n}\right]}, \quad \text{.....(H.10)}$$

Simplifying Eq.H.10 in terms of u, we have:

$$\overline{p}_{fD}(u) \approx \frac{\Gamma\left[\frac{1-n}{3-n}\right]\left[\frac{1}{3-n}\right]^{\frac{n+1}{3-n}}(\omega)^{\frac{n-1}{3-n}}}{\Gamma\left[\frac{2}{3-n}\right]}(u)^{\frac{2(n-2)}{3-n}} \quad \text{.....(H.11)}$$

Using Laplace Transform tables, Eq. H.11 can be inverted to yield:

$$p_{fD}(t_D) \approx \frac{\Gamma\left[\frac{1-n}{3-n}\right]\left[\frac{1}{3-n}\right]^{\frac{n+1}{3-n}}(\omega)^{\frac{n-1}{3-n}}}{\Gamma\left[\frac{2}{3-n}\right]} \frac{(t_D)^{\frac{1-n}{3-n}}}{\Gamma\left[-\frac{2(n-2)}{3-n}\right]} \quad \text{.....(H.12)}$$

Eq.H.12 is the approximation at "early-time" for the dual porosity non Newtonian model. For well test purposes a derivative is calculated. Taking the derivative multiplied by dimensionless time from Eq.H.12 for the "early-time" approximation as follows:

$$t_D \frac{dp_{fD}(t_D)}{dt_D} \approx \frac{\Gamma\left[\frac{1-n}{3-n}\right]\left[\frac{1}{3-n}\right]^{\frac{n+1}{3-n}}(\omega)^{\frac{n-1}{3-n}}}{\Gamma\left[\frac{2}{3-n}\right]\Gamma\left[-\frac{2(n-2)}{3-n}\right]}\left[\frac{1-n}{3-n}\right](t_D)^{\frac{1-n}{3-n}} \text{.....(H.13)}$$

APPENDIX I

LATE-TIME APPROXIMATIONS

This appendix presents the "late-time" approximation of the dual porosity non-Newtonian model in order to yield a direct Laplace transform inversion. Recalling the general solution in the Laplace domain:

$$\bar{p}_{Df}(r_D,u)=\frac{r_D^{\frac{1-n}{2}}K_{\frac{1-n}{3-n}}\left[\frac{2\sqrt{ug(u)}}{3-n}r_D^{\frac{3-n}{2}}\right]}{u\sqrt{ug(u)}K_{\frac{2}{3-n}}\left[\frac{2\sqrt{ug(u)}}{3-n}\right]}, \quad \text{.....(I.1)}$$

where:

$$g(u)=\frac{u(1-\omega)\omega+n\lambda D^{1-n}}{u(1-\omega)+n\lambda D^{1-n}} \quad \text{.....(I.2)}$$

When r_D=1 Eq. I.1 reduces to:

$$\bar{p}_{Df}(u)=\frac{K_{\frac{1-n}{3-n}}\left[\frac{2\sqrt{ug(u)}}{3-n}\right]}{u\sqrt{ug(u)}K_{\frac{2}{3-n}}\left[\frac{2\sqrt{ug(u)}}{3-n}\right]} \quad \text{.....(I.3)}$$

Considering Eq. I.2, as $u\rightarrow 0$ (large of "late" times), we have:

$$g(u\rightarrow 0)=\frac{0(1-\omega)\omega+n\lambda D^{1-n}}{0(1-\omega)+n\lambda D^{1-n}}=1 \quad \text{.....(I.4)}$$

Substituting Eq.I.4 in Eq.I.3 yields:

$$\bar{p}_{Df}(u)=\frac{K_{\frac{1-n}{3-n}}\left[\frac{2\sqrt{u}}{3-n}\right]}{u\sqrt{u}K_{\frac{2}{3-n}}\left[\frac{2\sqrt{u}}{3-n}\right]} \quad \text{.....(I.5)}$$

Recalling the Bessel functions when $u \to 0$

$$K_\nu(z) = \frac{1}{2}\Gamma(\nu)\left[\frac{1}{2}z\right]^{-\nu} \quad \text{.....(I.6)}$$

Substituting Eq.I.I.6 in Eq.I.5:

$$\overline{p}_{Df}(u) = \frac{\frac{1}{2}\Gamma\left[\frac{1-n}{3-n}\right]\left[\frac{1}{2}\frac{2\sqrt{u}}{3-n}\right]^{\frac{n-1}{3-n}}}{u\sqrt{u}\,\frac{1}{2}\Gamma\left[\frac{2}{3-n}\right]\left[\frac{1}{2}\frac{2\sqrt{u}}{3-n}\right]^{-\frac{2}{3-n}}} \quad \text{.....(I.7)}$$

Simplifying Eq.I.7:

$$\overline{p}_{Df}(u) = \frac{\Gamma\left[\frac{1-n}{3-n}\right]}{\Gamma\left[\frac{2}{3-n}\right]}\left[\frac{1}{3-n}\right]^{\frac{n+1}{3-n}}(u)^{\frac{2(n-2)}{3-n}} \quad \text{.....(I.8)}$$

We note that Eq.I.8 can be inverted directly using Laplace transform tables, which yields:

$$p_{Df}(t_D) = \frac{\Gamma\left[\frac{1-n}{3-n}\right]}{\Gamma\left[\frac{2}{3-n}\right](3-n)^{\frac{n+1}{3-n}}}\frac{t_D^{\frac{1-n}{3-n}}}{\Gamma\left[\frac{4-2n}{3-n}\right]} \quad \text{.....(I.9)}$$

Using the identity for the $\Gamma(n)$ function, we have:

$$\Gamma(n+1) = n\Gamma(n) \quad \text{.....(I.10)}$$

In order to use Eq.I.10, it is necessary to reform Eq.I.9 as follows:

$$p_{Df}(t_D) = \frac{\Gamma\left[\frac{1-n}{3-n}\right]}{\Gamma\left[\frac{2}{3-n}\right](3-n)^{\frac{n+1}{3-n}}}\frac{t_D^{\frac{1-n}{3-n}}}{\Gamma\left[\frac{1-n}{3-n}+1\right]} \quad \text{.....(I.11)}$$

Using the property shown by Eq.I.10 in Eq.I.11, we have:

$$p_{Df}(t_D) = \frac{\Gamma\left[\frac{1-n}{3-n}\right]}{\Gamma\left[\frac{2}{3-n}\right](3-n)^{\frac{n+1}{3-n}}\left[\frac{1-n}{3-n}\right]\Gamma\left[\frac{1-n}{3-n}\right]} \frac{t_D^{\frac{1-n}{3-n}}}{} \quad \text{.....(I.12)}$$

Finally rearranging terms in Eq.I.12 and simplifying, we have:

$$p_{Df}(t_D) = \frac{(3-n)^{\frac{2(1-n)}{3-n}}}{\Gamma\left[\frac{2}{3-n}\right](1-n)} t_D^{\frac{1-n}{3-n}} \quad \text{.....(I.13)}$$

Eq.I.13 is the approximation at long or "late-times" for our proposed dual porosity non Newtonian model. For application purposes, we require a derivative formulation as well. Taking the derivative multiplied by dimensionless time from Eq.I.13 yields the "late-time" approximation for this case:

$$t_D \frac{dp_{Df}(t_D)}{dt_D} = \frac{(3-n)^{\frac{2(1-n)}{3-n}}}{\Gamma\left[\frac{2}{3-n}\right](1-n)}\left[\frac{1-n}{3-n} t_D^{\frac{-2}{3-n}}\right] t_D \quad \text{.....(I.14)}$$

Reducing similar terms and simplifying Eq.I.14:

$$t_D \frac{dp_{Df}(t_D)}{dt_D} = \frac{(3-n)^{\frac{-(1+n)}{3-n}}}{\Gamma\left[\frac{2}{3-n}\right]} t_D^{\frac{1-n}{3-n}} \quad \text{.....(I.15)}$$